



Doctoral thesis

# Targeting angiogenesis with small antibody fragments and antibody-like molecules

Dragana Avramović



# Targeting angiogenesis with small antibody fragments and antibody-like molecules

Inauguraldissertation

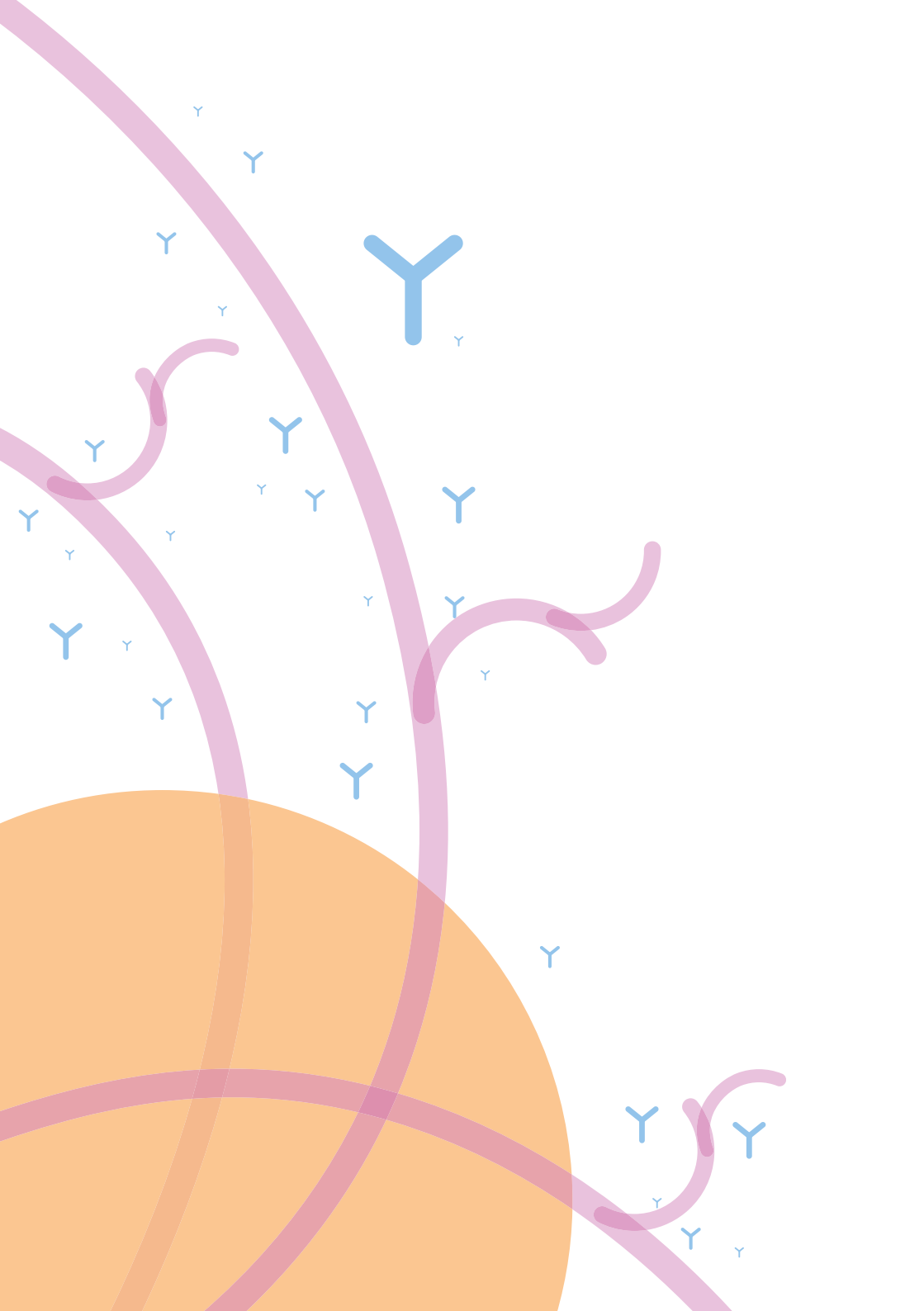
zur  
Erlangung der Würde eines Doktors der Philosophie

vorgelegt der Philosophische Naturwissenschaftlichen  
Fakultät der Universität Basel

Von  
Dragana Avramović  
aus Belgrad, Serbien

Basel, 2017

Originaldokument gespeichert auf dem Dokumentenserver der Universität Basel  
[edoc.unibas.ch](http://edoc.unibas.ch)



Genehmigt von der Philosophische Naturwissenschaftlichen Fakultät

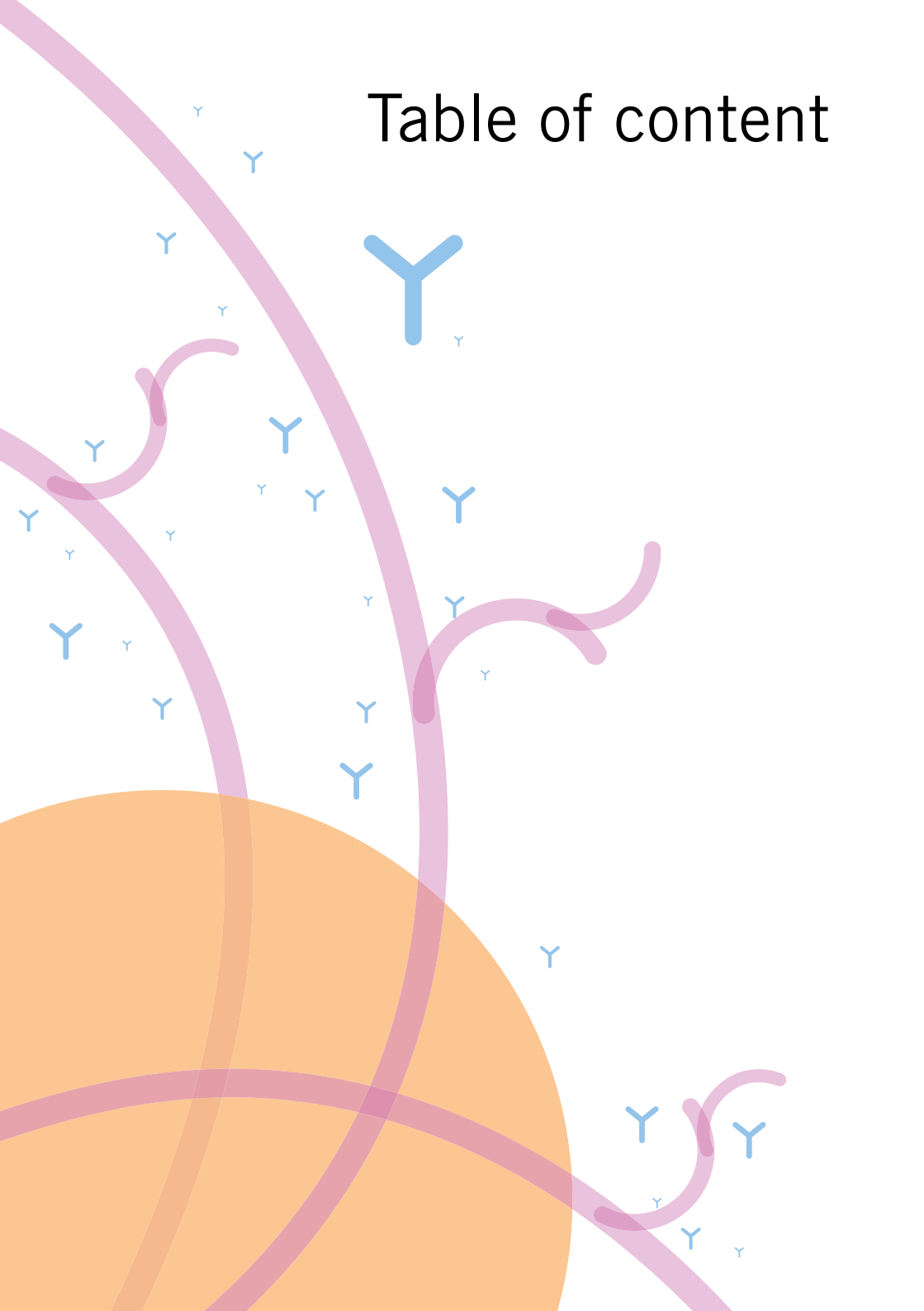
auf Antrag von:

Prof. Dr. Kurt Ballmer-Hofer  
Prof. Dr. Gerhard Christofori

Basel, 15.11.2016

Prof. Dr. Jörg Schibler, Dekan

# Table of content



**Summary**

**Zusammenfassung**

**1. HISTORY OF SINGLE CHAIN FRAGMENT VARIABLE (SCFVS) ANTIBODIES**

**DEVELOPMENT ..... 21**

1.1. Abstract ..... 22

1.2. Introduction ..... 22

1.3. Recombinant antibody technology ..... 23

1.3.1. ScFv antibodies ..... 24

1.3.2. Expression of scFv antibodies ..... 25

1.3.3. Phage display using recombinant libraries ..... 25

1.3.4. Ribosomal display technology ..... 27

1.3.5. Affinity maturation of scFvs selected from phage display libraries ..... 27

1.3.6. Antigen exposure for the scFvs selection process ..... 27

1.3.7. Advantages of scFv antibodies over full-size monoclonal ..... 28  
antibodies

1.4. Application of scFvs ..... 28

1.4.1. Medical application ..... 28

1.4.1.1. ScFvs in tumor therapy ..... 28

ScFvs as neutralizing antibodies ..... 29

ScFvs as recombinant immunotoxins ..... 29

ScFvs as cancer vaccine ..... 29

ScFvs as anticancer intrabodies ..... 29

1.4.1.2. Application of scFvs in neurodegenerative diseases ..... 31

Alzheimer's disease (AD) ..... 31

1.4.1.3. ScFvs against HIV infection ..... 31

1.4.2. *In vivo* imaging ..... 32

1.4.3. Diagnostic applications ..... 32

1.5. Discussion ..... 33

Aim of the thesis ..... 34

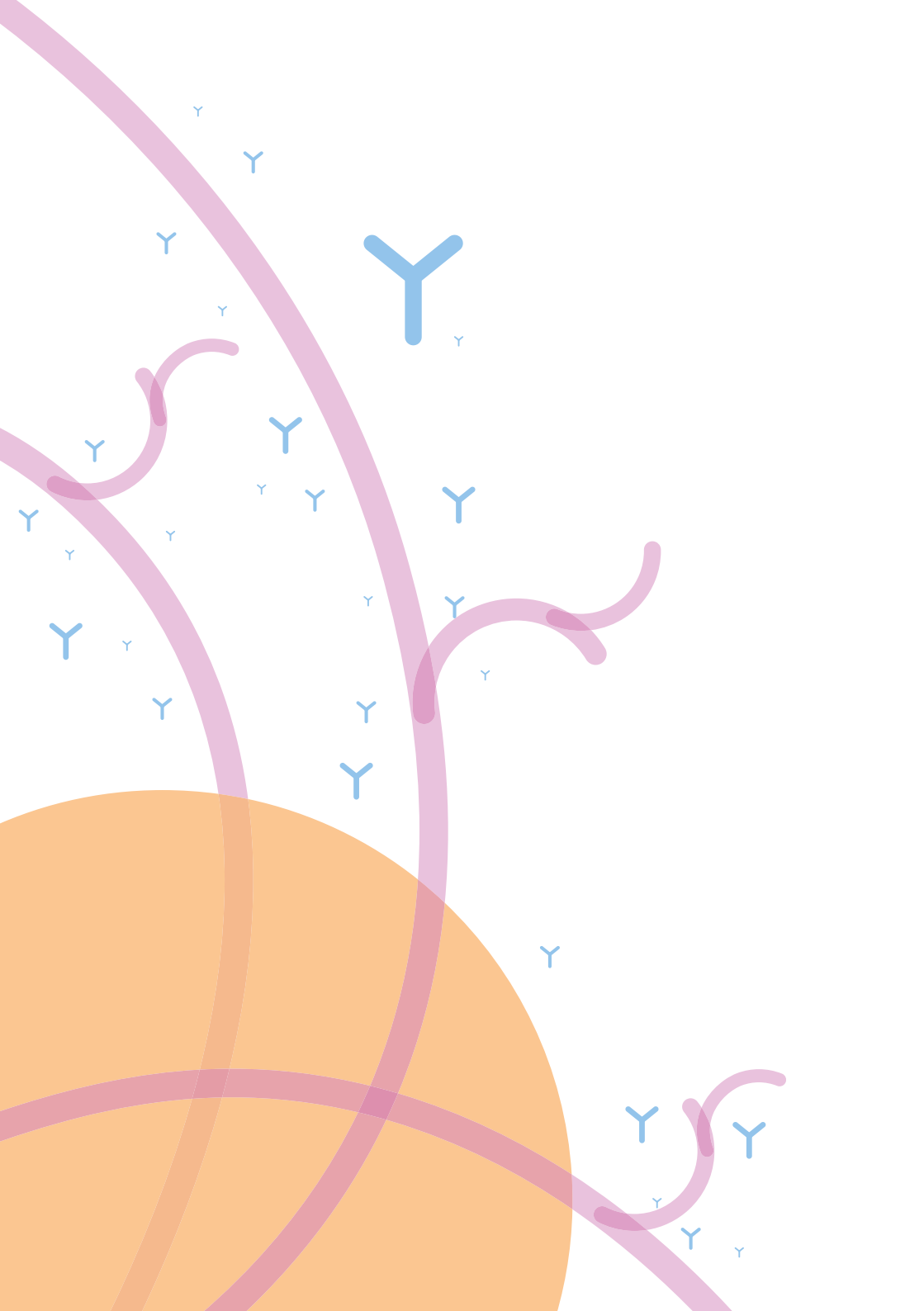
<b>2. DEVELOPMENT AND <i>IN VITRO</i> APPLICATION OF NOVEL VEGFR-2 INHIBITORY SINGLE CHAIN FRAGMENT VARIABLE ANTIBODIES</b> .....	<b>35</b>
2.1. Abstract .....	36
2.2. Introduction .....	36
2.3. Materials and methods .....	39
2.3.1. Cell culture .....	39
2.3.2. Transient transfection .....	39
2.3.3. VEGFR-2 kinase activity assay .....	39
2.3.4. Immunofluorescence microscopy .....	40
2.3.5. ETH-2 Gold library .....	40
2.3.6. ScFvs selection .....	40
2.3.7. ScFv A7 .....	41
2.3.8. Enzyme-linked immunosorbent assay (ELISA) .....	41
2.3.9. Expression and purification of scFvs .....	42
2.3.10. Size-exclusion chromatography (SEC) .....	42
2.3.11. Fluorescence size-exclusion chromatography (FSEC) .....	43
2.3.12. Binding affinity determination by ITC .....	43
2.3.13. HUVEC tube formation assay .....	43
2.3.14. HUVEC migration assay .....	44
2.3.15. Squash analysis of VEGFR-2 internalization .....	44
2.3.16. Trypsin digestion of cell surface exposed receptor .....	44
2.3.17. Statistical analysis .....	44
2.4. Results .....	45
2.4.1. Selection, production, and purification of scFvs antibodies .....	45
2.4.2. Binding of scFvs to recombinant and endogenous VEGFR-2 .....	50
2.4.3. Functional inhibition of VEGFR-2 phosphorylation with scFvs .....	51
2.4.4. Effect of antibodies on HUVEC tube formation and migration .....	52
2.4.5. VEGF and scFvs induce internalization of VEGFR-2 .....	55
2.5. Discussion .....	57



<b>3. REFORMATTING SCFV ANTIBODIES TO FRAGMENT ANTIGEN BINDING (FAB) ANTIBODY FRAGMENTS</b> .....	<b>59</b>
3.1. Introduction .....	60
3.2. Materials and methods .....	60
3.2.1. Cloning strategy for reformatting scFvs to Fabs .....	60
3.2.2. Expression and purification of soluble Fabs .....	61
3.2.3. Receptor kinase activity assay and HUVEC tube formation assay .....	61
3.3. Results .....	62
3.3.1. Construction of Fab format .....	62
3.3.2. Expression and purification of Fabs .....	62
3.3.3. Affinity determination with ITC .....	62
3.3.4. Receptor kinase activity assay and HUVEC tube formation assay .....	65
3.4. Discussion .....	67
<b>4. OBTAINING FULL-LENGTH IGGs FROM PREVIOUSLY CHARACTERIZED VEGFR-2 INHIBITORY SCFVS</b> .....	<b>69</b>
4.1. Introduction .....	70
4.2. Material and methods .....	70
4.2.1. Cloning, production, and purification .....	70
4.2.1.1. Cloning pcDNA3 vectors .....	70
4.2.1.2. Reformatting with MultiPrime expression system .....	71
4.2.1.3. IgGs purification .....	71
4.2.2. Fluorescence size-exclusion chromatography (FSEC), receptor kinase activity assay, tube formation assay .....	71
4.3. Results .....	72
4.3.1. IgG cloning and purification .....	72
4.3.2. Cloning into pcDNA3 vectors .....	72
4.3.3. Cloning with MultiPrime .....	73
4.3.4. Determination of IgGs binding to VEGFR-2 by FSEC .....	76
4.3.5. Functional inhibition of VEGFR-2 phosphorylation with IgGs .....	77
4.3.6. HUVEC tube formation assay .....	78
4.4. Discussion .....	79

<b>5. SELECTION AND CHARACTERIZATION OF SCFVS SPECIFIC FOR THE MOUSE VEGFR-2 ECD .....</b>	<b>81</b>
5.1. Introduction .....	82
5.2. Materials and methods .....	83
5.2.1. Production of recombinant mouse VEGFR-2 ECD .....	83
5.2.2. Selection of mouse specific scFvs against VEGFR-2 .....	83
5.2.2.1. Selection of mouse specific scFvs from ETH-2 Gold library .....	83
5.2.2.2. Selection of species cross-reactive scFv antibodies against mouse and human VEGFR-2 ECD .....	83
5.2.2.3. Selection of mouse specific scFvs from R3 EPFL library .....	84
5.2.3. Sequencing of selected mouse scFvs .....	84
5.2.4. Testing protein expression to select optimal bacterial strain .....	85
5.2.5. Expression and purification of scFvs against mouse VEGFR-2 .....	85
5.2.5.1. Expression and purification of soluble scFvs from ETH-2 Gold library ...	85
5.2.5.2. Expression and purification of scFvs from R3 EPFL library .....	85
5.2.6. ELISA for binder specificity .....	86
5.2.7. Cell culture .....	86
5.2.8. Receptor kinase activity assay .....	86
5.2.9. HUVEC tube formation assay .....	86
5.3. Results .....	87
5.3.1. Selection, production, and purification of scFvs antibodies .....	87
5.3.1.1. ETH-2 Gold library .....	87
5.3.1.2. R3 EPFL library .....	87
5.3.2. Functional inhibition of VEGFR-2 phosphorylation with mouse specific scFvs ..	90
5.3.3. Effect of antibodies on endothelial cell tube formation .....	92
5.4. Discussion .....	93

<b>6. TUMOR TARGETING WITH RADIOLABELED DARPINS</b> .....	<b>95</b>
6.1. Introduction .....	96
6.2. Materials and methods .....	96
6.2.1. Cell lines used in the study .....	96
6.2.2. DARPins .....	96
6.2.3. Fluorescence activated cell sorting (FACS) .....	97
6.2.4. Immunohistochemistry .....	97
6.2.5. Labeling of DARPins with $^{99m}\text{Tc}(\text{CO})_3$ .....	97
6.2.6. <i>In vivo</i> imaging .....	97
6.2.6.1. Animals .....	97
6.2.6.2. Cancer cell injections .....	97
6.2.6.3. Tumor targeting with radiolabeled DARPins .....	97
6.2.6.4. SPECT/CT imaging .....	97
6.2.7. Biodistribution .....	99
6.3. Results .....	99
6.4. Discussion .....	104
<b>7. CONCLUSIONS AND OUTLOOK</b> .....	<b>105</b>
<b>8. ACKNOWLEDGEMENTS</b> .....	<b>107</b>
<b>9. REFERENCES</b> .....	<b>109</b>



# Summary

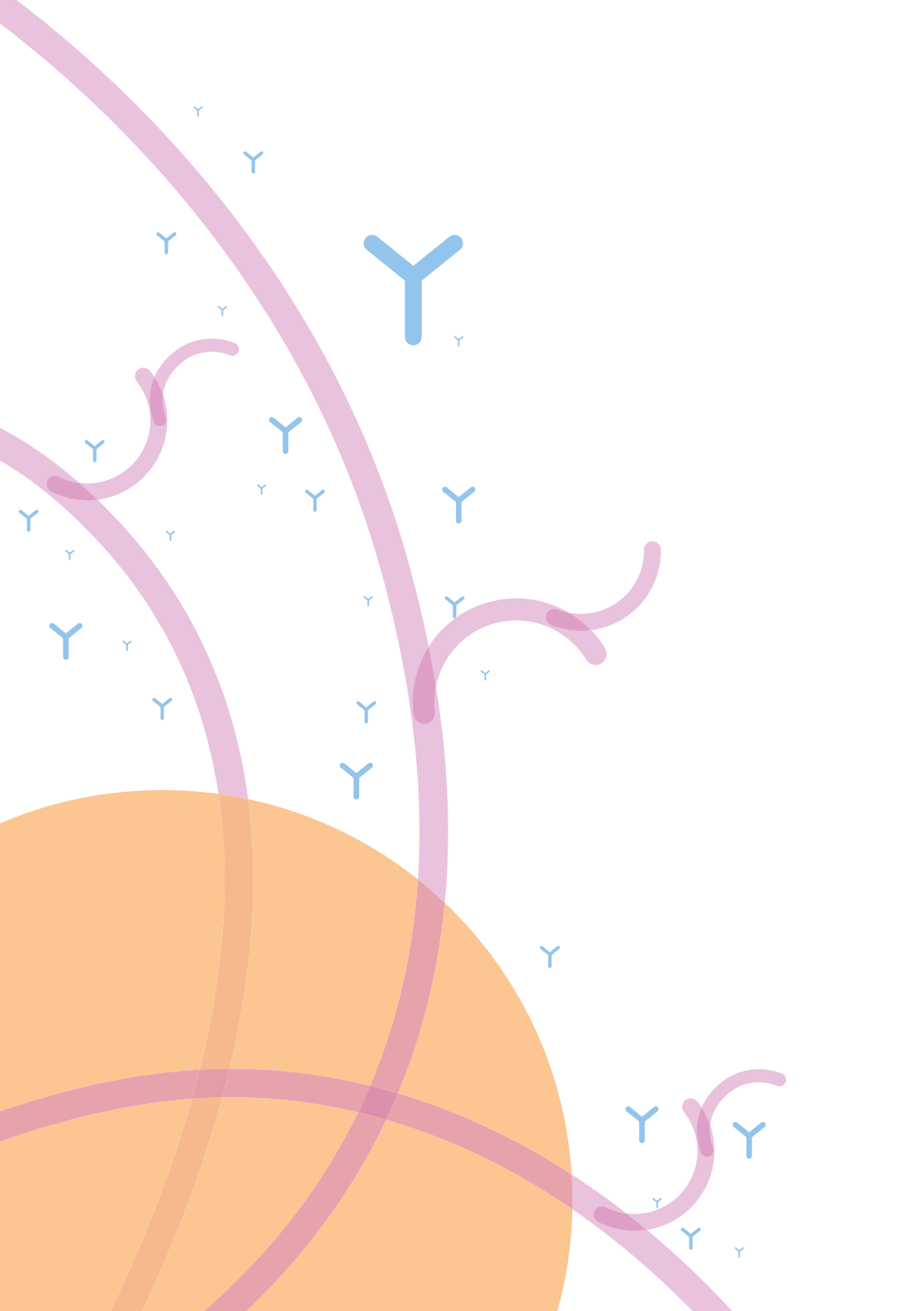
Angiogenesis is the formation of new blood vessels from pre-existing capillaries. It occurs throughout the life of higher organisms, in both health and disease. Metabolically active tissues in the body are found in the proximity of the blood capillaries, formed by the process of angiogenesis. The idea that control of angiogenesis could have a therapeutic potential has raised great interest during the past 40 years. Stimulation of angiogenesis can be therapeutic for ischemic heart disease, peripheral arterial disease and wound healing. Decreasing or inhibiting angiogenesis can be a therapeutic goal in cancer, some ophthalmic pathological conditions, rheumatoid arthritis, and other diseases.

Vascular Endothelial Growth Factors (VEGFs) and their receptors (VEGFRs) are major players in both physiological and pathological angiogenesis. VEGFs constitute a family of proteins that play important roles in blood and lymphatic vessel development. VEGFs bind VEGFR-1, -2, and -3, promoting cell survival, proliferation, differentiation, and migration. VEGFR-2 is the major mediator of angiogenic signaling in endothelial cells, and its activity is regulated at multiple levels. Ligand binding to the extracellular domain (ECD) of VEGFR-2 leads to receptor dimerization, followed by intracellular kinase domain activation, receptor internalization and downstream signaling.

The goal of this study was to develop novel antiangiogenic drugs targeting VEGFR-2, as an addition or alternative to existing cancer therapies. As for targeting tools, we used different antibody formats and antibody-like molecules. In this study, we generated and tested three types of ECD binders, single chain fragment variable antibodies (scFvs), fragment antigen-binding antibodies (Fabs) and full-length Immunoglobulins G (IgGs), specifically interacting with single Ig-homology domains, located in the receptor ECD. We identified several promising antibodies, interacting with the ECD of VEGFR-2 and blocking ligand-stimulated receptor activation. Different formats of antibodies showed similar effects with significant inhibition of VEGFR-2 phosphorylation at Tyr1175 and phosphorylation of PLC- $\gamma$ , as well as inhibition of *in vitro* angiogenesis in Human Umbilical Vein Endothelial cell (HUVEC) tube formation and HUVEC migration assays. Our findings provide the proof-of-principle that highly specific anti-VEGFR-2 agents targeting the membrane-proximal Ig-domains D4 and D7 inhibit receptor activity.

Interestingly, the binding of antibody fragments to VEGFR-2 led to receptor internalization as demonstrated by an increase in total volume of intracellular receptor-positive vesicles. Internalization independent of ligand binding represents a new, promising property of these VEGFR-2 antibodies. The new agents will be useful for *in vivo* studies aimed at vessel imaging or at inhibiting VEGFR-2 signaling.

Additionally, we tested the already characterized Designed Ankyrin Repeat Proteins (DARPs) for tumor targeting *in vivo*.



# Zusammenfassung

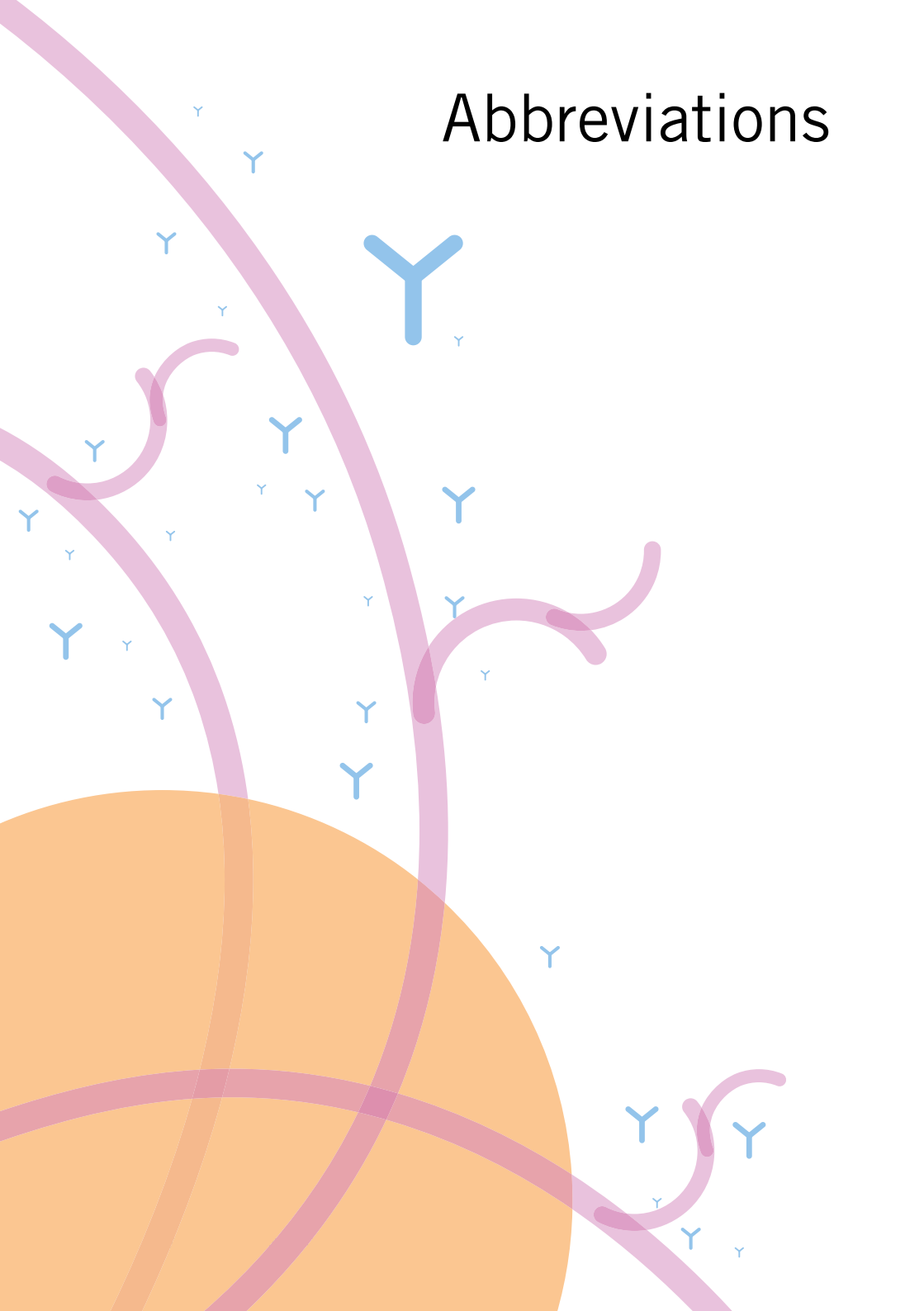
Angiogenese bezeichnet die Sprossung und Spaltung von existierenden Blutgefäßen. Dies ist ein permanenter Prozess in höheren Organismen und findet in gesundem sowie in krankem Zustand statt. Die Blutgefäßformierung ist besonders hoch in direkter Umgebung zu metabolisch aktivem Gewebe, wie den Organen. Während der letzten 40 Jahren fand bereits intensive Forschung im Bereich der Angiogenese statt, da ein großes Potential in der gerichteten Bildung von neuen Blutgefäßen gesehen wird und den daraus folgenden therapeutischen Effekten. Die ischämischen Herzkrankheiten, peripheren arteriellen Verschlusskrankheiten und Wundheilung sind dabei die wichtigsten potentiellen Anwendungsgebiete. Partielle oder vollständige Inhibierung von Angiogenese sind mögliche therapeutische Maßnahmen im Kampf gegen Krebs, einigen pathologischen Bedingungen, rheumatoider Arthritis und andere Krankheiten.

Die vaskulären endothelialen Wachstumsfaktoren (VEGFs) und dessen Rezeptoren (VEGFRs) sind dabei die wichtigsten Partner in physiologischer als auch pathologischer Angiogenese. VEGFs spielen eine essentielle Rolle in der Bildung von Blut- und Lymphgefäßen. VEGFs interagieren mit allen drei VEGFRs (VEGFR-1, 2 und -3) und stimulieren Proliferation, Differenzierung und Migration. VEGFR-2 ist vor allem verantwortlich für angiogene Aktivität in Endothelzellen. Dessen Aktivität wird schrittweise reguliert. Die Bindung vom VEGF an die extrazelluläre Domäne von VEGFR-2 führt zu dessen Dimerisierung, gefolgt von der Aktivierung der intrazellulären Kinasedomäne, welche die Internalisierung und weitere Signalwege aktiviert.

Das Ziel dieser Doktorarbeit war es eine neue anti-angiogene Therapie des VEGFR-2 zu entwickeln, die als zusätzliche oder alternative Maßnahme im Kampf gegen Krebs eingesetzt werden kann. Der Fokus liegt dabei auf dem möglichen Einsatz von verschiedenen Antikörpervarianten bzw. antikörper-ähnlichen Proteinen. Während dieser Studie wurden drei verschiedene Typen von ECD Bindern erzeugt und getestet: Einzelketten-Antikörper (scFvs), Antigen-bindendes Antikörperperfragment (Fab) und intaktes Immunglobulin G (IgG). Es ist uns gelungen mehrere potenzielle Antikörper zu identifizieren, die mit der EC Domäne von VEGFR-2 interagieren und dabei die Interaktion mit dessen Liganden VEGF blockieren. Die verschiedenen getesteten Interaktionspartner wiesen alle eine signifikante Inhibierung von der VEGFR-2 Phosphorylierungsstelle Tyr1175 und Phosphorylierung von PLC- $\gamma$  auf. Des Weiteren konnte eine deutliche Inhibierung von *in vitro* Angiogenese in humanen Nabelvenen-endothel Zellen (HUVEC) registriert werden. Es ist uns gelungen hoch spezifische Antikörper bzw. Antikörper-ähnlichen Proteinen zu erzeugen, die spezifisch an die Ig-Domäne D4 und D7 VEGFR-2 binden.

Die Bindung der Antikörperfragmente führte zu einer Internalisierung des VEGFR-2, welches durch ein höheres Ausmaß intrazellulärer Rezeptorvesikel bestätigt wurde. Die gesteuerte Internalisierung des Rezeptors in der Abwesenheit von VEGF öffnet neue potenzielle therapeutische Maßnahmen. Die Antikörper bieten ein nützliches Instrument für *in vivo* Studien im Bereich Imaging oder zur Inhibierung von VEGFR-2 Signalweges. Darüber hinaus haben wir die bereits charakterisierten Designed Ankyrin Repeat Protein (DARPs) für die gezielte Tumorbehandlung *in vivo* getestet.

# Abbreviations






AA	Amino acid
AMD	Age-related macular degeneration
AP	Alkaline phosphatase
BSA	Bovine serum albumin
CDR	Complimentarity determining region
CH / CL	Antibody heavy/light chain constant region
DARPinS	Designed Ankyrin Repeat Proteins
DMEM	Dulbecco's modified eagle's medium
DMSO	Dimethyl sulfoxide
DTT	Dithiothreitol
EC	Endothelial cells
ECD	Extracellular domain
ECM	Extracellular matrix
E. coli	Escherichia coli
EDTA	Ethylenediamine tetraacetic acid
EGF	Epidermal growth factor
EGFR	Epidermal growth factor receptor
ELISA	Enzyme linked immunosorbent assay
Erk	Extracellular signal-regulated kinase
Fab	Fragment antigen-binding antibody
Fc	Fragment crystallisable
FDA	Food and Drug Administration
FGF	Fibroblast growth factor
Flk-1	Fetal liver kinase-1 = murine VEGFR-2
Fv	Variable fragment
HEK293	Human embryonic kidney cells 293
HEPES	4-(2-Hydroxyethyl) piperazine-1-ethanesulfonic acid
HRP	Horseradish peroxidase
Ig	Immunoglobulin
IPTG	Isopropyl $\beta$ -D-1-thiogalactopyranoside
KDR	Kinase insert domain receptor
mAb	Monoclonal antibody

OD <sub>600</sub>	Optical density at 600 nm wavelength
PAEC	Porcine aortic endothelial cells
PAE KDR	Porcine aortic endothelial cells overexpressing VEGFR-2
PBS	Phosphate buffered saline
PCR	Polymerase chain reaction
PEG	Polyethylene glycol
PEI	Polyethylenimine
PET	Positron emission tomography
PEM	Protein expressing medium
PLC $\gamma$	Phospholipase C gamma
PVDF	Polyvinylidene fluoride
RT	Room temperature
RTK	Receptor tyrosine kinase
ScFv	Single chain variable fragment
SDS-PAGE	Sodium dodecylsulfate polyacryl gel electrophoresis
SEC	Size-exclusion chromatography
SH2	Src homology-2 domain
SHB	Src homology-2 protein in beta-cells
SPECT	Single photon emission computed tomography
SVEGFR	Soluble VEGFR
TBST	Tris buffered saline with 0.1% Tween 20
VEGF	Vascular endothelial growth factor
VEGFR	VEGF receptor
V <sub>H</sub> / V <sub>L</sub>	Antibody heavy/light chain variable region

1

# History of single chain fragment variable (scFvs) antibodies development

The background is a warm orange color. It features several faint, light-colored Y-shaped symbols representing antibodies, scattered across the page. There are also abstract, flowing lines and a large, semi-transparent yellow circle in the lower right quadrant.

1.1.

# Abstract

As high affinity, protein-based binding reagents, antibodies have proven to be the superior choice in many applications in biological research, medical therapy, and diagnosis. The development of monoclonal antibodies (mAbs) and its standardized production, led to regulatory approvals for IgGs as treatment options for cancer, infectious and inflammatory disease, in the last two decades. Recombinant mAbs expressed in a form of smaller binding fragments solved some of the issues encountered with full-length Immunoglobulins G (IgGs) and alleviated problems such as the high costs, demanding production schemes and low tissue penetration due to IgGs' large size. Easier selection and genetic manipulation of antibody fragments enabled such antibodies to become part of standard laboratory practice to produce completely functional antigen-binding fragments in bacterial systems. The focus on structural designs led to improved *in vivo* pharmacokinetics, extended recombinant library generation and enabled selection against challenging targets. At the same time, new molecular strategies have enhanced affinity, stability and expression levels. The simplicity of the technique allowed agile development of the method and led to the development of small antibody fragments. Such ScFvs can be fused to marker proteins (fluorescent proteins, alkaline phosphatase, radionuclides), can be expressed in the form of bifunctional scFvs with two antigen specificities and can be formatted to larger formats (Fabs, Fab2, IgG). Alternatively, antibody fragments could also be used in the immunotoxin construction, for therapeutic gene delivery and generation of anticancer intrabodies for therapeutic purposes. Redesigned mAb-based fragments provide the next generation of antibody-based reagents for immunotherapy and *in vivo* imaging, with many having being tested in late-phase clinical trials.

1.2.

# Introduction

Antibodies are an integral part of the immune defense system that identifies and neutralizes foreign or innate objects such as bacteria, viruses or infected cells, which represent a threat to the system. An antibody carries an antigen-binding site (paratope) that recognizes a unique target-specific antigen (epitope). Paratope specifically binds the epitope. (Figure 1.1, A). This highly precise mechanism allows an antibody to neutralize microbes as well as to target infected cells that are then further recognized and attacked by other components of the immune system<sup>1</sup>. The most abundant type of antibody is immunoglobulin G (IgG)<sup>2</sup>, a large molecule of about 150 kDa that consists of two distinct regions: the fragment antigen-binding (Fab) and fragment crystallizable (Fc) part. The Fab fragment consists of a constant (C<sub>1</sub>)

and a variable ( $V_L$ ) light-chain domain, linked to the constant ( $C_H$ ) and the variable ( $V_H$ ) heavy chain domains (Figure 1.1, B).  $V_L$  and  $V_H$  carry each three solvent-exposed loops that bind the antigen, named complementary determining regions (CDRs, Figure 1.1, C). Today researchers can select antibodies against virtually any target; it is not surprising that these molecules and their small conjugates are used extensively in clinical and basic research.

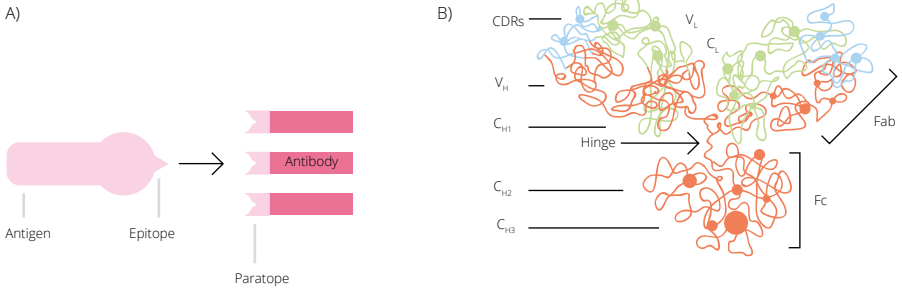


Figure 1.1. Antibody structure. A) IgG structure representation with the focus on paratope-epitope binding adapted from<sup>3</sup>. B) Overall crystal structure of intact antibody protein with the focus on Fab and Fc parts and complementary determining regions (CDRs) adapted from<sup>4</sup>.

### 1.3.

# Recombinant antibody technology

The immune system relies on antibodies. This important role in first line defense is possible due to the diversity of antibody molecules and their high antigen specificity. The immense diversity is achieved through somatic recombination and hypermutation of a set of variant genes<sup>5</sup> (Figure 1.2, A). These unique properties of antibodies proved to be an attractive tool in research, medical diagnosis and therapy<sup>6</sup>. Further development of the field led to the manipulation of the affinity and specificity of antigen binding by mimicking naturally occurring somatic hypermutation during an immune response. It opened new possibilities for replacing the existing practices of animal immunization applying hybridoma technology (Figure 1.2, B). In 1975, the era of hybridoma technology began with the results of Köhler and Milstein<sup>7</sup>. In 1984, their work was awarded the Nobel Prize in Medicine. Their findings led to the development of monoclonal antibodies with defined specificity, and consistent quality in large scale production.

Monoclonal antibody therapy faced several difficulties: monoclonal antibodies are almost exclusively of murine origin and are thus recognized as foreign by the human

immune system. Delivery of mature immunoglobulin requires extensive post-translational modifications (disulfide bond formation and glycosylation). Due to the large size and molecular complexity of full-size antibodies, their production requires mammalian expression systems<sup>8</sup>, which is time-consuming and costly. Primary attempts to move antibody production from hybridoma cells to bacteria failed due to challenges such as improper folding of the polypeptide and consequent aggregation in the cytoplasm of bacterial cells<sup>9,10</sup>. Monoclonal antibodies provided additional formats of antibodies with different application possibilities (Fab, or Fv fragments).

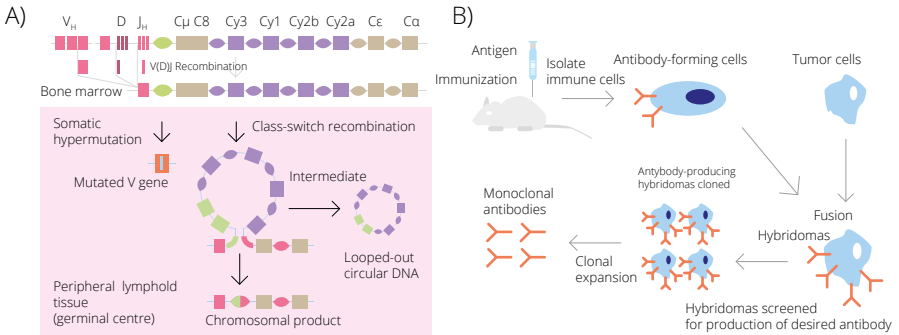


Figure 1.2. IgG technology. A) Schematic representation of V(D)J recombination and somatic hypermutation adapted from<sup>11</sup>. B) Scheme of hybridoma technology developed by Georges Köhler and César Milstein 1970. The figure was adapted from<sup>12</sup>.

### 1.3.1.

## ScFv antibodies

In 1988 scFv antibodies were reported for the first time as the minimal form of antibody<sup>13</sup>. The Fv fragment is the smallest unit of an immunoglobulin molecule that can recognize an antigen and that consists of variable domains of heavy (V<sub>H</sub>) and light (V<sub>L</sub>) chains joined by a flexible peptide linker (Figure 1.3 A, B). With a size of 28 kDa, scFvs can be functionally expressed in *E. coli*. Simple protein expression additionally allows improvement of scFvs properties, including their affinity, by protein engineering<sup>14</sup>. ScFv is a covalently linked heterodimer of heavy and light chain variable domains derived from hybridoma<sup>13,15-17</sup>, spleen cells from immunized mice<sup>18-20</sup>, or B lymphocytes from humans<sup>21-23</sup>. mRNA is isolated from antibody-producing cells and reversely transcribed into cDNA to serve as a template for DNA amplification by PCR. This enabled construction of large libraries with a diverse range of antibody genes<sup>22</sup>.

### 1.3.2.

## Expression of scFv antibodies

To date, scFvs have been successfully expressed in different expression systems such as bacteria, mammalian cells<sup>24</sup>, yeast<sup>25</sup>, plant cells<sup>15</sup> and insect cells<sup>26</sup>. Each expression system demonstrates advantages and disadvantages in the production of active scFvs. Correct folding and secretion of the scFvs remain the critical criteria. Nevertheless, the bacterial expression system remains preferable for the production of scFv antibody fragments among the various expression strategies available. The use of *E. coli*, as an easy and well-established expression system allows proper folding of scFvs and represents a simple technique applicable in a standard molecular biology laboratory at low cost.

This approach allows the optimization of both screening<sup>27</sup> and protein production<sup>28</sup>. Challenges when using *E. coli* as expression system include the reducing environment of the bacterial cytoplasm which leads to insoluble aggregate and inclusion body formation<sup>29,30</sup>. The inclusion bodies must be renatured and the scFvs correctly folded *in vitro*<sup>8</sup> which complicates the expression procedure. This problem was overcome with the introduction of a signal peptide into the expression vectors to direct scFvs into the periplasmic space located between the inner and the outer membrane<sup>31,32</sup>. This periplasmic space contains proteins such as chaperones and disulfide isomerases, which assist proper folding of recombinant proteins<sup>33</sup>.

### 1.3.3.

## Phage display using recombinant libraries

New techniques opened the opportunity for *in vitro* selection of scFvs from large libraries of variable domains, avoiding the traditional hybridoma method. In 1985, Smith<sup>37</sup> postulated that foreign DNA could be fused to the gene encoding the pIII coat protein of a nonlytic filamentous phage. The protein is then expressed as a fusion protein on the phage surface without disturbing the infectivity of the virus (Figure 1.3, C). McCafferty et al.<sup>38</sup> have demonstrated that scFv fragments can be displayed on the phage surface as functional proteins, retaining antigen-binding capability. This technology allows rare clones to be selected and isolated from a large population of phages using any desirable antigen<sup>39</sup>. After this breakthrough discovery, the technology has been widely exploited for the production of antibody fragment molecules including Fab fragments<sup>40</sup>, Fv fragments<sup>41</sup>, and their derivatives<sup>42</sup>. Based on the source of antibody genes, scFv libraries can be immune, naïve, and synthetic.

1. Immune libraries are derived from variable domains of antibody genes of B cells from an immunized animal (mouse, rabbit, rat, goat, camel, sheep, donkey). Therefore, this approach always results in higher affinities of isolated binders as well as a greater number of antigen-specific binders than antibodies derived from naïve libraries. However, the construction

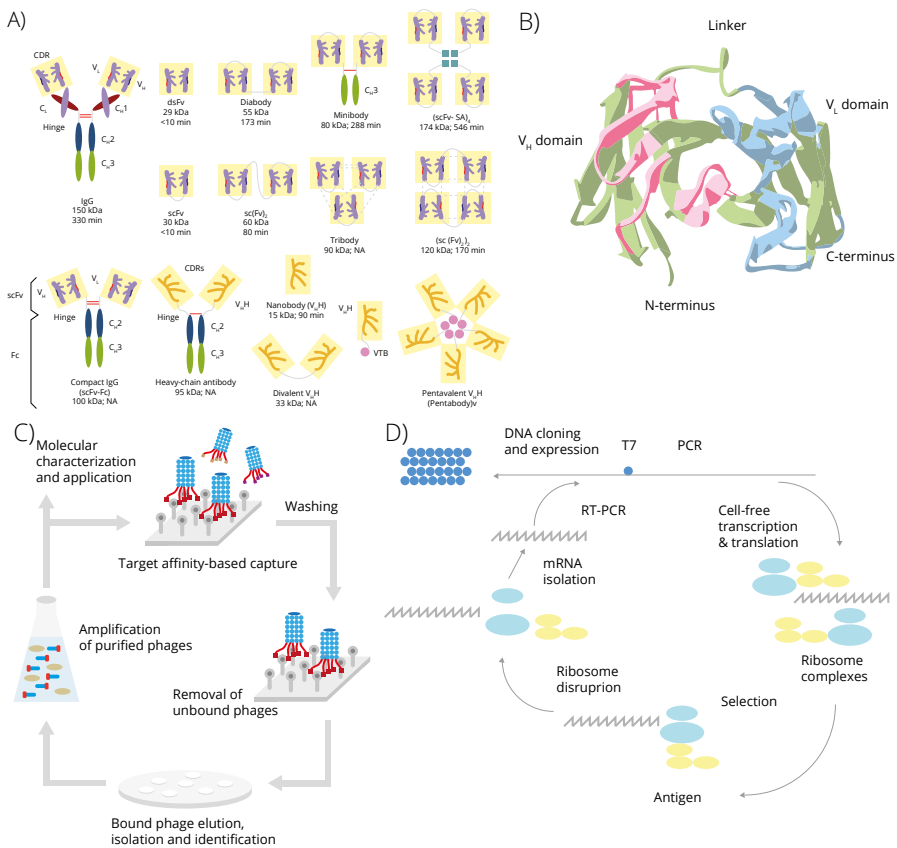


Figure 1.3. ScFvs and display technologies. A) Overview of engineered antibodies and antibody fragments engineered for clinical application adapted from<sup>34</sup>. B) Crystal structure of scFv adapted from<sup>35</sup>. C) A schematic of an affinity-based selection procedure adapted in phage display technology adapted from<sup>36</sup>. D) A schematic representation of a ribosome display selection process adapted from Creative BioLabs (<http://www.creative-biolabs.com>).

of a new library for each antigen is necessary. Antibodies from immune libraries are biased towards the antigen that was used for immunization.

- Naïve libraries are derived from nonimmunized B cells and constructed from a pool of IgM genes<sup>43,44</sup>. A single library can be utilized for any antigen. The selected antibodies demonstrate various specificities. Naïve libraries are not biased towards any antigen. Such libraries are particularly useful for the production of antibody fragments difficult to generate with hybridoma technology, particularly against nonimmunogenic or toxic antigens. The affinities of scFv isolated from naïve libraries are typically lower compared to those isolated from immune libraries<sup>14,43-45</sup>.



3. Synthetic libraries are also derived from nonimmune sources, assembled synthetically by combining the gene sequences from germ lines with randomized complementary determining regions (CDRs) responsible for antigen binding<sup>14,46</sup>. The majority of synthetic human antibody libraries rely on randomizing CDR3, the region which shows the largest diversity and which is directly responsible for antigen binding. These libraries provide high-affinity monoclonal antibodies and are therefore extensively used today. A large number of semisynthetic libraries are also available; one of the largest is the Griffin-1 library with a total diversity of  $1.2 \times 10^9$  scFv fragments (H Griffin, MRC, Cambridge, UK).

1.3.4.

## Ribosomal display technology

Besides phage display, there are also libraries using ribosomal display technology for antibody selection. They use an *in vitro* method of isolating scFvs directly without involving phages and bacteria (Figure 1.3, D). The DNA library of scFv is transcribed and translated *in vitro* to create complexes of linked mRNA-ribosome-scFv proteins. Such complexes are used for selection on immobilized antigen. The mRNAs specifically recognizing the antigen are eluted, reversely transcribed and finally employed for the next round of selection<sup>47,48</sup>.

1.3.5.

## Affinity maturation of scFvs selected from phage display libraries

Phage display technology favors the selection of phages from a significant number of clones that can bind to the target of interest with high affinity. This is achieved by multiple rounds of exposing phages to the antigen, washing steps to remove the unbound phage and elution of specifically bound phages. The eluted phages are amplified *E. coli* and used in the next round of selection. After the third round, infected *E. coli* is diluted and plated to yield single colonies. Single colonies are randomly selected, and the phage is tested for antigen binding. The best binders are identified, expressed in large quantities and characterized.

1.3.6.

## Antigen exposure for the scFvs selection process

To properly present the desired epitope, there are various ways to expose the antigen to phage particles<sup>49</sup>. In the majority of protocols, the antigen is immobilized on a solid surface, such as an immunotube<sup>46</sup>, a microtiter plate well<sup>14</sup>, a BIAcore sensor chip<sup>50</sup>, or a column<sup>14</sup>. Alternatively, the antigen can be biotinylated in solution, where

the antigen-phage complex is captured on a streptavidin surface<sup>14</sup>.

Unique advantages of phage display technologies come to light when the antigen is not available or is unknown, when antibodies are selected against whole cells, tissue fragments or heterogeneous antigen mixture<sup>51-53</sup>.

1.3.7.

## Advantages of scFv antibodies over full-size monoclonal antibodies

There are several benefits of phage-displayed scFv over full-size monoclonal antibodies including inexpensive production in *E. coli*, easy gene manipulation<sup>54</sup>, and the lack of the requirement of immune response stimulation. The smaller scFv fragments penetrate more rapidly and evenly into target tissues, e.g. tumors, in comparison to whole antibodies and display lower retention times in nontarget tissue<sup>55-57</sup>. As scFvs are cleared from circulation more rapidly, exposure of the healthy tissue<sup>58-60</sup> is shorter, which makes such antibody fragments preferable for imaging and drug delivery, using radionuclides and drug coupled scFvs. Additionally, the steps of the scFvs selection and production protocol can be standardized and automated. Therefore such a strategy is used in high throughput approaches<sup>61</sup>.

1.4.

## Application of scFvs

Due to their favorable properties, scFvs are used in medicine, laboratory diagnosis, and research. Furthermore, new ways of utilizing scFvs have appeared in noninvasive tumor labeling and detection. scFvs proved especially applicable in *in vivo* imaging, allowing real-time detection.

1.4.1.

### Medical application

1.4.1.1.

#### ScFvs in tumor therapy

The exciting idea that monoclonal antibodies can specifically recognize extracellular markers expressed on tumor cells has been present for a while<sup>62,63</sup>. Its limitation in solid tumor application was quickly revealed, due to IgGs' poor tissue penetration<sup>62</sup>. ScFvs were offered as an alternative with an improved tissue penetration. Tumor therapy using scFvs requires specific markers on tumor cells and is either aimed

at neutralizing the targeted protein or at efficiently delivering further therapeutic agents, such as toxins, drugs or siRNAs.

## ScFvs in tumor therapy

One of the first applications of scFvs was the neutralization of targeted protein (receptors) on tumor cells or accompanying tissue (endothelium, extracellular matrix). One successful example of a targeted neutralizing antibody is a humanized scFv-Fc (scFvFc or “minibody”) fusion protein derived from an anti-CCR4 monoclonal antibody (mAb) h1567. The CC chemokine receptor 4 (CCR4) ligands are highly expressed in several cancers, such as breast cancer, ovarian cancer and cutaneous T-cell lymphoma<sup>64-66</sup>, and represent well-characterized targets for tumor-therapy<sup>64</sup>.

## ScFvs as recombinant immunotoxins

ScFvs in the form of recombinant immunotoxins (RIT) serve to carry cytotoxic drugs to kill cancer cells<sup>67,68</sup>. RITs are hybrid proteins consisting of an scFv binding an antigen on cancer cells and *Pseudomonas* exotoxin A<sup>69</sup>. Either alone or in combination with chemotherapy, a number of such RITs are undergoing clinical trials for different types of cancer malignancies<sup>68,69</sup>. Many antibody fragments were tested in clinical trials as toxin carriers (Table 1.1).

## ScFvs as cancer vaccine

Antibody fragments also play a considerable role in cancer gene therapy. ScFvs serve as platforms delivering therapeutic agents. Two examples of such treatments are retroviral vectors that display anti-CEA-scFv against carcinoembryonic antigen (CEA) and deliver the therapeutic gene of nitric oxide synthase. As a result, this recombinant retrovirus can bind, infect and kill the CEA-expressing cancer cells<sup>70</sup>. Li et al.<sup>71</sup> targeted Epidermal Growth Factor Receptor 2 (HER2) in breast cancer, which is overexpressed in 20% of invasive breast cancer cases<sup>72,73</sup>. A vaccine with anti-HER2 specificity delivers therapy genes into breast cancer cells by integrating HER2-specific scFv as a DNA condensing fusion protein. Many antibody fragments were tested in clinical trials as cancer vaccines carrying therapeutic genes (Table 1.1).

## ScFvs as anticancer intrabodies

Apart from immunotoxins and therapeutic gene delivery, scFvs can also be used as anticancer intrabodies. Numerous studies have reported that such antibodies, when they reach cells, specifically bind and neutralize a vast range of oncogene products or signaling molecules. Such treatments can inhibit tumor growth or trigger apoptosis in tumor cells. Such an anti-HER2 intrabody was tested in phase I clinical trials. The treatment involved adenoviral-mediated gene therapy using an intrabody in the treatment of HER2-overexpressing ovarian cancer<sup>74</sup>. Another study

by Strube and Chen<sup>75</sup> confirmed that anticyclin E (expressed in the nucleus of the breast cancer cell) scFv intrabody inhibits the growth of the targeted cells.

Name	NP type	Target	Ligand	Bioactive compound	Indication	Phase
SGT-53	Lipid	Transferrin receptor	Anti-transferrin receptor ScFv	p53 DNA	Solid tumors	Ib
SGT-94	Lipid	Transferrin receptor	Anti-transferrin receptor ScFv	RB94 DNA	Solid tumors	I
C225-ILS-Dox	Lipid	EGFR	Cetuximab Fab	Doxorubicin	Solid tumors	I
Erbix-EDVspac	Bacterially derived mini-cell	EGFR	Bispecific monoclonal antibody (mAb)	Paclitaxel	Solid tumors	II
MM-302	Lipid	HER2	Anti-HER ScFv	Doxorubicin	Breast cancer	I
Lipovaxin-MM	Lipid	Dendritic cell CD209	dab	Melanoma antigens + IFN $\gamma$	Melanoma vaccine	I
MCC-465	Lipid	Uncharacterised (GAH)	Anti-GAH F(ab') <sub>2</sub>	Doxorubicin	Metastatic stomach cancer	I
Anti-EGFR ILS-Dox	Lipid	EGFR	Cetuximab Fab	Doxorubicin	Solid tumors	I

Table 1.1. A list of nanoparticle–antibody conjugates undergoing clinical trials adapted from Roy van der Meel 2013<sup>76</sup>.

#### 1.4.1.2.

### Application of scFvs in neurodegenerative diseases

Neurodegenerative diseases are a heterogeneous group of chronic disorders typically characterized by the progressive degeneration of the structure and function of the central nervous system or the peripheral nervous system. The ability of scFvs to cross the blood-brain barrier, to be overexpressed long-term *in vivo*, as well as their invisibility to the immune system, open the way for attractive new strategies for the treatment of neurodegenerative diseases.

#### Alzheimer's disease (AD)

The accumulation of amyloid- $\beta$ -peptide (A $\beta$ ) in the brain is the hallmark of the pathogenesis of Alzheimer's disease (AD)<sup>77,78</sup>. Over the last decade, antibodies have been introduced to target and reduce high levels of A $\beta$  in the brain and neutralize its toxic effects<sup>79</sup>. Conventional immunotherapies employing full-length IgGs demonstrated promising potential of immunotherapy, but also caused a vast range of undesirable side effects such as meningoencephalitis, vasogenic edema or cerebral microhemorrhages in the mouse model and in humans<sup>80</sup>. Therefore, smaller antibody fragments that circumvent the immune response were explored in search of a safer and more efficient therapy<sup>79</sup>.

Ryan et al.<sup>81</sup> observed that the expression of a human scFv directed against the N-terminal region of A $\beta$  in the triple transgenic AD mouse model (3 $\times$  Tg mice, carrying PS1M146V, APPSw, and tauP301L mutations) resulted in the reduction of amyloid plaques. The amount of hyperphosphorylated tau, correlated with an improvement of cognitive functions, was assessed in the Morris Water Maze test. A rAAV encoding a scFv directed against the N-terminal epitope of A $\beta$ , administered via an intramuscular injection, reduced amyloid deposition and cognitive impairment in the APPsw/PS1dE9 double transgenic mice<sup>82,83</sup>. Frenkel et al.<sup>84</sup> delivered a scFv expressed on a phage, which bound amyloid plaques in the hippocampus of Tg APP mice. More recently, Cattepoel et al.<sup>85</sup> showed that a preventive intranasal administration of a humanized scFv directed against the C-terminal region of A $\beta$  could reduce the number of amyloid plaques in the cortex of Alzheimer model mice.

#### 1.4.1.3.

### ScFvs against HIV infection

ScFvs as vehicles for delivery of different drugs, siRNA and toxins are emerging as promising therapeutics for several diseases<sup>86,87</sup>. In HIV-infected mice, CD7 specific scFv was coupled with anti-viral siRNA suppressing HIV-1 infection. ScFv as an immune-nanoparticle (CD7 antibody conjugated with PLGA/HDAC inhibitor) targets and delivers the therapeutic drugs (histone deacetylase inhibitor (HDACi)) to CD4+ T-cells hiding latent HIV particles<sup>88</sup>.

#### 1.4.2.

## *In vivo* imaging

The small size of scFvs enables conjugation with radionuclides, quantum dots, nanoparticles, and fluorophores. They can provide a non-invasive tool to visualize the location and distribution of a particular target *in vivo*. Critical properties are pharmacokinetics, tissue penetration and blood clearance without compromising binding affinity. The scFv format combines all of the above criteria and thus represents an ideal imaging tool. Interestingly, despite posing a challenge for therapeutic applications, the fast clearance of scFvs is a much-desired property in *in vivo* diagnostic applications. Radionuclide-conjugated scFv fragments against tenascin-c were used for visualization of heart disease in a rat model<sup>89</sup>. Radiolabeled scFv specifically binding tenascin-c showed a higher uptake of radioactivity in infarcted myocardium compared to the non-infarcted muscle. Fluorescent complexes of quantum dots and anti-EGFR or anti-HER2/neu scFv antibodies enabled visualization of cancer cells<sup>56</sup>. Moreover, Quantum dot-anti-GRP78 scFv (Qdot-GRP78) not only visualized the tumor but also demonstrated biological anti-tumor activity by inhibiting breast cancer growth in a xenograft model<sup>90</sup>. scFvs specific for histone H3 lysine 9 acetylation (H3K9ac), fused with green fluorescent protein (minibodies), tracked post-translational histone modification *in vivo* in fruit fly and zebrafish<sup>91</sup>. Recently, a scFv-based technique (SunTag) was employed for long-term fluorescent imaging of single protein molecules in living cells by recruiting up to 24 copies of GFP. Additionally, SunTag can be used to create a potent synthetic transcription factor by recruiting multiple copies of a transcription activation domain fused to a scFv targeting nuclease-deficient CRISPR/Cas9 protein and thus activating endogenous gene expression<sup>92</sup>. ScFvs can be used to improve the sensitivity of magnetic resonance imaging (MRI). scFv specific for carcinoembryonic antigen (CEA) conjugated to superparamagnetic iron oxide nanoparticles (SPIONs) could be used to target and image cancer cells more efficiently than the standard MRI technique<sup>93</sup>.

#### 1.4.3.

## Diagnostic applications

Another important application of scFvs is in the field of immunodiagnosics, where antibody fragments are increasingly replacing “conventional” immunodiagnostic reagents<sup>94</sup>. Highly specific antibody fragments recognize a variety of antigens such as proteins, nucleic acids, carbohydrates, lipids, but also entire pathogens. ScFvs can be used in numerous immunoassays (immunoblotting, ELISA, immunohistochemical staining and lateral flow immunochromatographic assays)<sup>95</sup>. Antibodies are detected using secondary antibodies recognizing a specific tag fused to the C- or N-terminus of the scFv (myc, his, E-tag). ScFvs can be fused to fluorescence proteins (fluorobodies) and used for direct labeling in flow cytometry and immunofluorescence microscopy<sup>96</sup>. These fluorobodies do not fade after illumination compared to (FITC-) conjugated antibodies. A new technique called fluorophore-linked immunosorbent assay (FLISA) has been developed, in which a scFv is fused to a fluorescent protein

and antigen binding is detected by measuring the fluorescence, circumventing the need for secondary antibodies. Compared to ELISA, FLISA is a faster and simpler method<sup>97</sup>.

1.5.

## Discussion

After a decade of extensive engineering followed by preclinical and clinical studies, antibody fragments partially replaced full IgGs as therapeutic and diagnostic agents. Especially when it comes to targeting cancer cells, inflammatory tissue or autoimmune and viral diseases, smaller forms of antibodies have ousted full-size IgGs. Recent advances in scaffold design, repertoire construction and selection methods, have allowed for the production of specific, high-affinity mAb fragments against virtually any target. Owing to the fact that they are simpler to express and can be handled in a standard laboratory, truncated structural forms of antibodies play an increasingly important role in human health. The creative use of these proteins will continue to represent a growing field of protein science, basic and applied biological research, and therapeutic discovery. Currently, small fragment antibodies are used for the discovery of new cancer biomarkers and are increasingly exploited for the development of sensitive microarrays, diagnostic and nanosensor tools. Efforts were directed at defining critical parameters for scFv applicability, and their properties have been altered to provide improved expression, pharmacokinetics and *in vivo* efficacy. Lately, scFvs technology was used as a base for the design of scFv multimers, such as diabodies, triabodies, minibodies. Such scFvs derivatives have achieved impressive tumor-to-blood ratios and maintain the right balance between ideal size and blood clearance as limiting factors. The ability of scFvs to safely deliver toxic chemicals to their targets remains their preferable application in therapy. In the form of immunotoxins and nanoparticle-antibody conjugates, scFvs have so far shown great potential, and several promising candidates have entered clinical trials (Table 1.1). Notably, their primary job is to deliver these cargos selectively to diseased cells. The majority of these strategies employ antibody fragments as the targeting ligand and delivery platform.

# Aim of the thesis

More than 30 years ago, Judah Folkman proposed a revolutionary new idea for a novel cancer therapy<sup>98</sup>. He postulated that, to survive and grow, tumors required blood vessels, and that by cutting off blood supply, cancer could be starved into remission. The development and use of antiangiogenesis agents, particularly those targeting VEGF, have become an integral component of anticancer treatment for many tumor types. Since then, a vast spectrum of antiangiogenic inhibitors has been developed, and used, either as monotherapy or in combination with other cytotoxic and chemotherapy drugs, in clinical trials for the treatment of cancer. Despite early success, antiangiogenic therapy was followed by a number of controversies and failed to become a reliable option for cancer therapy.

The VEGF/VEGFR-2 axis remains an important and attractive target when targeting tumor growth and metastasis. There is a clear need for a new generation of VEGF/VEGFR-2 inhibitors. Previously, our group and others demonstrated the importance of homotypic interactions in the receptor ECD for VEGFR-2 activation. Allosteric regulatory sites in Domain (D) 4-7 of the VEGFR-2 ECD were identified as attractive targets for inhibitory molecules such as DARPins and antibodies<sup>99-104</sup>. The work presented in this thesis is focused on targeting the membrane-proximal Ig-homology domains 4-7 in the VEGFR-2. Based on our functional analysis of VEGFR-2 activation, we aimed at the generation of specific inhibitors binding to D4 and D7 of the ECD, which might block receptor activation. We generated four different types of inhibitors. First, we selected scFvs against human VEGFR-2 from the ETH-2 Gold library. The best VEGFR-2 inhibitors were fully biophysically characterized and extensively tested in *in vitro* angiogenesis assays. We then reformatted the obtained scFvs into larger fragments such as Fabs and IgGs. To identify mouse-specific VEGFR-2 binders we used the synthetic ETH-2 Gold library and the R3 EPFL library. In collaboration with Molecular Partners AG in Schlieren, our group developed and characterized DARPins interacting with the receptor ECD that we further tested for tumor targeting *in vivo*.



2

Development and *in vitro* application of novel VEGFR-2 inhibitory single chain fragment variable antibodies

2.1.

# Abstract

The role of Vascular endothelial growth factor receptor 2 (VEGFR-2) in tumor angiogenesis, growth and metastasis is well appreciated. Unfortunately, available biotherapeutics largely failed to show significant improvement in tumor therapy. Here we offer allosteric receptor inhibitors as novel inhibitory tools. Instead of competing with the ligand for receptor binding, our antibodies block receptor activity by preventing homotypic interaction of extracellular subdomains 4-7 (D4-7) of VEGFR-2, previously described to play a role in receptor activation<sup>104</sup>. To target the VEGFR-2 extracellular immunoglobulin homology domains D4-7, we isolated novel single chain recombinant antibodies, scFvs. ScFvs were obtained from either a synthetic human library<sup>105</sup> or an antigen-biased immune V-gene phage display library generated from murine lymphocytes<sup>106</sup>. The antibodies were tested for binding to recombinant VEGFR-2 extracellular domain protein as well as to live cells expressing the full-length receptor. The best binders were biophysically and biologically characterized, in particular their ability to compete with VEGF binding to VEGFR-2, and their inhibitory activity for ligand-mediated VEGFR-2 kinase activation. The antibodies did not block VEGF binding to D23, but significantly reduced receptor activity in ligand-stimulated VEGFR-2-expressing porcine aortic endothelial cells (PAE KDR). The best inhibitors were cloned into a larger format, Fab. Selected binders showed dramatic inhibition of VEGFR-2 phosphorylation at Y1175 in a dose-dependent manner and also inhibited downstream signaling. Phosphorylation of PLC $\gamma$  and AKT were inhibited, without an effect on total protein levels. In addition, scFvs targeting D4-7 of VEGFR-2 inhibited VEGF-induced Human Umbilical Vein Endothelial Cells (HUVEC) tube formation and migration. Moreover, the cellular mechanism of inhibition was investigated in receptor internalization studies. Upon binding of the scFvs, the receptor was rapidly cleared from the cell surface, and the internalization was shown to be ligand-independent. These findings brought attention to the possibility of using VEGFR-2 scFvs as immunotoxin or nanoparticle-antibody conjugates for endothelial cell targeting.

2.2.

# Introduction

The term angiogenesis comes from the Greek word *Angêion*, meaning vessel. Angiogenesis is the process of formation of blood vessels from existing vasculature<sup>107</sup>. It occurs throughout life in both health and disease, beginning in utero and continuing through old age. Embryonic blood vessels are formed from precursor cells (angioblasts) differentiated into endothelial cells that form a vascular network<sup>108</sup>. Metabolically active tissues are generally located a few hundred micrometers from

a blood capillary, formed by the process of angiogenesis. Capillaries are needed in all tissues for the exchange of nutrients and oxygen metabolites. Changes in metabolic activity of the tissues are accompanied by proportional changes in capillarity. Oxygen plays a critical role in this regulation. VEGFs and their receptors represent the key drivers of embryonic vascular development of both physiological and pathological neovascularization<sup>109</sup>, particularly during rapid tissue growth and metastasis of solid tumors. Tumor cells release VEGF, a mitogen and angiogenesis inducer predominantly found in endothelial cells. VEGF is often detected in tumors *in situ*. Early findings indicated that inhibiting the angiogenic factor produced by tumor cells might suppress tumor growth *in vivo*<sup>110</sup>.

The pioneer of the field of tumor angiogenesis is considered to be Juda Folkman, despite the fact that Folkman expanded earlier concepts previously introduced by other scientists. In 1939, Ide et al.<sup>111</sup> observed that tumor growth was accompanied by infiltration of newly formed blood vessels in a rabbit tumor model. Algire<sup>112</sup> and Chalkeley<sup>113</sup> demonstrated that tumors actively promoted new blood vessel formation in 1945. Finally, the term tumor angiogenesis was coined for the first time 1968 by Shubi<sup>114</sup>. Ide, Shubi, Greenblatt, Algire, Chalkeley, Warren<sup>111-115</sup> are considered to be the founding fathers of the field of tumor angiogenesis, together with Juda Folkman<sup>98,116,117</sup>

The idea of antiangiogenic therapy was pioneered by Judah Folkman in the early 1970s. He proposed that by cutting off the blood supply, cancer cells would be deprived of nutrients and, consequently, die. Validation of his hypothesis followed when bevacizumab, a monoclonal antibody targeting VEGF, was approved as antiangiogenic therapy in 2004 for the treatment of colon cancer<sup>100</sup>.

Since then, various strategies that target VEGFR signaling have been developed. No satisfactory therapy is available at this time, however. Inhibition of VEGF signaling by ligand sequestering agents (bevacizumab)<sup>100</sup> or antibodies that block VEGF-VEGFR-2 interaction is overcome by high ligand concentration in the tumor, whereas the available tyrosine kinase inhibitors are not exclusively specific for VEGFR-2. Here we offer a new approach, novel allosteric inhibitors that inhibit VEGFR-2 signaling independent of VEGF concentration and relying on a new mechanism of inhibition. VEGFR-2 is the most prominent receptor in angiogenic signaling by VEGF ligands. The extracellular part (ECD) of VEGF receptors consists of seven immunoglobulin homology domains (Ig-domains). The analysis of the role of specific subdomains of the VEGFR-2 ECD in receptor activation showed that domains 2 and 3 are required for ligand binding<sup>118,119</sup>, while D4, D5, and D7 are required for stabilizing receptor dimers and properly positioning receptor monomers in active dimers<sup>102,103</sup>. Finally, at the functional level we showed that homotypic contacts in D4 and D7 are indispensable for receptor activation<sup>104</sup>.

To target the VEGFR-2 extracellular Ig domains D4-7, we isolated novel scFvs from the ETH-2 Gold library (Figure 2.1). The antibodies were biophysically and biologically characterized. Inhibitory scFvs were reformatted to larger formats such as Fabs and IgGs. We determined the biological activity of these antibodies, in particular, their ability to compete with VEGF binding to VEGFR-2, and their inhibitory activity for ligand-mediated VEGFR-2 kinase activation. The antibodies did not block VEGF binding to D23, but did significantly reduce receptor activity and interrupted down-

stream signaling in a dose-dependent manner. In addition, the series of *in vitro* angiogenesis assays, such as endothelial cell tube formation and migration assays, document the therapeutic potential of these antibodies. Moreover, we investigated in detail the mechanism of inhibition of these antibodies via receptor internalization, trafficking, and signaling studies.

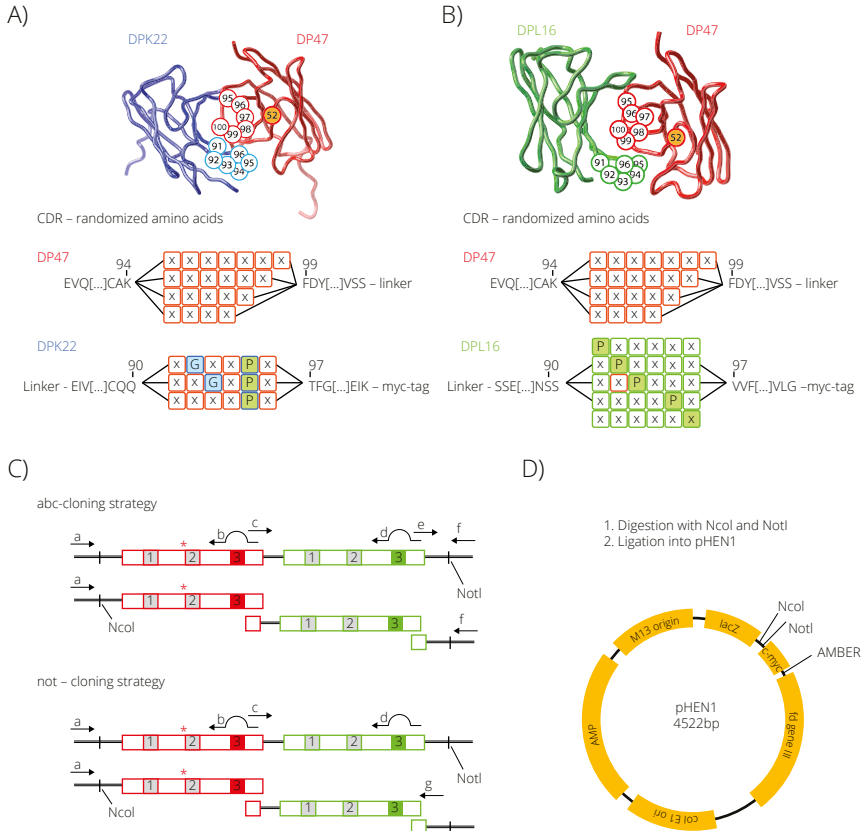


Figure 2.1. Design and cloning strategy of the Philo scFv antibody library. A, B) Three-dimensional structure of a scFv antibody fragment, with randomized amino acids, highlighted in circles. In the DP47 heavy chain fragment (in red), positions 95–100 were randomly mutated, with the length of the CDR varying from 4 to 7 amino acids. The antibody in A) shows the DPK22 light chain fragment (in blue). The antibody in B) contains a light chain based on the DPL16 germline segment. C) Cloning strategy for the construction of different sub-libraries. D) All DNA fragments were amplified, double digested and ligated into the pHEN1 phagemid vector. The figure was adapted from<sup>120</sup>.

2.3.

# Materials and methods

2.3.1.

## Cell culture

Porcine Aortic Endothelial Cells overexpressing VEGFR2 (PAE KDR) and Human Embryonic Kidney epithelial 293 cells (HEK293) were grown in Dulbecco's modified Eagle's medium (DMEM; BioConcept, Basel, Switzerland) supplemented with 10% fetal bovine serum (FBS) and 1% Penicillin-Streptomycin. Cells were propagated in a humidified atmosphere at 37°C and 5% CO<sub>2</sub>. Human umbilical vein endothelial cells (HUVEC), (Lonza) were cultured in EGM-2 medium (Lonza). Cells were grown in a humidified atmosphere at 37°C and 5% CO<sub>2</sub>.

2.3.2.

## Transient transfection

HEK293 cells were grown in standard, previously described conditions until reaching 60% cell confluency. Transfection with pBE plasmid bearing the full-length VEGFR-2 sequence was performed with FuGENE (Promega) in Optimem medium (Life Technologies). 2:3 ratio of DNA:FuGENE was shown to be the most efficient for transient cell transfection. Immunostaining was performed 24 hours after transfection.

2.3.3.

## VEGFR-2 kinase activity assay

PAE KDR cells were serum starved in DMEM supplemented with 1% bovine serum albumin (BSA) and stimulated with 1.5 nM VEGF for 10 min at 37°C with or without 30 min of preincubation with antibody fragments (0.1 to 1 μM). Cell lysates were prepared in lysis buffer (50 mM Tris [pH 7.5], 100 mM NaCl, 0.5% [wt/vol] Triton X-100) supplemented with protease inhibitor cocktail (Complete Mini EDTA-free, Roche) and phosphatase inhibitors (200 μM Na<sub>3</sub>VO<sub>4</sub>, 20 μM phenylarsine oxide). Lysates were diluted in 5x loading buffer (0.25 M Tris-HCl pH 6.8, 0.5 M DTT, 10% SDS, 50% Glycerol, 0.5% Bromophenol Blue), boiled at 50°C for 30 minutes and resolved by 7% SDS-PAGE, transferred to PVDF membranes (GE Healthcare), and immunodecorated with primary antibodies (dilution 1:1000) followed by secondary alkaline phosphatase-coupled antibodies (1:10000), and developed with Novex AP Chemiluminescent Substrate (Invitrogen). Immunoblot assays were analyzed with Amersham Imager 600, GE. Antibodies used were as follows: pY1175-VEGFR-2 (2478, Cell Signaling), tVEGFR-2 (2479, Cell Signaling; ab11939, Abcam), pPLCy1 (2821, Cell Signaling), tPLCy1 (2822, Cell Signaling), pAKT (4060, Cell Signaling), tAKT (4051, Cell Signaling), his-tag (34660, Qiagen), myc-tag (2276S, Cell Signaling), anti-rabbit IgG HRP-linked (7074S, Cell Sig-

naling), anti-mouse IgG HRP-linked (7076S, Cell Signaling); alkaline phosphatase (AP) conjugated antibodies were obtained from Jackson ImmunoResearch, fluorescently labeled Dylight 488, Cy3 and Cy5 were purchased from Abcam. Protein marker used for all SDS-PAGE and western blots gels was PageRuler™ Plus Prestained Protein Ladder, 10 to 250 kDa (26619, ThermoFisher).

2.3.4.

## Immunofluorescence microscopy

Cells were grown on glass coverslips coated with Poly-L-Lysine (P4707, Sigma) to 60% confluency. Antibody fragments and VEGF were added to cells in serum starvation conditions. Cells were fixed with 3.7% formaldehyde (FA) in phosphate-buffered saline (PBS) for 20 min at 37°C, permeabilized for 10 min with 0.1% NP-40 in PBS and blocked for 20 min in 5% BSA in PBS at room temperature (RT). Samples were exposed to primary (1:1000) and fluorescently labeled secondary (1:1000) antibodies in PBS containing 5% BSA and embedded in Gelvatol (15% Gelvatol, 33% glycerol, 0.1% sodium azide). Cells were extensively washed with PBS after each step. Images were acquired with an Olympus IX81 equipped with an Andor iXonEM camera and with Leica SP5 laser scanning confocal microscope.

2.3.5.

## ETH-2 Gold library

The ETH-2 Gold library was kindly provided by Prof. Dario Neri from ETH, Switzerland. ETH-2 Gold is a synthetic human antibody library in scFv format. The library has been cloned in phagemid vector, encoding for scFv-pIII fused proteins. The ETH-2 Gold library is based on a single  $V_H$  segment (DP47) and a single  $V_K$  (DPK22) or  $V_\lambda$  (DPL16) segment, respectively. These germline variants are dominant in the human functional repertoire and represent 12%, 25% and 16% respectively of the antibody repertoire in humans. In the ETH-2 Gold library, the flexible polypeptide Gly4Ser-Gly4SerGly4<sup>13</sup> was chosen as the linker. ETH-2 Gold scFv antibody fragments were cloned into the phagemid vector pHEN<sup>121</sup> bearing the short peptidic myc-tag at the C-terminus. The ETH-2 Gold library consists of  $3 \times 10^9$  different antibody clones, and it was shown to be highly functional<sup>105</sup>.

2.3.6.

## ScFvs selection

Anti-VEGFR-2 ECD ScFvs were selected from ETH-2 Gold.<sup>105</sup> Immunotubes (470319K, Nunc) were coated with antigen at a concentration of  $10^{-6}$  M in PBS overnight at room temperature. The following day, the antigen-coated immunotubes were washed three times with PBS and blocked with 5% BSA in PBS for 2 hours at room temperature on the orbital shaker. After the tubes were washed three times with PBS, the

phage library ( $10^{12}$ - $10^{13}$  t.u.) was added and incubated for 1.5 h at RT. To remove the unbound phage, the tubes were extensively washed with PBS containing 0.1% Tween 20 (TPBS) and PBS. Bound phages were eluted with 100 mM Triethylamine followed by neutralization with 1M Tris-HCl, pH 7.4. The eluted phage was used for the infection of exponentially growing *E. coli* TG1. Bacterial dilution series were then plated on small 2xTY-Amp-Glu agar plates and incubated at 30°C overnight to determine the titer of the eluted phage. The remaining phage-infected bacteria were centrifuged for 10 min at 4150 rpm at 4°C. Pelleted cells were resuspended in 0.5 ml 2xTY, spread on the large 2xTY-Amp-Glu agar plates and incubated at 30°C overnight. Eluted phages were used to infect exponentially growing *E. coli* TG1 cells and amplified for the next round of selection. After the third round, infected *E. coli* was diluted and plated to obtain single colonies. Single colonies were randomly selected, and the scFvs were tested for binding reactivity with recombinant VEGFR-2 by ELISA. Therefore, small-scale bacterial cultures were grown in 96-well plates for 4 h at 30°C. The expression of scFv antibody fragments was induced by 1 mM isopropyl  $\beta$ -D-thiogalactoside (IPTG), and the cells were grown overnight at 30°C. Following centrifugation, supernatants of bacterial cultures containing soluble scFvs were incubated for 1 h at RT in 96-well VEGFR-2-coated (10  $\mu$ g/ml in PBS) microtiter plates and blocked with 5% MPBS. Reactivity of scFvs was detected by anti myc-tag 9E10 antibody (diluted 1:4000) and horseradish-peroxidase (HRP)-conjugated goat anti-mouse IgG (diluted 1:1000). After extensive washing with TPBS and PBS, the color was developed using HRP substrate. Color development was stopped after 20 min with 1 M  $H_2SO_4$  and the absorbance at 450 nm was read using a microplate reader. The best binders were identified and used to infect the *E. coli* non-suppressor strain Mach1 for the production of soluble scFv antibodies. The first selection of scFvs against human VEGFR-2 was performed by Thomas Schleier.

2.3.7.

## ScFv A7

ScFv A7 used in this study, was obtained from an antigen-biased immune V-gene phage display library generated from murine lymphocytes<sup>106</sup>.

## Enzyme-linked immunosorbent assay (ELISA)

Binders' specificity was determined by enzyme-linked immunosorbent assay (ELISA) using immobilized recombinant VEGFR-2 ECD protein Domain (D) 1 to D7, D1 to D3, D1 to D6. Ninety-six-well maxisorp ELISA plates (Nunc) were coated overnight with 3 g/ml of the target protein. Plates were washed and blocked in PBS/1% BSA/0.1% Tween 20. Supernatants from cultured colonies were diluted in blocking solution and incubated for 2 h at RT. Plates were washed, and binding was detected using myc-tag antibody as primary and HRP-conjugated anti-mouse antibody as second-

ary antibodies, followed by peroxidase substrate (ThermoFisher). The reaction was quenched by adding 100  $\mu$ l of 2 M sulphuric acid ( $H_2SO_4$ ) to the wells and the  $OD_{450}$  value for each well was measured with an ELISA reader (TECAN Safire2).

2.3.9.

## Expression and purification of scFvs

Soluble scFv antibodies were expressed in *E. coli* Mach1 cultured in 2xYT medium. The media containing 100  $\mu$ g/ml ampicillin and 0.1% glucose was incubated at 37°C until bacteria reached an  $OD_{600}$  of 0.8. IPTG was added to a final concentration of 1 mM to induce expression of antibody fragments. Following a 10-hour incubation at 30°C, the bacteria were pelleted by centrifugation at 4000 g for 20 min. The culture supernatant was filtered through a 0.45  $\mu$ m filter (Millipore) and purified using immobilized metal affinity chromatography (IMAC). Soluble scFv antibodies were purified by protein A chromatography (GE) or with Ni-affinity chromatography (GE) for scFv A7. Buffers used for Protein A chromatography purification were: binding buffer: 20 mM Tris pH 8.0; washing buffer: 20 mM glycine pH 6.0 and elution buffer: 0.1 M glycine pH 2.5. Affinity chromatography purification was performed with the fully-automated liquid chromatography instrument Äkta (GE Healthcare). The flow rate was 2 ml/min. Before sample loading, the column was equilibrated with 25 ml of binding buffer. Bound scFvs were washed with 60 ml of binding buffer followed by a lower pH washing step with 60 ml of washing buffer. The scFvs were eluted with 40 ml elution buffer in 2 ml fraction wells containing 100  $\mu$ l 1 M Tris-base, pH 8.0. The absorption signal was detected at 280 nm. Fractions containing the protein were pooled together and dialyzed overnight against PBS. The next day, the scFvs solutions were concentrated and stored at -80°C.

Soluble scFv A7 was purified by Ni-affinity chromatography purification, with the following buffers: binding buffer: 50 mM sodium phosphate, 300 mM NaCl, 10 mM imidazole, pH 7.4 and elution buffer: 50 mM sodium phosphate, 300 mM NaCl, 500 mM imidazole, pH 7.4.

2.3.10.

## Size-exclusion chromatography (SEC)

SEC was performed with Superdex S-200 (Amersham Pharmacia Biotech, Switzerland) chromatography. The column was equilibrated with 5 column volumes of HEPES buffer. The flow rate was 2 ml/min and protein absorption was detected at 280 nm. 500  $\mu$ l of the samples were injected onto the column for each run. ScFv A7 was incubated for 1 h at 4°C with ECD VEGFR-2 at a molar ratio of 2:1.



2.3.11.

## Fluorescence size-exclusion chromatography (FSEC)

An Agilent 1200 series high-performance liquid chromatography (HPLC) system kept in a cold-room was used. The system was equipped with an auto-sampler. A Shodex semi-micro KW404-4F (4.6×300 mm) column on the Ettan LC system (GE Healthcare) was used for SEC analysis. Running buffer was PBS, pH 7.4 and the column temperature was maintained at 4°C. Samples were ultra-centrifuged at 40000 rpm. The settings were the following: FLD1: excitation/emission 435/470 nm, gain 12; FLD2: excitation/emission 515/535 nm, detector gain 10. Data was analyzed in OriginLab.

2.3.12.

## Binding affinity determination by ITC

Isothermal titration calorimetry (ITC) was performed at 15°C. The sample cell and syringe were filled with 15  $\mu\text{M}$  of scFvs proteins (monomer equivalents) and 400  $\mu\text{M}$  of ECD VEGFR2, respectively. Both the protein and the peptides were equilibrated in the same buffer (PBS), filtered and degassed before titration. The scFvs (400  $\mu\text{M}$ ) were loaded in the syringe and were titrated in 2.5  $\mu\text{l}$  injections against 14  $\mu\text{M}$  of the protein placed in the sample cell in a MicroCal iTC200 microcalorimeter (Microcal, Northampton, UK). Similarly, the control experiments were performed by titrating the proteins against buffer. The binding isotherms were fitted by a nonlinear least-squares minimization method using Origin v8.0 (Microcal Inc., Northampton, MA).

2.3.13.

## HUVEC tube formation assay

15-well  $\mu$ -Slides (Ibidi, Germany) were coated with 10  $\mu\text{l}$  of Geltrex® Matrix (ThermoFisher) 10 mg/ml and incubated at 37°C for 30 minutes to promote solidification. 6000 HUVECs were resuspended in growth medium (serum concentration 10%) and added to each well with 0.5 - 5  $\mu\text{M}$  inhibitor concentration. After 18 h, the plates were fixed with 3.7% formaldehyde (FA). Images were acquired with wide-field fluorescent microscope (Olympus IX81 equipped with Andor iXonEM camera). Images were analyzed using automated image analysis software (<http://ibidi.wimasis.com/>).

2.3.14.

## HUVEC migration assay

Migration assay was used to assess HUVEC migration (Ibidi, Germany). Cells were seeded at 21,000 cells per chamber and allowed to attach overnight. The following day, culture inserts were removed and cells were stimulated with 1.5 nM VEGF in the presence and the absence of increasing concentrations of scFvs. During the migration assay, cells were cultured under normal conditions, and images were acquired after 8 h. Images were acquired with a wide-field fluorescent microscope (Olympus IX81 equipped with Andor iXonEM camera) and analyzed using automated image analysis software (<http://ibidi.wimasis.com/>).

2.3.15.

## Squassh analysis of VEGFR-2 internalization

Image analysis was performed using the ImageJ plugin Squassh<sup>122</sup>. Squassh combines segmentation and deconvolution in a single step, yielding better results for small objects close to the diffraction limit of the microscope. Squassh was used to segment intracellular vesicles and cells. Squassh Analyst was used for data analysis and normalization of the vesicle count relative to cell area<sup>123</sup>.

2.3.16.

## Trypsin digestion of cell surface exposed receptor

Protection of VEGFR-2 from extracellular trypsin treatment was exploited in quantification of the internalized VEGFR-2. Following treatment in conditioned media, PAE KDR cells were washed three times with ice cold PBS and then incubated on ice with freshly prepared trypsin (1 mg/mL, Sigma) for 30 minutes. Reactions were then quenched by the addition of soy bean trypsin inhibitor (50 mg/mL, Sigma). Cells were collected very gently with soft scrapers into tubes for centrifugation at 500 rcf, 4°C for 5 minutes. The PBS was aspirated and the pellet suspended in a small volume of ice-cold PBS; the cells were then lysed by the addition of the sample buffer for gel electrophoresis. Lysates were boiled at 95°C and analyzed by Western blot.

2.3.17.

## Statistical analysis

For statistical analysis of experimental data, multiple comparisons were investigated for significant differences by 1-and 2-way ANOVA. Individual comparisons were subsequently performed by using the Bonferroni post-test or unpaired Student's t-test, as

appropriate. Unless otherwise stated, experiments were performed in triplicate. Data is expressed as mean  $\pm$  SD, where n is the number of individual experiments; p values  $\leq 0.05$  were considered statistically significant in two-sided tests. Unless otherwise stated, all numerical and graphical analyses were performed in Microsoft Office Excel 2010 (Microsoft, USA) and GraphPad Prism version 7.0 (GraphPad Software, USA).

2.4.

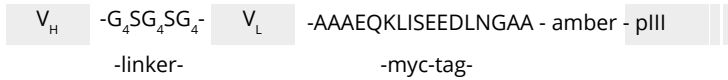
## Results

2.4.1.

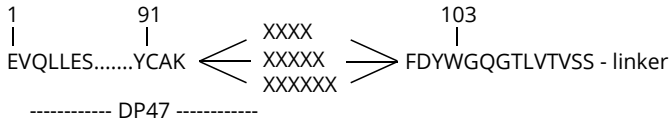
### Selection, production, and purification of scFvs antibodies

ScFvs specific for human VEGFR-2 were generated with the ETH-2 Gold phage library<sup>105</sup> (Figure 2.2, A, B). After three rounds of selection, positive clones were chosen at random for further analysis. Selected clones were tested for specificity for VEGFR-2 by ELISA. Binders with the highest ELISA signal were sequenced and scFvs with unique sequences were selected for further analysis (Figure 2.2, C). The large-scale expression of scFvs was performed in Mach-1 *E. coli* and soluble scFv antibodies were purified from the filtered culture supernatant with Ni-affinity chromatography and protein A chromatography. ScFv antibodies were expressed in *E. coli* Mach1. The bacteria were cultured in 2xYT medium containing 100  $\mu\text{g/ml}$  ampicillin and 0.1% glucose at 37°C until they reached an  $\text{OD}_{600}$  of 0.8 IPTG was added to a final concentration of 1 mM to induce expression of scFv antibodies. Following 10 hours incubation at 30°C, the bacteria were pelleted by centrifugation at 4000 g for 20 min. Soluble scFv antibodies were purified from the filtered culture supernatant by Ni-affinity chromatography (GE) (Figure 2.3, A) and protein A chromatography (GE) (Figure 2.3, C). The eluted peak fractions were loaded on 12% polyacrylamide gel and analyzed by Coomassie blue staining (Figure 2.3, B, D). The obtained yield of scFvs was in the range of 1 – 4 mg from 1 l of bacterial culture.

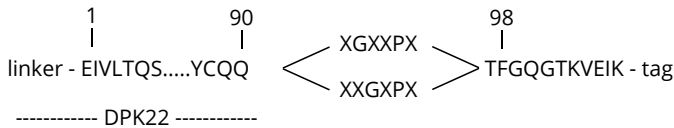
A) scFv sequence



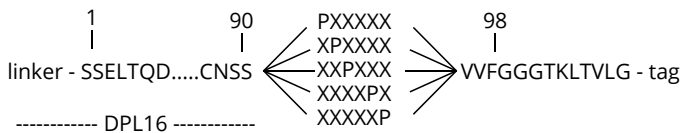
V<sub>H</sub> (based on DP47):



V<sub>K</sub> (based on DPK22):



V<sub>Y</sub> (based on DPL16):



B)

V<sub>H</sub>  
 AEV QLLES G G G L V Q P G G S L R L S C A A S G F T F S S Y A M S W V R Q A P G K G  
 L E W V S A I S G S G G S T Y Y A D S V K G R F T I S R D N S K N T L Y L Q M N S L R A E D  
 T A V Y Y C A **K K K K K** F D Y W G Q G T L V T V S S

V<sub>L</sub>  
 S S E L T Q D P A V S V A L G Q T V R I T C Q G D S L R S Y A S W Y Q Q K P G Q A P V L V  
 I Y G K N N R P S G I P D R F S G S S S G N T A S L T I T G A Q A E D E A D Y Y C N S S **K K K**  
**K K K** V V F G G G T K L T V L G

C)

scFv	V <sub>H</sub>	V <sub>L</sub>	library	Tag	Domain specificity
G3	P G F S A	D P R G A H	DP47DPL16	myc	D6
F1	P G A S A	A P G G A Y	DP47DPL16	myc	D7
H5	S P P A A	S L S V I P P	DP47DPL16	myc	D7
C11	Q S H R G T	R P R R H R	DP47DPL16	myc	D7
A7	GLWGGMDY	QQWNTYPYT	mouse synthetic V -Gene	his	D2-3

Figure 2.2. The amino acid sequences of the scFvs. A) Schematic of scFvs amino acid sequences from ETH-2 Gold library used for selection<sup>105</sup> B) Full amino acid sequences of scFvs selected against human VEGFR-2 where randomized CDR3 was represented with letters K in red C) Randomized CDR3 amino acid sequence of scFvs selected against human VEGFR-2.

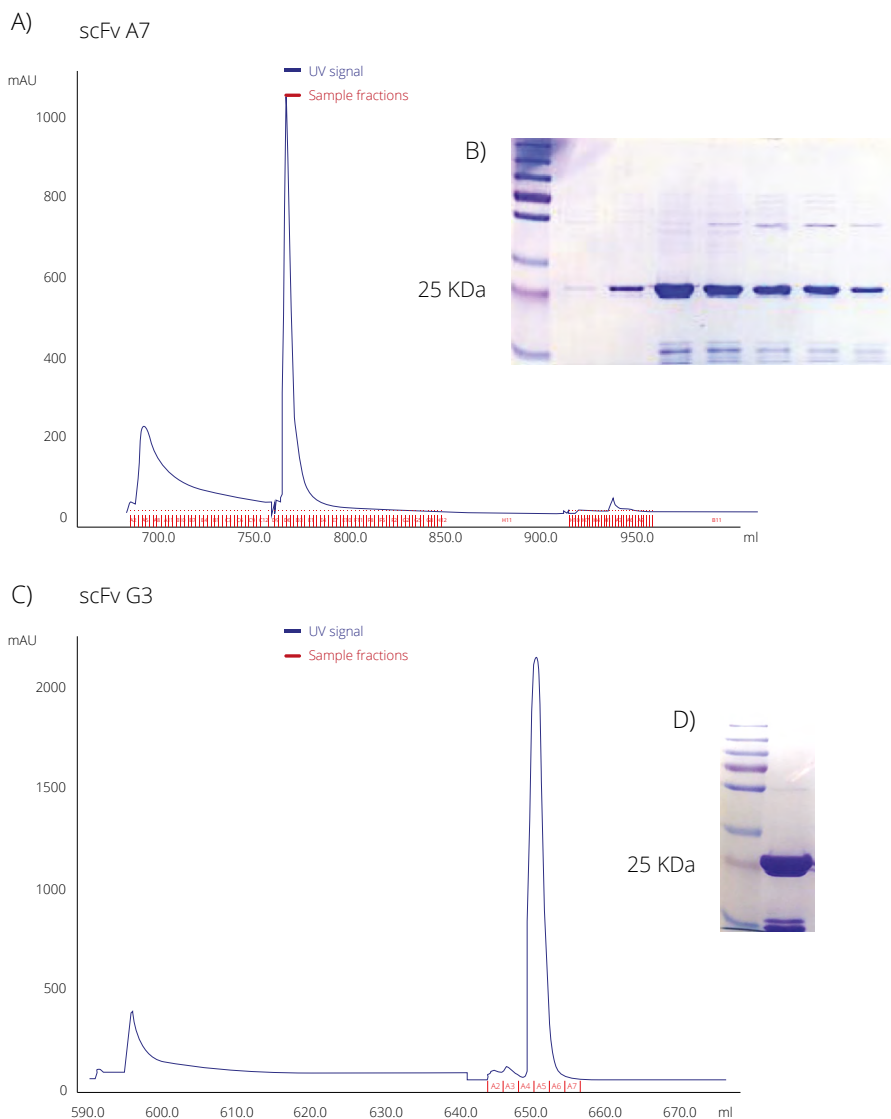
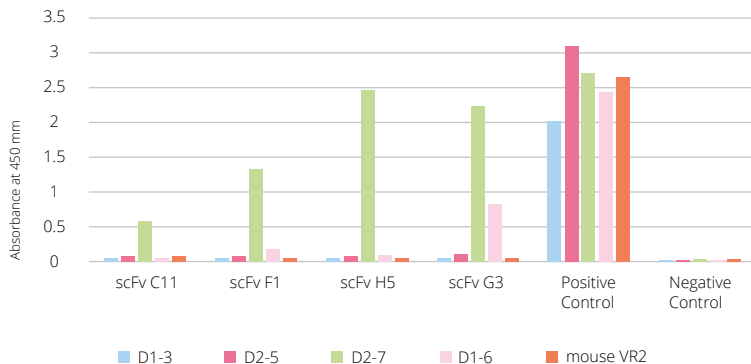


Figure 2.3. ScFvs purification by protein A and Ni-affinity chromatography. A) Elution profile of scFv A7 after purification by Ni-affinity chromatography. B) The eluted peak fractions loaded on 12% polyacrylamide gel and analyzed with a Coomassie blue staining. C) Elution profile of scFv G3 after purification by protein A. D) The eluted peak fraction loaded on 12% polyacrylamide gel and analyzed by Coomassie blue staining.

A) ELISA: scFvs domain specificity



B)

Binder	scFv A7	scFv G3	scFv F1	scFv H5	sFv C11
Domain specificity	D2-3	D6	D7	D7	D7

C)

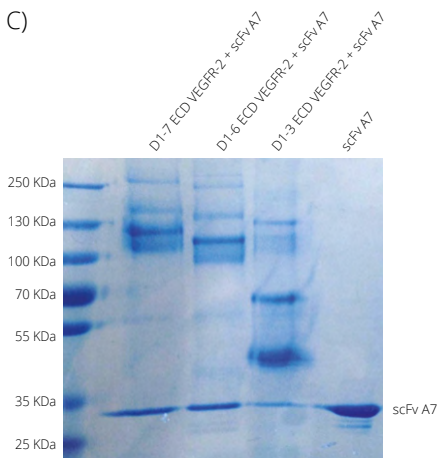


Figure 2.4. Determining domain specificity of selected scFvs by ELISA. A) ELISA results show VEGFR-2 domain specificity by measuring absorbance at 450 nm. ELISA was performed with different length VEGFR-2 ECDs. B) Overview of scFvs domain specificity. C) Determining domain specificity of scFv A7 by size-exclusion chromatography (SEC) of scFv A7 in complex with different length VEGFR-2 ECDs. Proteins from collected peak fractions were concentrated and resolved on 12% SDS-PAGE gel.

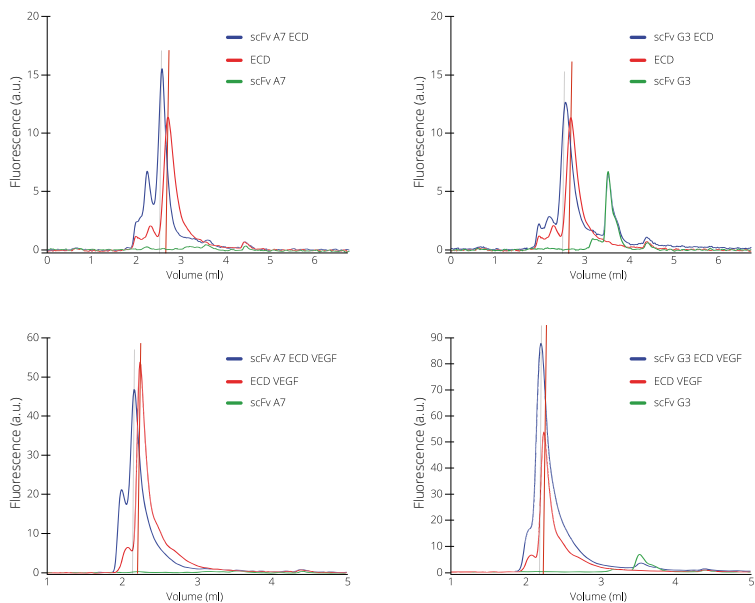


Figure 2.5. ScFvs binding to recombinant VEGFR-2 in FSEC. FSEC analysis shows scFvs binding to both VEGFR-2 ECD and VEGFR-2 ECD/VEGF complex. The shift in the peak to the left (from red to blue peak) demonstrates the formation of new larger species in the combination of VEGFR-2 ECD and scFvs (top panel) and VEGFR-2 ECD/VEGF and scFvs (bottom panel).

### 2.4.2.

## Binding of scFvs to recombinant and endogenous VEGFR-2.

Binder specificity was confirmed with ELISA on human VEGFR-2 (hVEGFR-2) and mouse VEGFR-2 (mVEGFR-2) (Figure 2.4, A, B). The positive signal was detected at the OD<sub>450</sub>. All presented antibodies were specific for hVEGFR-2, but were not binding mVEGFR-2. The binding specificity for scFv A7 was determined by SEC where scFv A7 was incubated with ECD VEGFR-2 at a 2:1 molar ratio for 1 h at 4°C and consequently loaded on a Superdex S-200 (Amersham Pharmacia Biotech, Switzerland). Collected peak fractions were concentrated and resolved on 12% SDS-PAGE gel (Figure 2.4, C). Purified scFv A7 was loaded in the last well to serve as a size control. ScFv A7 forms complexes in combination with full-length ECD (D1-7), D1-6 and D1-3, which means that it binds VEGFR-2 ECD D1-3. SDS-PAGE shows all protein species collected as a single peak, including a 30 kDa protein, which is the size of scFv A7. Larger protein species are D1-7, D1-6 and D-3 respectively. Multiple bands visible on the gel are degradation products.

FSEC (Figure 2.5) on hVEGFR-2 (top panels) and on hVEGFR-2 VEGF complex (bottom panels) show a shift of the peak to the left (from red to blue peak), meaning that a larger protein species was formed. This demonstrates that scFvs bind both VEGFR-2 ECD and VEGFR-2 ECD VEGF complex, confirming that scFvs and VEGF have different VEGFR-2 binding sites. Live cells binding was confirmed in HEK293 cells by immunostaining. First, VEGFR-2/Dylight 488 staining was used to confirm VEGFR-2 expression on the cell surface (green); subsequently, myc-tag/Cy3 (red) staining showed that scFvs bind the receptor on the surface of transiently transfected HEK293/VEGFR-2 cells (Figure 2.6). Affinities of the scFvs were determined by ITC (Figure 2.7, A). The calculated K<sub>d</sub> values are shown in the Table (Figure 2.7, B).

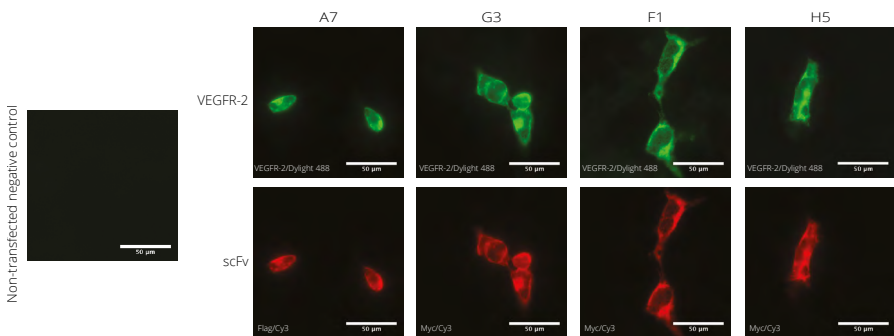


Figure 2.6. ScFvs binding to VEGFR-2 expressed on HEK293 cells. Green signal (top panel) represents VEGFR-2 immunostaining with Abcam antibody (11939). Red signal demonstrated scFvs binding to HEK cells transfected with VEGFR-2 (bottom panel). Non-transfected HEK293 control (left, middle panel) shows the background signal.



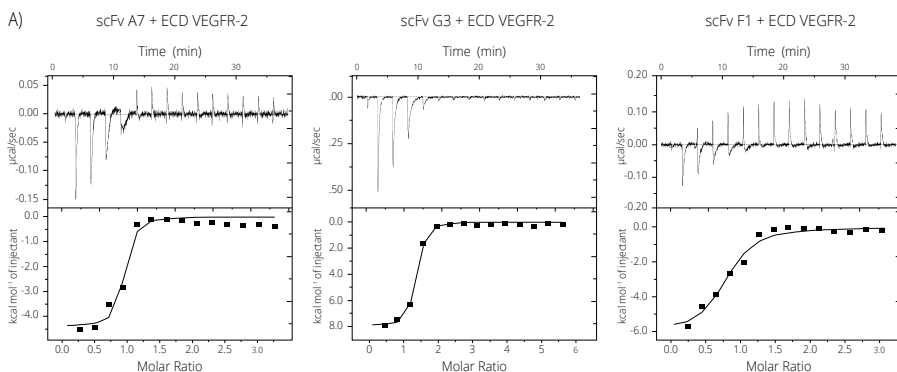


Figure 2.7. Thermodynamic analysis of antibody-VEGFR-2 interaction. A) ITC analysis of scFvs in complex with VEGFR-2 ECD. Raw data and binding isotherms are shown. B) Calculated thermodynamic parameters of interactions are summarized in the Table.

#### 2.4.3.

## Functional inhibition of VEGFR-2 phosphorylation with scFvs

Activation of VEGFR-2 is a key step in angiogenesis. We, therefore, investigated the potential of scFvs to inhibit this process by blocking VEGFR-2 signaling *in vitro*. We exposed PAE KDR cells to various concentrations of scFvs in the presence or absence of VEGF. Analysis revealed that increasing concentrations inhibited kinase phosphorylation at Y1175 in a dose-dependent manner. VEGFR-2 was phosphorylated by the addition of exogenous VEGF to PAE KDR cells (Figure 2.8). Pretreatment of cells with increasing concentrations of scFvs in the presence of VEGF showed inhibition of Y1175 phosphorylation in a dose-dependent manner, without affecting overall VEGFR-2 expression levels. In order to identify the effects of scFvs on downstream signaling, we examined the expression and phosphorylation of PLC $\gamma$ , AKT, and p38. While PLC $\gamma$  signaling was clearly inhibited, AKT signaling did not show statistically significant change. The challenges in quantifying phospho-AKT are the consequence of the small difference between basal and fully activated phospho-AKT levels. While treatment of PAE KDRs with antibodies inhibited VEGF-dependent phosphorylation of downstream signaling in a dose-dependent manner, total protein levels were unaffected (Figure 2.8, A). All kinase assays were performed in triplicates and quantified with Imagej software. Quantified data was analyzed with GraphPad (Figure 2.8, B).

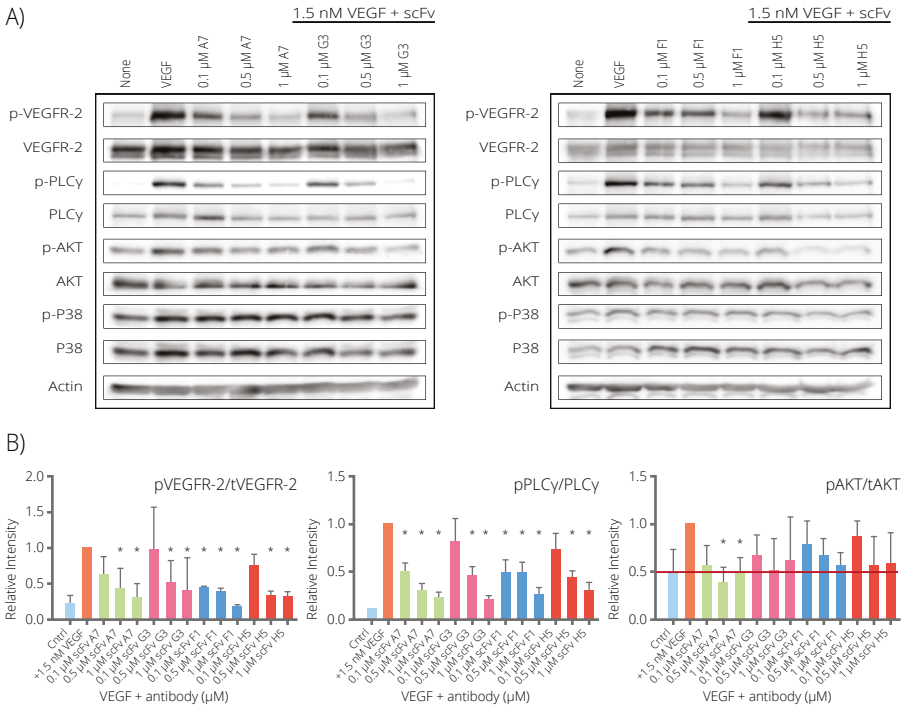


Figure 2.8. Effect of antibody treatment on VEGF-induced signaling in PAE KDR cells. A) scFvs inhibit phosphorylation of Y1175-VEGFR-2, PLCγ and AKT in a dose-dependent manner. B) The western blot data was analyzed and quantified with ImageJ. Quantification of western blot data shown as n-fold increase over the activity of ligand-induced receptor activity in the absence of scFv antibodies. Data distribution and statistical analysis were performed using GraphPad, Prism 7. It demonstrates a representative experiment of four independent experiments. Error bars represent  $\pm$  Standard Deviation (SD). The statistical significance based on a Student's t-test is indicated by \* representing  $P < 0.05$ .

#### 2.4.4.

## Effect of antibodies on HUVEC tube formation and migration.

We examined the role of our antibodies in the formation of capillary-like tubes formed by endothelial cells in Matrigel. HUVEC cells were embedded in Matrigel and treated for 8 h with VEGF in the presence or absence of increasing concentrations of scFvs. After the incubation period, the formation of tubes was examined by phase contrast microscopy. Results show that VEGF triggers the formation of a dense network of tubule-like structures when added to control HUVEC in Matrigel. This effect was markedly repressed in cells to which scFvs were added (Figure 2.9, A). Four independent experiments were performed for each concentration of scFvs and an-

alyzed with Wimasis online software (<http://ibidi.wimasis.com/>). Data was quantified with GraphPad (Figure 2.9, B).

The migration and invasion of endothelial cells are critical features in the formation of new blood vessels and in the repair of injured vessels. Therefore, we investigated the effects of scFvs on the movement of HUVECs from a wounded edge to an open area using wounding migration assays (Figure 2.10). Treatment with scFvs decreased the migration of HUVECs compared to that of control in a dose-dependent manner (Figure 2.10, B).

A)

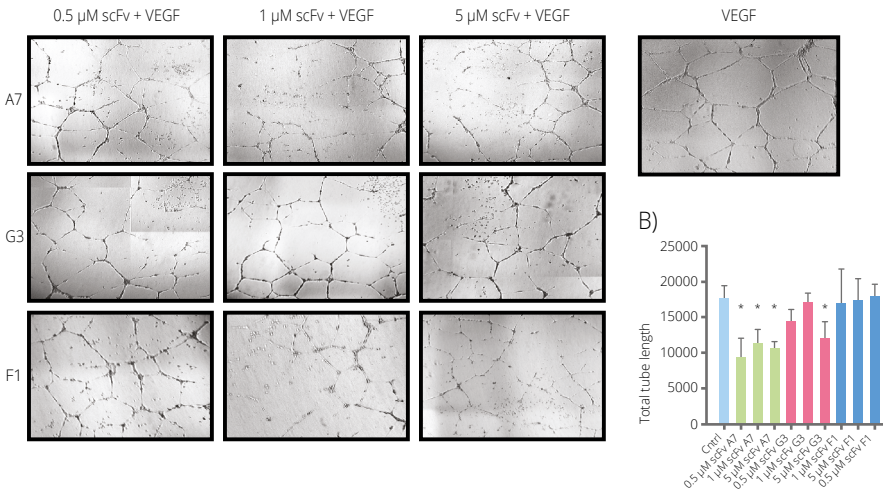


Figure 2.9. Effect of antibody treatment on VEGF-induced capillary-like tube formation in HUVECs. A) Light microscopy of capillary-like tubes formed in the presence and absence of increasing concentrations of antibodies. The total tube length was quantified with Wimasis online software (<http://ibidi.wimasis.com/>). B) Quantification of data shown as n-fold increase over the activity of ligand-induced tube formation in the absence of scFv antibodies. Data distribution and statistical analysis were performed using GraphPad, Prism 7. It shows the results of a representative experiment, out of four independent experiments. Error bars represent  $\pm$  SD. The statistical significance based on a Student's t-test is indicated by \* representing  $P < 0.05$ .

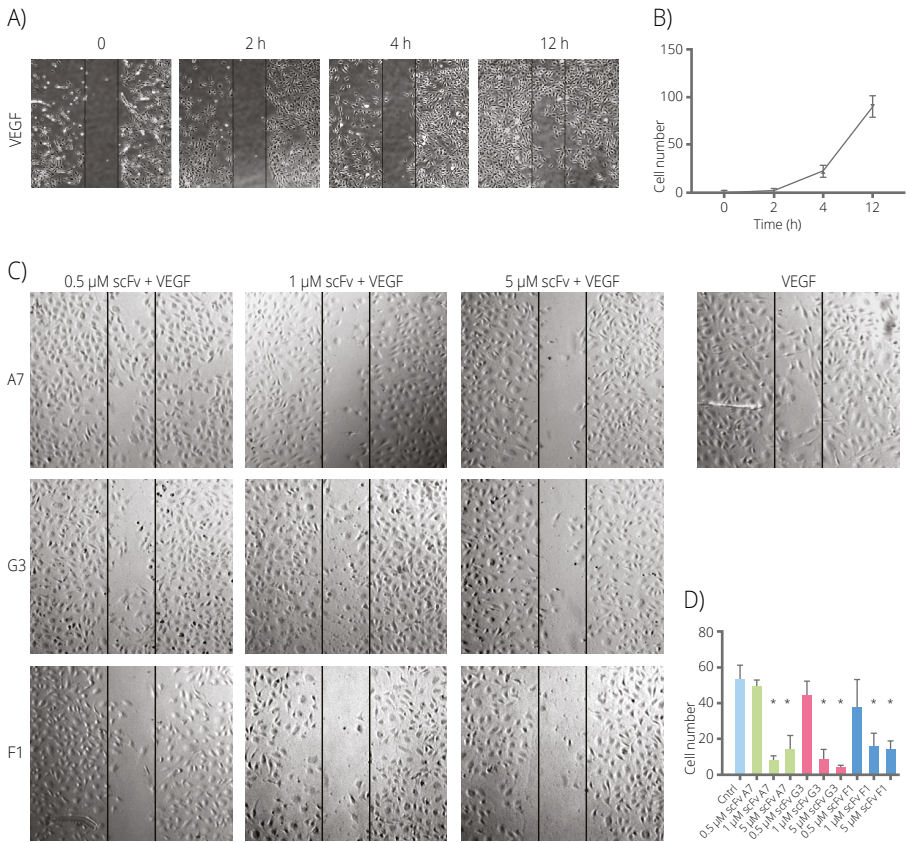


Figure 2.10. Effect of antibody treatment on VEGF-induced wound healing assay in HUVECs. A) Time course of VEGF-induced cell migration. B) Growth curve of HUVEC cells. C) Cells migrating in presence and absence of increasing concentrations of antibodies. D) Quantification of data shown as n-fold increase over the activity of cell migration in the absence of scFv antibodies. Data distribution and statistical analysis were performed using GraphPad, Prism 7. It shows a representative experiment out of three independent experiments. Error bars represent  $\pm$  SD. The statistical significance based on a Student's t-test is indicated by \* representing  $P < 0.05$ .

## VEGF and scFvs induce internalization of VEGFR-2

Two approaches were used to determine receptor internalization. Firstly, immunostained VEGFR-2 was used to follow the time-dependent increase of intracellular vesicles and vesicle volume upon VEGF or scFv addition (Figure 2.11, A). Individual incubation, not only with VEGF but also with scFv alone led to a dramatic increase of both critical parameters. When both scFv and VEGF were present at the same time, we could observe an additive effect on total vesicle volume after 10 minutes, which suggests that a similar mechanism of internalization is involved in both VEGF and scFv mediated internalization. To quantify the observed phenomenon, we used Squassh software and analyzed 25 images per condition (Figure 2.11, B).

To confirm that VEGFR-2 is indeed internalized upon scFvs binding, a simple method that distinguishes between internalized and cell surface proteins was used. Trypsin was used for proteolysis of membrane-bound extracellular proteins. Upon incubation with trypsin cell surface proteins are cleaved, including VEGFR-2, while the internalized proteins are protected from the extracellular trypsin and remain intact. The cell lysis was followed by Western blot analysis (Figure 2.11, C). Two time points were assessed. A basal level of internalization was detected in the absence of both scFvs and VEGF (blue arrow). However, the most pronounced band was the lower band (red arrow) representing the product of receptor degradation. Incubation with scFv C11, non-inhibitory control led to the same outcome. In the presence of VEGF, VEGFR-2 is quickly internalized and protected from trypsin degradation, therefore only the band that corresponds to the size of intact VEGFR-2 (blue arrow) can be observed. When incubating with inhibitory scFvs only, both the trypsin digestion product and a more pronounced intact VEGFR-2-sized band can be observed. Interestingly, 45 minutes incubation with scFv A7 yielded the same outcome as incubation with VEGF, demonstrating that scFv A7 leads to slower but complete VEGFR-2 internalization. Incubation with scFv G3 did not lead to a complete internalization after 45 minutes, which can be explained by the higher affinity of scFv A7 compared to scFv G3 (Figure 2.7, B). However, at the same time, this is in line with the better inhibitory effect of scFv A7 in kinase assay (Figure 2.8) and Tube formation assay (Figure 2.9). The trypsin degradation assay thus confirmed the immunostaining data, indicating that both VEGF and scFv led to receptor internalization.

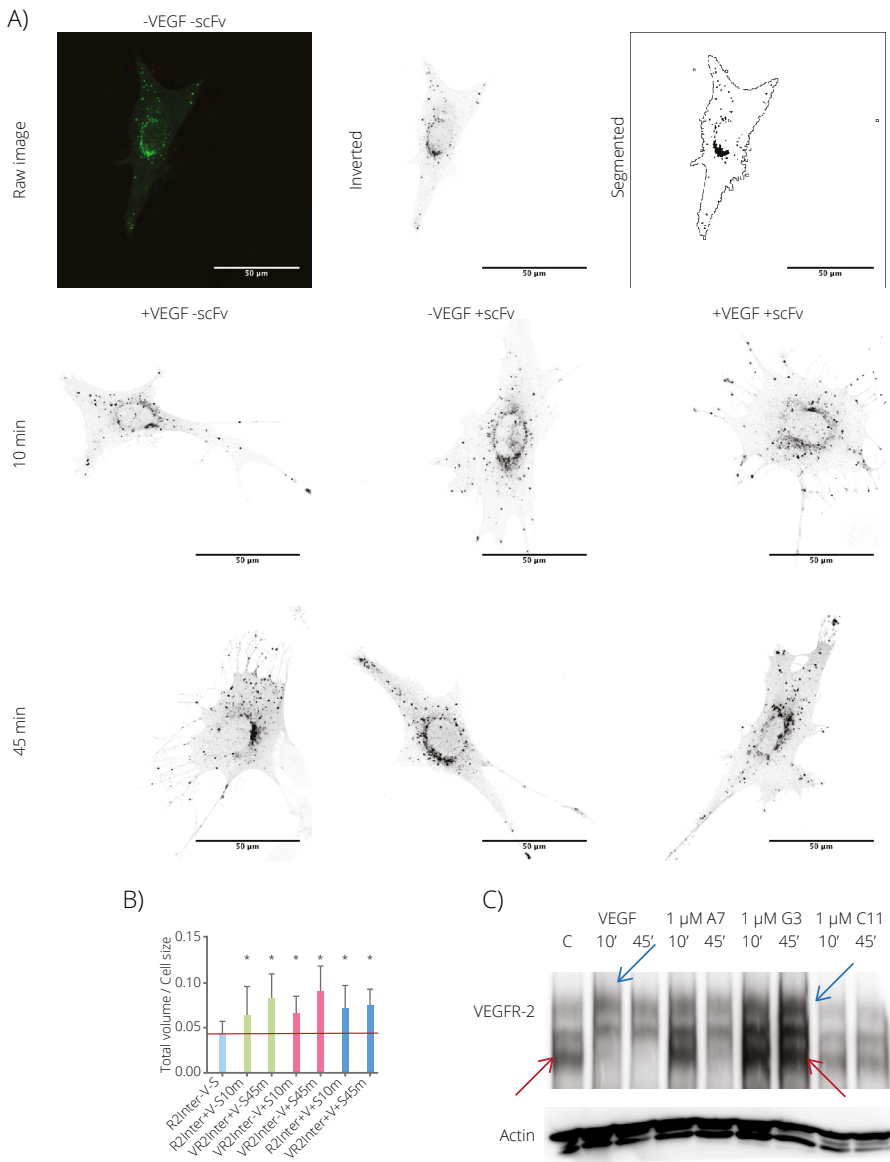


Figure 2.11. VEGFR-2 internalization study. A) Immunostaining of VEGFR-2 receptor with Abcam antibody (ab11939) shows the receptor dynamics upon scFv G3 or VEGF binding, or a combination of both. PAE KDR cells were fixed at different time points after addition of scFv G3, VEGF or scFv + VEGF. Vesicle number/volume was analyzed upon VEGF or/and scFv binding. B) Squash analysis of immunostaining data was performed<sup>122</sup>. Data distribution and statistical analysis were performed using GraphPad, Prism 7. It shows

a representative experiment out of 25 independent experiments. Error bars represent  $\pm$  SD. The statistical significance based on a Student's t-test is indicated by \* representing  $P < 0.05$ . C) Trypsin degradation profile of VEGFR-2 upon scFvs or/and VEGF binding.

2.5.

## Discussion

Several antiangiogenic inhibitors have been developed and used in clinical trials for the treatment of cancer, either as monotherapy or in combination with other cytotoxic and chemotherapy drugs. Despite an early success, antiangiogenic therapy was plagued by a number of controversies and failed to become a viable option for cancer therapy.

The VEGF/VEGFR-2 axis remains an important and attractive target when targeting tumor growth and metastasis. There is a clear need for a new generation of VEGF/VEGFR-2 inhibitors. Our group and other researchers have previously demonstrated the importance of homotypic interactions in the receptor ECD for VEGFR-2 activation. Allosteric regulatory sites in D4-7 of VEGFR-2 were identified as an attractive target for inhibitory molecules such as DARPin and antibodies<sup>99-104</sup>. VEGFR-2 specific antibody fragments were therefore produced as a potential therapeutic tool. Selected scFvs showed species-specificity by binding to both purified human receptor and HEK293 cells transiently expressing hVEGFR-2 on the surface. The affinity of scFvs differed significantly depending on scFv variant. The best binders demonstrated affinity in the nanomolar range. The  $K_d$  values of here presented inhibitors were in the range reported for several therapeutic antibodies<sup>124</sup>. Selected antibodies showed consistent inhibition of different aspects of VEGF-driven angiogenesis in a number of *in vitro* assays. ScFvs fully suppressed VEGF-induced VEGFR-2 phosphorylation and downstream signaling. Inhibitory potential of scFvs was further demonstrated in HUVEC tube formation and wound healing migration assays, where VEGF-dependent properties of HUVECs including the formation of capillary-like tubes, demonstrating vessel formation, as well as migration from a wounded edge to an open area, demonstrating wound healing, were inhibited. Most interestingly, internalization studies revealed a possible cellular mechanism of inhibition. Antibody fragments binding to VEGFR-2 led to receptor internalization as demonstrated by an increase in total volume of intracellular receptor-positive vesicles. Internalization independent of ligand binding represents a new promising property of these VEGFR-2 antibodies. Drebin et al.<sup>125</sup> and Hudziak<sup>126</sup> et al. have demonstrated that anti-HER2 MAbs reduce the amount of HER2 protein expressed on the cell surface. The mechanism by which anti-HER2 MAbs induce HER2 downregulation is unclear, although it is shared by other anti-growth factor receptor antibodies such as anti-EGFR<sup>127</sup> antibodies. The indication is that the antibodies synthesized in this study share some propriety with the well characterized anti-HER2 MAbs. It still remains to be determined why scFvs lead to VEGFR-2 internalization. Two possible explanations are offered herein. One possible reason may be antibody-induced receptor clustering; clustering of scFv-VEGFR-2 complexes could cause efficient internalization. Similar effects have been described for Pertuzumab-HER2<sup>128,129</sup>. The second ex-

planation could lay in allosteric properties of scFvs. By binding VEGFR-2, scFvs could be causing structural alteration of the receptor which cells recognize as improperly folded receptors that need to be internalized and recycled or degraded.

The ability of scFvs to selectively and safely deliver a cocktail of toxic chemicals to the target cell remains their preferable application in therapy. Due to the demonstrated receptor internalization propriety, these antibodies might be useful as immunotoxin or nanoparticle–antibody conjugates with the potential to deliver therapeutic cargos to diseased cells. Such a strategy would employ antibody fragments as the targeting ligands.

Here, antibody fragments have been described as an attractive alternative to inhibit the VEGF/VEGFR-2 activation. Currently available antiangiogenic strategies, ligand sequestering antibodies, small molecular weight tyrosine kinase inhibitors (TKIs), and VEGFR ligand blocking antibodies, are affected by high local VEGF concentrations. Compared to available therapeutics, the antibodies presented herein might even function at high ligand concentrations. It is believed that free ECDs regulate the local VEGF excess. By neutralizing the ligand, the fine balance between free and bound VEGF is disrupted and may consequently lead to aberrant signaling. In addition, VEGFR-2 forms dimers with VEGFR-1 and VEGFR-3<sup>130</sup>. The activity of VEGFR-1 as a kinase is low, but in heterodimeric form with VEGFR-2, VEGFR-1 participates in angiogenic signaling<sup>131,132</sup>. VEGFR-2/VEGFR-3 heterodimers are described to play a role in full VEGFR-3 activation<sup>133</sup>. We believe that a similar mode of action, requiring D4-7 interactions as described for VEGFR-2 homodimers is present in heterodimers. Although no heterodimer structure was yet solved, the hypothesis is that interactions in domains 4-7 are necessary to position all members of the VEGF receptor family in an active conformation in the ligand binding dimer. It would seem reasonable to assume that the antibodies presented herein, targeting these interactions in both homodimeric and heterodimeric receptor complexes could represent promising new tools for antiangiogenic therapy.


In summary, a series of novel antibody fragments with a new mode of action to target VEGFR-2 mediated signaling has been described and it has been shown that allosteric inhibition of VEGFR-2 is an effective mechanism for inhibiting VEGFR-mediated effects in several tissue culture models. The next step would be to apply these new tools in animal models such as matrigel implant assays in mice.

Also, it would be interesting to further examine scFvs-induced VEGFR-2 internalization. What is the exact mechanism of internalization? To which cellular compartment does receptor go upon internalization? What happens with scFvs when VEGFR-2 is internalized? What is the ultimate destiny of the internalized receptor? Is it recycled or degraded? All these questions remain to be answered.



3

# Reformatting scFv antibodies to Fragment Antigen Binding (Fab) antibody fragments

The background features a warm orange-to-yellow gradient. It is decorated with several faint, stylized antibody structures, which are Y-shaped molecules with two long arms and a shorter stem. These structures are scattered across the page, some appearing as simple outlines and others with more detail. Additionally, there are numerous small, light-colored Y-shaped symbols, similar to the antibody structures, scattered throughout the background, creating a thematic pattern related to immunology.

3.1.

# Introduction

Recombinant antibodies, including antibody fragments, have become a fundamental tool in medical research and therapy<sup>134-139</sup>. In the previous chapter, we discussed scFv antibodies in detail, with the focus on advantageous properties such as smaller molecular sizes, easy production, higher penetrability and elimination of the Fc region when compared to the full-length IgGs. Therefore, smaller particles penetrate tumors more rapidly and uniformly than larger particles<sup>140</sup>, and smaller particles carrying drugs are more effective against tumors than larger particles<sup>141</sup>. On the other hand, smaller particles are eliminated more quickly from the blood<sup>142</sup>. The choice of nanomedicine drug size for a cancer type involves finding a balance between maximizing tumor penetration and minimizing both toxicity to normal tissue and blood clearance. Both scFv and Fab formats share the above-mentioned advantages. However, the Fab format appears to be more stable<sup>143</sup> and to have considerably slower blood clearance when compared to the scFv format<sup>142</sup>. In some reports reformatting scFv to Fab lead not only to improved stability but to improved neutralization activity as well<sup>144</sup>. Preserving the properties of the small antibody fragments and at the same time, improving blood clearance, Fab format proved to be the preferential tool for tumor and tissue imaging<sup>145</sup>. In order to obtain a Fab and to compare its properties with scFv format, we used the best VEGFR-2 inhibitory scFvs previously selected and characterized (Chapter 2).

3.2.

# Materials and methods

3.2.1.

## Cloning strategy for reformatting scFvs to Fabs

To transfer the heavy chain variable domain ( $V_H$ ) and light chain variable domain ( $V_L$ ) from pHEN to pEA and pMX9 vectors already bearing heavy chain constant domain  $C_H$  and light chain constant domain ( $C_L$ ) respectively,  $V_H$  and  $V_L$  were PCR amplified by using the following primers:

SMM17 scH9\_ $V_H$ -SapF 5'-atatatGCTCTTctAGTgaggtgcagctggtggagtctg-3';

SMM18scH9\_ $V_H$ -SapR 5'-tatataGCTCTTcaTGCTCTCGACACGGTGACCAGG-GTT-3' for  $V_H$  and

SMM15 scH9\_ $V_L$ -SapF 5'-atatatGCTCTTctAGTtctgagctgactcaggaccctg-3';

SMM16 scH9\_ $V_L$ -SapR 5'-tatataGCTCTTcaTGC GCCTAGGACGGTCAGCTTG-GTC-3' for  $V_L$  PCR amplification.

Amplified DNA was gel-purified and assembled. The assembly was performed in two steps. Firstly,  $V_H$  and  $V_L$  were ligated in pEA and pMX9 vectors respectively by using SapI (New England Biolabs); secondly, heavy chain ( $V_H + C_H$ ) was digested with SfiI (New England Biolabs) and ligated into pMX9 already bearing the light chain ( $V_L + C_L$ ). The obtained DNA was sequenced with sequencing primers:

SMM25 primer (pMX9\_ompAseq for  $V_H$ ): 5'-AAGACAGCTATCGCGATTG-3`  
and

SM03 primer (pMX9\_ompAseq for  $V_L$ ): 5'-ATGTTGTGTGGAATTGTGAGCGG-3`

3.2.2.

## Expression and purification of soluble Fabs

Each pMX9 vector containing the corresponding Fab was electro-transformed into Mach1 E. coli competent cells. The cells were cultured in Terrific Broth (TB) medium supplemented with 0.1% glucose plus chloramphenicol (17 µg/ml) at 37°C and induced with 1 mM IPTG when the culture reached an  $OD_{600} = 0.8$ . After induction, the culture was grown at 30°C for 12 h, centrifuged at 6000 rpm at 4°C for 15 min and the pellet was resuspended in the lysis buffer containing 50 mM Tris pH 7.5, 150 mM NaCl, with the addition of 1 mg/ml lysozyme, 20 µg/ml DNase and 2 complete protease inhibitor tablets. The cells were homogenized with Turrax disperser (IKA) and lysed by high-pressure Emulsi-Flex C-3 (Avestin®) at 15000 psi. Unlysed cells, cell debris, and aggregates were removed by centrifugation at 17000 rpm for 45 minutes. Fabs were purified from the filtered supernatant by Ni-affinity chromatography, equilibrated with 5 ml of binding buffer: 50 mM Tris pH 7.5, 150 mM NaCl, 10 mM imidazole. Samples were eluted with elution buffer: 50 mM Tris pH 7.5, 150 mM NaCl, 500 mM imidazole. Eluted fractions, containing the Fabs were collected and used immediately for analysis or stored at -80°C.

3.2.3.

## Receptor kinase activity assay and HUVEC tube formation assay

To confirm that obtained Fabs preserved the same inhibitory properties as scFvs, kinase activity assay and HUVEC tube formation assay were performed as previously described in chapter 2.

3.3.

# Results

3.3.1.

## Construction of Fab format

The scFvs described in the previous chapter to inhibit VEGFR-2 phosphorylation were now transformed into Fabs, and their specificity, affinity and inhibiting capacity were assayed. Gel-purified DNA fragments encoding the variable domains of the light and heavy chains of the corresponding scFv were amplified by PCR (Figure 3.1).  $V_L$  and  $V_H$  were cloned into two distinct plasmids (pMX9 and pEA, respectively). The assembly was performed using SapI. Final ligation of heavy chain ( $V_H + C_H$ ) into pMX9 bearing light chain ( $V_L + C_L$ ) was performed with SfiI (Figure 3.1). The DNAs were sequenced with sequencing primers SMM26 and SM03.

3.3.2.

## Expression and purification of Fabs

The Fabs sub-cloned into pMX9 vector were expressed by IPTG induction using the Mach1 E. coli strain. The recombinant Fabs were extracted from the periplasm and purified by Ni-affinity chromatography (Figure 3.2, A). The typical yield was around 1 mg of soluble protein per liter of culture. The Fab fractions under SDS-PAGE conditions showed a MW of approximately 50 kDa (Figure 3.2, B).

3.3.3.

## Affinity determination with ITC

ITC was performed for Fab F1 as previously described for scFvs. Kd values for Fab F1 showed approximately 10-fold increased activity when compared with Kd values for scFv F1. (Figure 3.3).

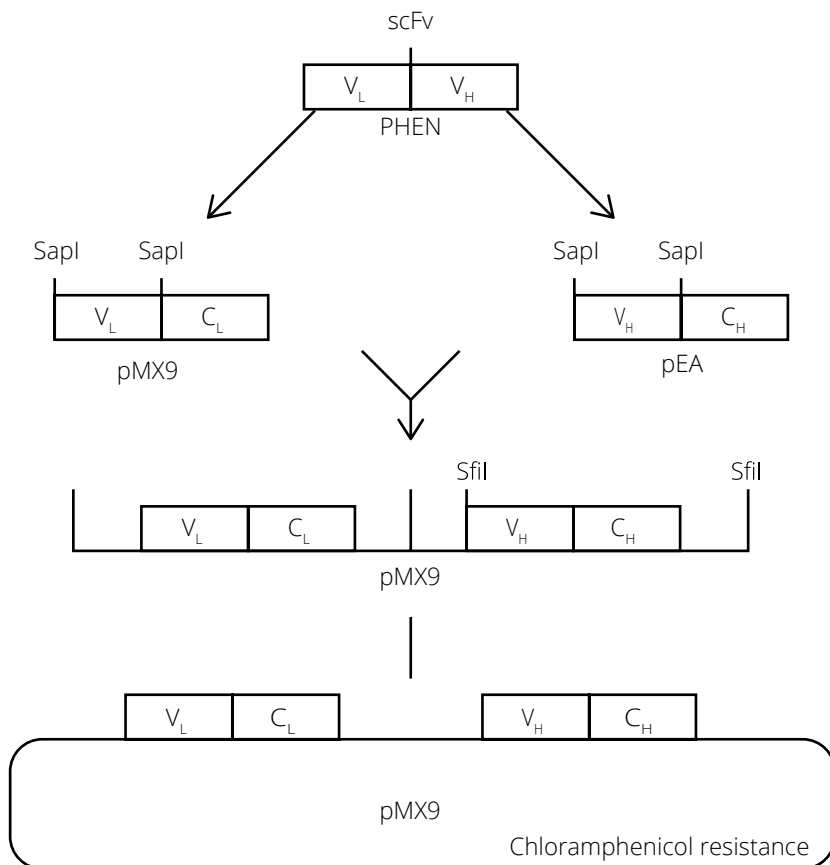


Figure 3.1. Construction of Fabs. DNA fragments encoding the variable domains of the light and heavy chains of the corresponding scFv, were amplified by PCR and cloned into two distinct plasmids (pMX9 and pEA, respectively), which contained the human C<sub>L</sub> or C<sub>H</sub> constant domains by digestion with S<sub>ap</sub>I. Heavy variable fragment, previously cloned into pEA, was subcloned into pMX9 vector containing the light Fd fragment by digestion with S<sub>fi</sub>I, resulting in pMX9Fab vector.

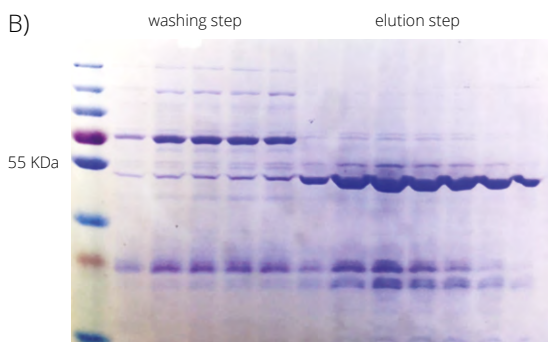
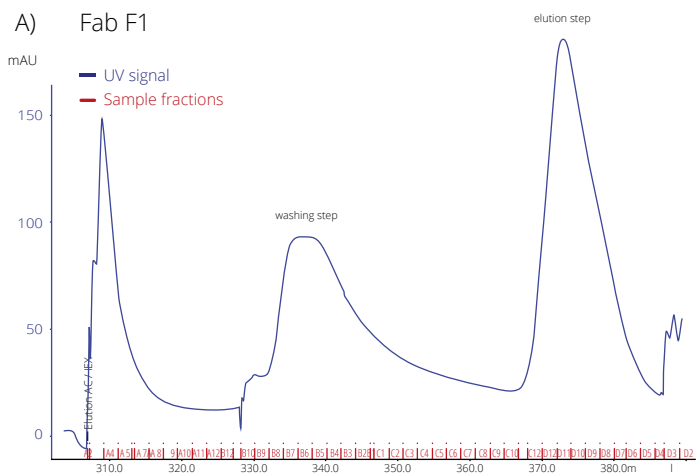
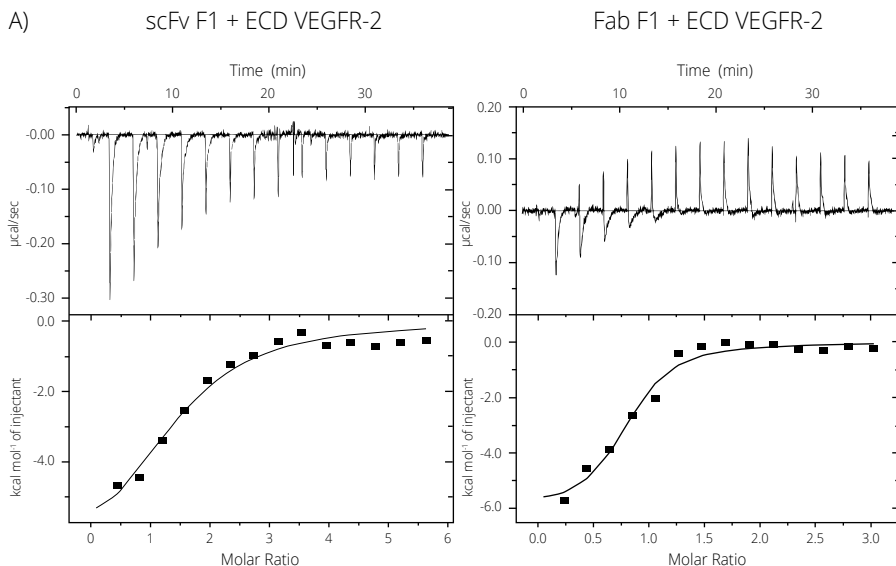


Figure 3.2. Fab purification by protein Ni-affinity chromatography. A) Elution profile of Fab F1 after purification by Ni-affinity chromatography shows two peaks in washing step and in elution step. B) The eluted peak fractions loaded on 12% polyacrylamide gel and analyzed with a Coomassie blue staining.



B)

Complex	Stoichiometric Coefficient, N	Kd (nM)	$\Delta H$ (kcal mol <sup>-1</sup> )	$T\Delta S$ (kcal mol <sup>-1</sup> )
ECD + scFv F1	1.38	6800	-7283	-1.63
ECD + Fab F1	0.754	869	-6075	6.64

Figure 3.3. Comparison of thermodynamic analysis of antibody-VEGFR-2 interactions. A) ITC analysis and of scFv F1 and corresponding Fab F1 in complex with VEGFR-2 ECD. Raw data and binding isotherms are shown. B) Calculated thermodynamic parameters of interactions are summarized in the Table.

3.3.4.

## Receptor kinase activity assay and HUVEC tube formation assay

Both assays were performed as previously described for scFvs in chapter 2. Analysis of the kinase assay revealed that increasing concentrations of Fabs inhibited kinase phosphorylation at Y1175 in a dose-dependent manner. VEGFR-2 was phosphorylated by the addition of exogenous VEGF to PAE KDR cells (Figure 3.4). Pretreatment of cells with increasing concentrations of scFvs in the presence of VEGF showed inhibition of Y1175 phosphorylation in a dose-dependent manner, without affecting overall VEGFR-2 expression levels. To identify the effect to downstream signaling by Fabs, the expressions and phosphorylation of PLC $\gamma$ , AKT, and p38 were examined. PLC $\gamma$  signaling was clearly inhibited, whereas p38 and AKT signaling did not show a statistically significant change. While treatment of PAE KDRs with antibodies inhibit-

ed VEGF-dependent phosphorylation of downstream signaling in a dose-dependent manner, total protein levels were unaffected (Figure 3.4, A). All kinase assays were performed in triplicates and quantified with ImageJ software. Quantified data was analyzed with GraphPad (Figure 3.4, B). For Fab H5 we observed a high standard deviation at 0.1  $\mu\text{M}$  concentration which can be explained by having one quantified point with considerably different value compared to others in triplicates. HUVEC tube formation assay shows that VEGF triggers the formation of a dense network of tubule-like structures. Added Fab F1 repressed this effect (Figure 3.5, A). Four independent experiments were performed for each concentration and the tube-like structures were analyzed with ImageJ software. Data was quantified with GraphPad (Figure 3.5, B).

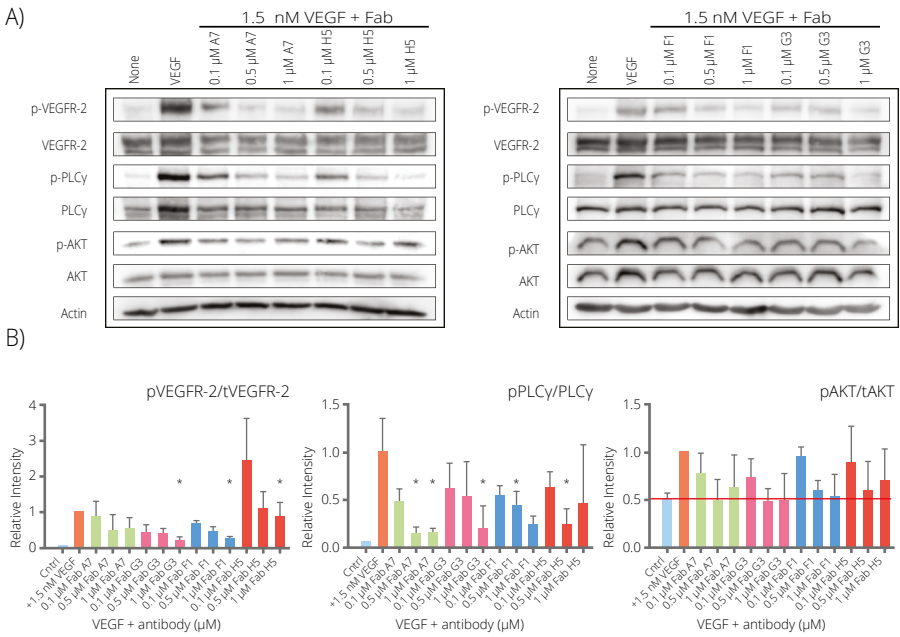


Figure 3.4. Effect of antibody treatment on VEGF-induced signaling in PAE KDR cells. A) Fabs inhibit phosphorylation of Y1175-VEGFR-2, PLCy and AKT in a dose-dependent manner. The western blot data was analyzed and quantified with Image J. B) Quantification of data shown as n-fold increase over VEGF-induced signaling in the absence of Fabs antibodies. Data distribution and statistical analysis were performed using GraphPad, Prism 7. A representative experiment, out of three independent experiments, is shown. Error bars represent  $\pm$  SD. The statistical significance based on a Student's t-test is indicated by \* representing  $P < 0.05$ .



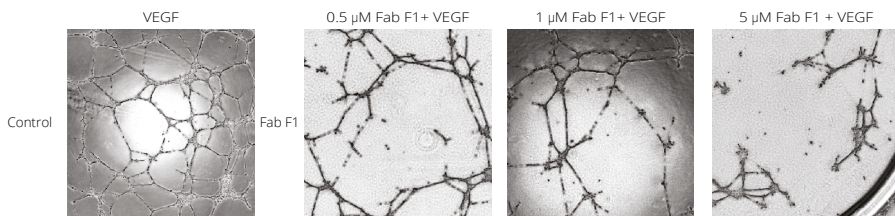


Figure 3.5. Effect of antibody treatment on VEGF-induced capillary-like tube formation in HUVECs. A) Light microscopy of capillary-like tubes formed in the presence and absence of increasing concentrations of Fab antibody.

### 3.4.

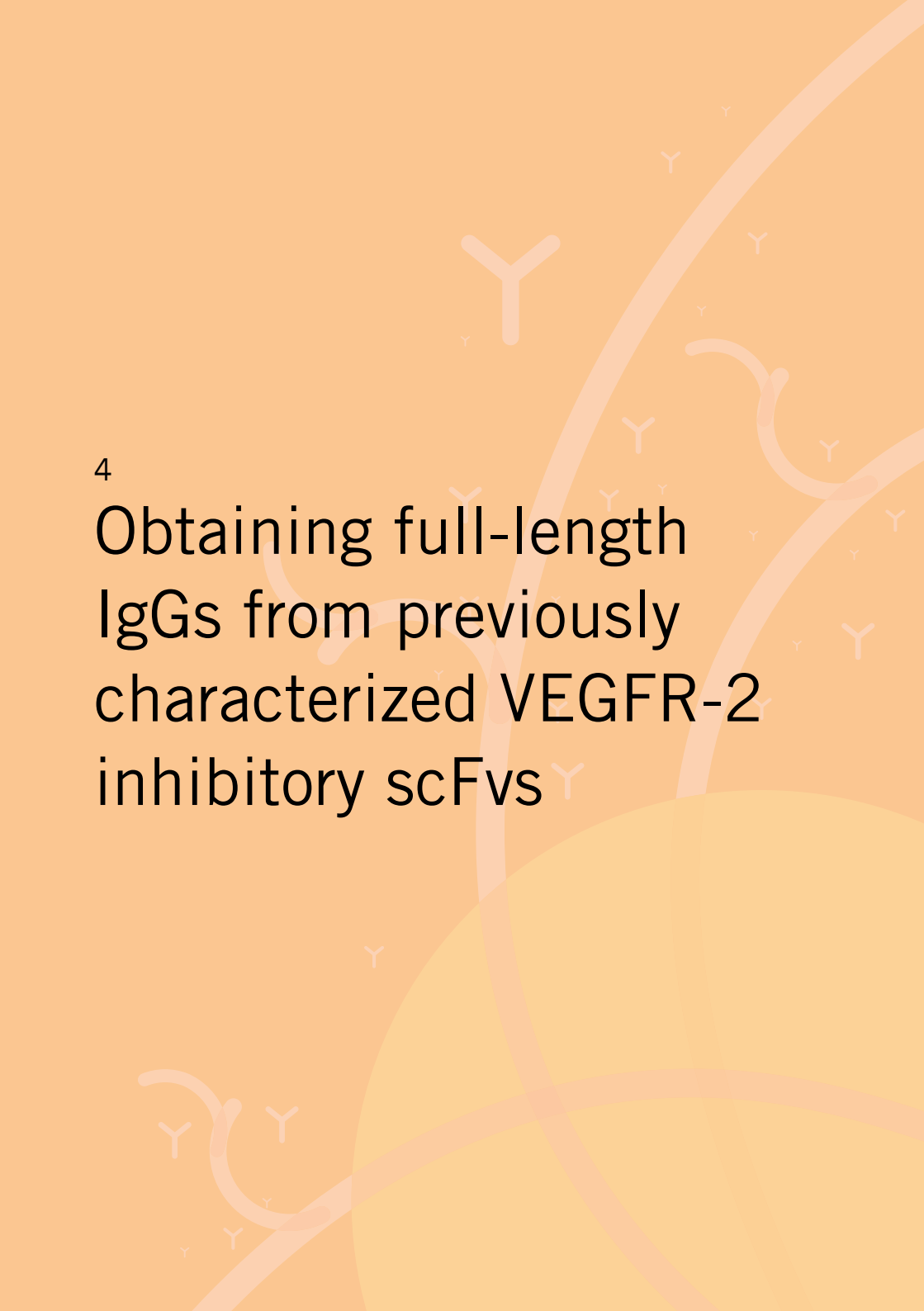
## Discussion

To provide the best VEGFR-2 imaging tool for *in vivo* studies, some of the previously synthesized scFvs were reformatted to Fabs. A method for the production of Fabs from preselected scFvs from ETH-2 Gold library previously developed by Prof. Dr. Raimund Dutzler's group from the University of Zürich was tested.  $V_H$  or  $V_L$  domains were PCR amplified and cloned into a single bacterial pMX9 vector. Fabs were functionally expressed in Mach-1 E. coli. Fabs maintained domain specificity. The affinity of the Fab F1 was compared to that of corresponding scFv F1, and we observed 10-fold increase in affinity. This can be explained by the findings that Fabs are generally more stable compared to the scFv format<sup>144</sup>. Since ITC data for other scFv/Fab pairs is not available, it is impossible to determine whether the increase of affinity for reformatted scFv F1 to Fab F1 is a single event or is consistent for all the observed Fabs. The Fabs preserved inhibitory activity previously demonstrated for scFvs in the kinase activity assay in PAE KDR cells and in the HUVEC tube formation assay. Future experiments could, therefore, consist of further characterization of the obtained Fabs, including the determination of missing affinities against D1-7 by Isothermal Titration Calorimetry. The Fabs may further be tested for inhibition of HUVEC migration discussed in section 3.5 for the scFvs and in *in vivo* imaging experiments.



4

Obtaining full-length  
IgGs from previously  
characterized VEGFR-2  
inhibitory scFvs

The background is a warm orange color. It features several white Y-shaped symbols representing antibodies, scattered across the page. There are also large, abstract, curved shapes in shades of orange and yellow, some resembling antibody structures or molecular pathways. The overall aesthetic is clean and scientific.

4.1.

# Introduction

Despite the wealth of available antibody formats, immunoglobulin G (IgG) remains the most accepted therapeutic antibody format<sup>2</sup>, whereas small recombinant antibodies<sup>18,21,40,41</sup> are required for *in vitro* antibody generation and engineering during drug development. Single chain antibody fragments such as scFvs or Fabs are especially well suited for phage display and bacterial expression<sup>20,40</sup>. One of the major drawbacks of the scFv format is its reduced affinity compared to the full-length IgG. In general antibody affinity of 1 nM or less is required for clinical application; thus, one or several cycles of affinity maturation are important steps during antibody generation<sup>44,146</sup>. Conversion of *in vitro* optimized antibody fragments back to IgGs will result in similar or improved antigen binding affinity<sup>147</sup>. Surprisingly, some studies have demonstrated a loss of affinity after reformatting scFv fragments into IgGs<sup>148</sup>, which can partially diminish the benefit from affinity maturation in the scFv format<sup>149</sup>. Increasing efforts are being made to address the challenges related to IgG reformatting from small antibody fragments, such as screening of vast numbers of scFv clones, full batch conversion into the IgG format after selection in combination with mammalian expression system for screening<sup>150</sup> or Fab display on yeast<sup>47</sup>. Changing the expression host during screening may overcome restrictions of the *E. coli* expression system. However, this requires more time and effort, and also introduces a risk of error in the additional subcloning steps. For the purposes of this study, two different strategies were tested for the conversion of anti-human VEGFR-2 scFvs into full IgGs, so that they could be used in animal angiogenesis models.

4.2.

# Materials and methods

4.2.1.

## Cloning, production, and purification

4.2.1.1.

### Cloning pcDNA3 vectors

The method used for reformatting with the pcDNA3 vector was previously developed and described by Grünberg et al. 2003<sup>151</sup>. To obtain IgG formats, the DNA of heavy chain ( $V_H$ ) and light chain ( $V_L$ ) variable regions from scFvs were PCR amplified. Purified DNA was subcloned into two separate pcDNA3 vectors (Invitrogen, Basel, Switzerland), one encoding the human  $\kappa$  light chain and the other the human  $\gamma 1$  heavy chain by using restriction digestion. The vectors encoding heavy and light chains were transiently transfected into HEK293, and the cells were propagated in standard growing conditions. Large-scale purification of antibodies was performed using stably transfected cells. HEK293 cells were co-transfected by using in-house prepared 1 mg/ml

PEI (Polyethylenimine), and selection was performed after 24 h by adding 500 µg/ml of G418 (Geneticin) to the medium. Colonies were picked after 10 days. Stable HEK293 cells were grown in 2 l shaking flasks in PEM (Protein Expression Medium, GIBCO) for 2 weeks when 1M sodium butyrate was added to enhance protein expression. IgGs were purified from the filtered supernatant by Protein A chromatography.

4.2.1.2.

## Reformatting with MultiPrime expression system

The method used for reformatting with MultiPrime was developed in our group by Mansouri et al. 2016<sup>152</sup>. The genes encoding  $V_H$  and  $V_L$  were inserted into a modified donor and acceptor vector, respectively, bearing the constant domains by using BamHI and XbaI restriction sites. Positive clones were selected by antibiotic screening. Integration of the donor expression cassette comprising the heavy chain ( $V_H + C_H$ ) into acceptor vector bearing the light chain ( $V_L + C_L$ ) was performed with Cre-LoxP recombination<sup>152</sup>. In this way, both heavy and light chains were located on the same vector, having separate promoters (CMV) in separate expression units. IgGs were expressed in transiently transfected HEK293. Cells were grown in the standard growing conditions in large 15-cm plates in adherent cultures. When cultures reached confluency, cells were transiently transfected with MultiPrime bearing both heavy and light chains. Transfected cells were incubated at 37°C for 4 h, and the medium was then replaced with fresh mammalian cell culture medium.

4.2.1.3.

## IgGs purification

Soluble full-length IgG antibodies were concentrated and filtered through a 0.45 µm filter (Millipore) and purified by protein A chromatography (GE). Buffers used for Protein A chromatography purification were: binding buffer: 20 mM Tris pH 8.0; washing buffer: 20 mM glycine pH 6.0 and elution buffer: 0.1 M glycine pH 2.5. The affinity chromatography purification was performed as previously described for scFvs in chapter 2. Purified IgGs were concentrated and resolved on 12% and 7% SDS-PAGE gels.

4.2.2.

## 4.2.2. FSEC, receptor kinase activity assay, tube formation assay

FSEC, kinase activity assay, and tube formation assay were performed as previously described in chapter 2.8.11.

4.3.

# Results

4.3.1.

## IgG cloning and purification

The most promising antibodies were converted into full-length IgGs consisting of light and heavy chains. Two different strategies were used to reformat scFvs to IgG.

4.3.2.

## Cloning into pcDNA3 vectors

First, the reformatting approach used allowed functional antibody production from stably transfected cells. Heavy and light chain variable regions from scFvs were PCR amplified using oligonucleotides (Table 4.1). Purified DNA was subcloned into two separate pcDNA3 vectors (Figure 4.1), one encoding human  $\kappa$  light chain and the other human  $\gamma 1$  heavy chain by using restriction digestion enzymes HindIII and Bsi-Wi for  $V_H$  and HindIII and NheI for  $V_L$ .

The DNA was sequenced using primers (Table 4.1). The vectors encoding heavy and light chains were transiently cotransfected into HEK293 cells propagated in standard growing conditions. Large-scale purification of antibodies was performed using stable transfection. When the cultures reached 60% cell confluency, they were transfected with PEI. After 4 h, transfection medium was replaced with fresh growing medium. 24 h later, the selecting antibiotic was added. The following days cell death and resistant cell colony formation was carefully observed. After 10 days, well-defined colonies were picked and cultured separately. Colonies with the highest IgG expression were selected and used in large scale expression.

IgGs were grown in large shaking flasks (2 l) in standard growing conditions in PEM media. Cell number was regularly monitored in order not to exceed 3 million cells/ml. When culture reached 4 l it was filtered, concentrated and IgGs were purified using Protein A chromatography (Figure 4.3, A). The eluted peak fractions were loaded on 12% polyacrylamide gel and analyzed by Coomassie blue staining and anti-human IgG immunoblotting (Figure 4.3, B, C). The obtained yield for pcDNA3 strategy was  $\sim 1$  mg from 1 l of culture.

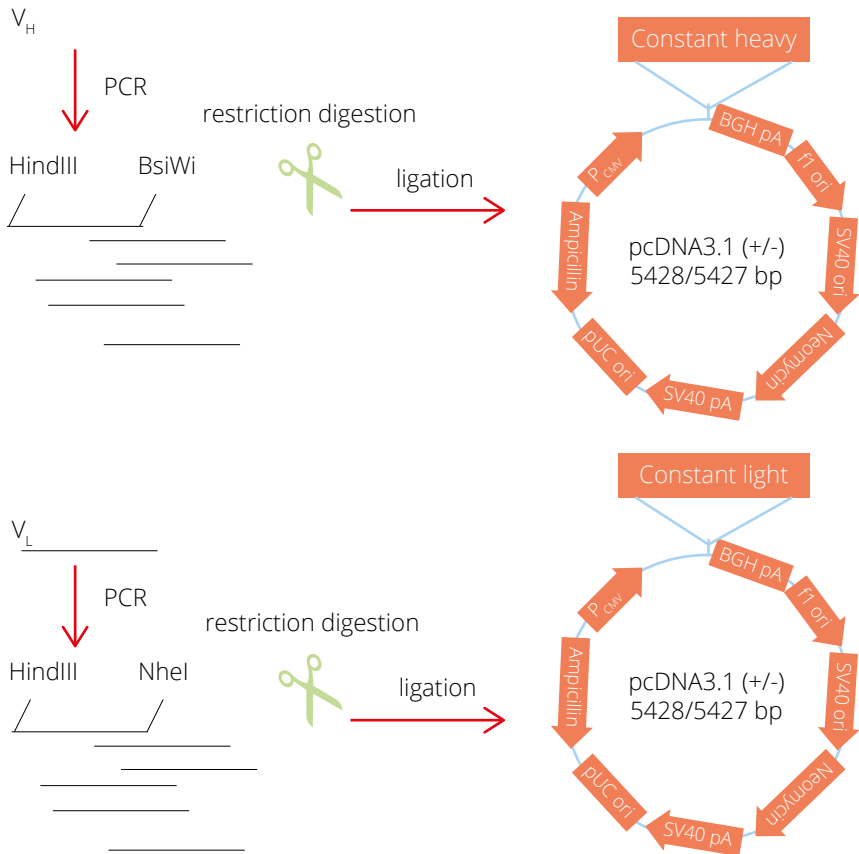


Figure 4.1. Schematic representation of the pcDNA3 cloning workflow.  $V_H$  and  $V_L$  were PCR amplified with sequence addition of HindIII and BsiWI to  $V_H$  and HindIII and NheI to  $V_L$  DNA sequences. Digested DNAs were ligated to pcDNA3 vectors already bearing  $C_H$  and  $C_L$  respectively.

#### 4.3.3.

## Cloning with MultiPrime

MultiPrime approach was used to express functional antibodies in HEK293 cells. Cloning was performed in two steps (Figure 4.2). First, the genes encoding  $V_H$  and  $V_L$  were inserted into the modified donor and acceptor vector, respectively, bearing the constant domains by using BamHI and XbaI restriction sites. Subsequently, donor expression cassette bearing the DNA encoding the heavy chain was integrated into acceptor vector bearing the DNA encoding the light chain with Cre-LoxP recombination<sup>152</sup>. The cloning was performed with great help by Jonas Mechttersheimer.

## Workflow of IgG reformatting with MultiPrime

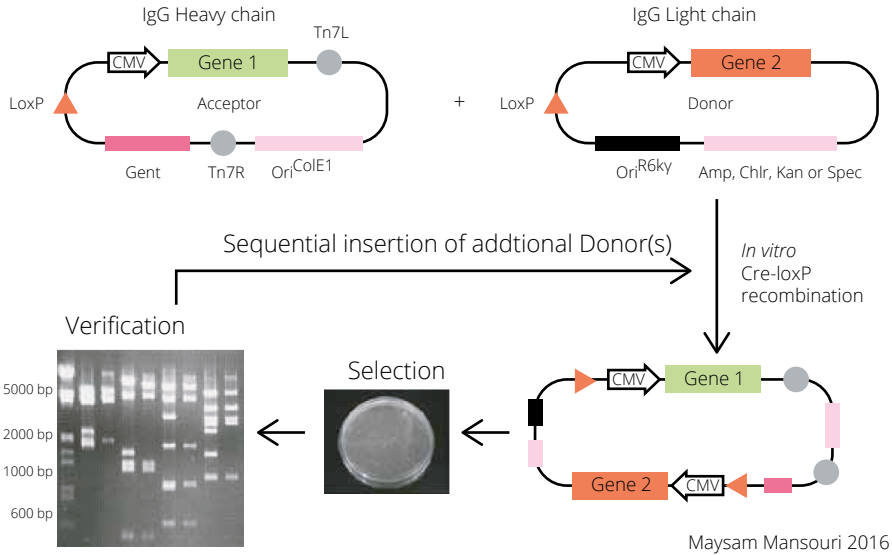


Figure 4.2. Schematic presentation of the MultiPrime cloning workflow.  $V_H$  was ligated to acceptor vector already bearing  $C_H$  and  $V_L$  was ligated into donor vector already bearing  $C_L$ . Full-length light chain ( $V_L + C_L$ ) was fused to the donor containing full-length heavy chain ( $V_H + C_H$ ). Acceptor-donor fusions are selected on plates with appropriate antibiotics, and verified by restriction mapping<sup>152</sup>.

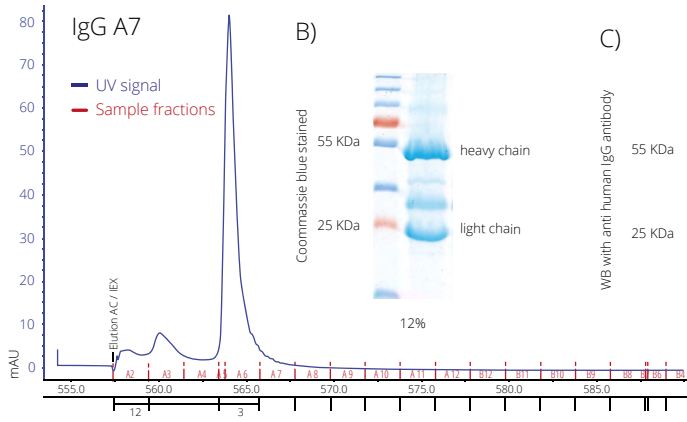
The single-host promoter CMV was utilized to drive recombinant IgG expression. The resulting MultiPrime vector was successfully tested for expression in HEK293. All IgG antibodies tested were expressed at comparable levels. HEK293 were propagated in adherent culture in standard conditions until reaching necessary cell number and density. Transient transfection was performed by using Lipofectamine 2000. Soluble IgGs were purified 48 h after transfection from filtered supernatant using Protein A chromatography as previously described (Figure 4.3, D). The eluted peak fractions were loaded on 12% polyacrylamide gel and analyzed with a Coomassie blue staining and anti-human IgG immunoblotting (Figure 4.3, E, F). The blots showed bands of the right size for both heavy (~50 kDa) and light chains (~25 kDa). Also, an unidentified strong band of ~35 kDa could be observed for all purified IgGs. The yield obtained using MultiPrime strategy was ~1 mg from 250 ml of culture.

	Primer 1 (melting temperatures)	Primer 2 (melting temperatures)
$V_H$	gatcGCTCTCCATGGGTTGGAGCCTCATC(67)	catcGCTCTTCcTCAGGCTCAACTTCTTGTC(67)
$V_L$	gatcGCTCTCCATGGAGACAGACACACTCCTG(68)	catcGCTCTTCcTCAGACTCCGCCTTCTTGGT(69)

Table 4.1: Oligonucleotides used for IgG cloning into pcDNA3 vectors.



A) MultiPrime strategy



D) pcDNA3 strategy

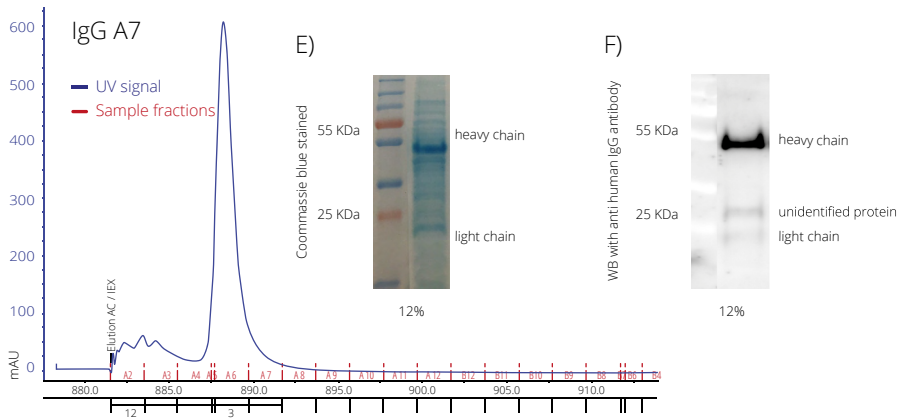


Figure 4.3. A) & D) Purification profiles of IgG A7 obtained with MultiPrime and pcDNA 3 cloning strategies. B) & E) IgG proteins stained with Coomassie blue staining and C) & F) anti-human IgG antibody.

4.3.4.

# Determination of IgGs binding to VEGFR-2 by FSEC

Thermodynamic analysis of antibody-VEGFR-2 interaction revealed a loss of binding in the case of IgGs using pcDNA3-based expression (Figures 4.4, B). IgGs cloned with MultiPrime maintained binding specificity towards hVEGFR-2 ECD (Figures 4.4, A). Coomassie blue staining of resolved IgG showed that the light chain from pcDNA3 cloning strategy is shorter compared to the light chain from MultiPrime cloning (Figure 4.4, C). This may explain the lost binding properties. The same shorter band was observed in other cloned IgGs as well, indicating that there is probably a problem with the vector (pcDNA3) bearing the light chain. Again, an unidentified strong band of the size ~35 kDa could be observed for the purified IgGs (Figure 4.4, C).

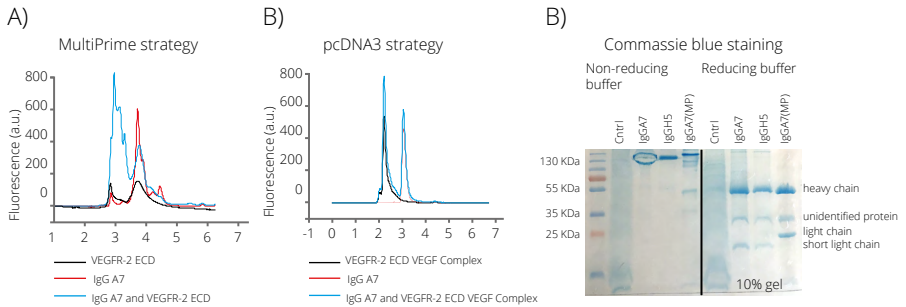


Figure 4.4. IgG binding to recombinant VEGFR-2 in FSEC. A) FSEC analysis shows IgG A7 obtained with MultiPrime strategy binding VEGFR-2 ECD. The shift in the peak to the left (from red to blue peak) demonstrates the formation of a new, larger protein species in the combination of VEGFR-2 ECD and IgG A7. B) The shift from right to left is missing for IgG obtained with pcDNA3 strategy. C) To compare IgGs obtained with MultiPrime and pcDNA3 strategy obtained IgGs were resolved with SDS-PAGE. Coomassie blue staining and comparison of IgGs obtained with MultiPrime (MP), and pcDNA3 strategy shows the difference in size of the light chains.

4.3.5.

# Functional inhibition of VEGFR-2 phosphorylation with IgGs

We investigated the potential of IgG A7 to inhibit VEGFR-2 signaling *in vitro*. We exposed PAE KDR cells to various concentrations of IgGA7 in the presence or absence of VEGF (Figure 4.5). Analysis revealed that IgG A7 significantly inhibited kinase phosphorylation at the Y1175 position, which was also reflected in reduced downstream signaling by PLC $\gamma$  and AKT. P38 signaling did not show statistically significant change.

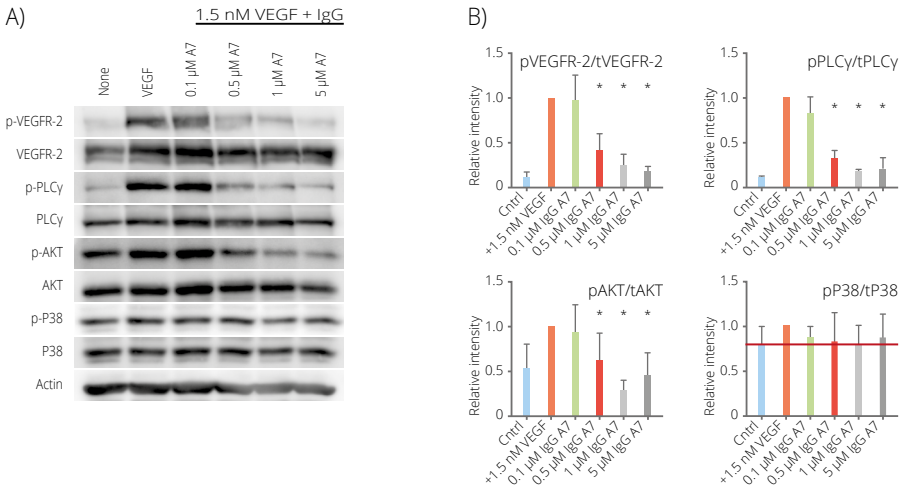


Figure 4.5. Effect of antibody treatment on VEGF-induced signaling in PAE KDR cells. A) scFvs effect on phosphorylation of VEGFR-2, PLC $\gamma$ , AKT and p38. B) Quantification of western blot data. Quantification of data shown as n-fold increase over VEGF-induced signaling in the absence of antibodies. Data distribution and statistical analysis were performed using GraphPad, Prism 7. A representative experiment out of four independent experiments is shown. Error bars represent  $\pm$  SD. The statistical significance based on a Student's t-test is indicated by \* representing  $P < 0.05$ .

4.3.6.

## HUVEC tube formation assay

The effect of IgG A7 on the formation of capillary-like tubes by endothelial cells in Matrigel was examined. HUVEC were embedded in Matrigel and treated for 8 h with VEGF in the presence or absence of increasing concentrations of IgG A7. The formation of tubes was then examined under phase contrast microscopy. Results show that VEGF triggers the formation of a dense network of tubules when added to control HUVEC in Matrigel. This effect was markedly repressed in cells to which IgG A7 was added (Figure 4.6, A). Four independent assays were performed for each concentration of IgG A7 and analyzed with ImageJ Angiogenesis analyzer software. Data was quantified with GraphPad (Figure 4.6, B).

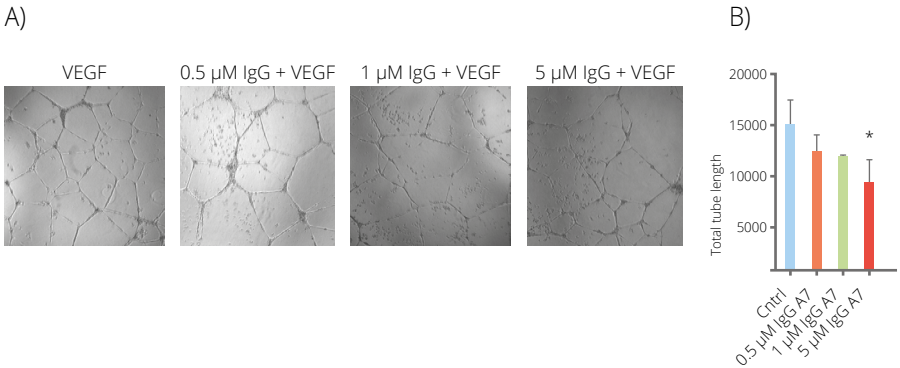


Figure 4.6. Effect of antibody treatment on VEGF-induced capillary-like tube formation in HUVECs. A) Light microscopy of capillary-like tubes formed in the presence and absence of increasing concentrations of antibodies. The total tube length was quantified with Wimasis online software (<http://ibidi.wimasis.com/>). B) Quantification of data shown as n-fold increase over VEGF-induced tube formation in the absence of antibodies. Data distribution and statistical analysis were performed using GraphPad, Prism 7. A representative experiment is shown, out of three independent experiments. Error bars represent  $\pm$  SD. The statistical significance based on a Student's t-test is indicated by \* representing  $P < 0.05$ .

# Discussion

Two methods were tested using MultiPrime and pcDNA3 expression vectors for the production of IgGs by using the natural dimerization mechanism between IgG heavy and light chains. The original  $V_H$  or  $V_L$  domains of an IgG molecule were replaced by scFvs, resulting in the full-length antibody. IgGs were functionally expressed and assembled in mammalian cells<sup>153</sup>. These two approaches are believed to be applicable to a wide range of scFv antibodies. The small-size scFv fragments may be preferable to the full-size IgG for some clinical applications, for example, to promote rapid clearance for improved tumor imaging<sup>55,56,89</sup> and to facilitate efficient tumor penetration<sup>57</sup>. In many other applications, however, IgGs may offer additional advantages as this format provides an IgG Fc region that can confer long serum half-life and support secondary immune functions<sup>154</sup>. The major hurdles in traditional methods of IgG production from scFvs include heterogeneity of the products, low yield, and difficulty with the purification process. For example, co-expression of IgG heavy and light chains gives different expression levels (Figure 4.3, E, F), compromising the yield of functional IgGs and imposing significant problems with purification. The first method for IgG production described herein (pcDNA3 method) provided pure IgG in high yield, but binding to VEGFR-2 ECD was lost. As discussed in the “Results” section, this probably occurred due to a cloning error in the pcDNA3 vector bearing the light chain sequence. A new method was recently developed to improve the production of IgG-like molecules<sup>152</sup>. Mansouri et al. have demonstrated that MultiPrime bearing both heavy and light chains can be used to overcome non-uniform expression of heavy and light chains. IgGs expressed with the MultiPrime strategy retained the biological functions of scFvs. The IgGs bind the same target and efficiently neutralize VEGF-induced VEGFR-2 phosphorylation in a dose-dependent manner. It is noteworthy that the IgGs are equally potent as scFvs in neutralizing VEGF-induced receptor phosphorylation. In HUVEC tube formation assay IgGs showed comparable inhibitory effect on total tube length. In conclusion, IgG antibodies were constructed from scFvs and characterized *in vitro*. Further, IgG A7 may be expressed in higher quantities with MultiPrime strategy and tested in mouse matrigel plug assay.



5

# Selection and characterization of scFvs specific for the mouse VEGFR-2 ECD

# Introduction

Before reaching humans, potential therapeutics must be tested in increasingly complex model systems ranging from cell culture to animal models, and such tests are still invaluable in discovering new technologies for the detection, management and treatment of cancer in humans. Preclinical research represents the evaluation of potential therapeutics in cells and animals. Regardless of ethical issues associated with *in vivo* studies, preclinical characterization remains a necessary step before propagating a therapy to the clinic<sup>155</sup>. The mouse (*Mus musculus*) represents one of the best model-systems for cancer investigations. The animals are small and show a good propensity to breed in captivity, they have a relatively short lifespan of 3 years, extensive physiological and molecular similarities to humans, and an entirely sequenced genome<sup>156,157</sup>. Mouse cancer models offer several phases of increasing complexity, including xenograft tumors derived from human tumor cell lines or explants, chemical and viral carcinogens, and genetically engineered mice<sup>158</sup>. Each approach has its advantages and disadvantages, and it is important to choose the most appropriate system to address the particular questions. Importantly, mouse cancer models represent a tremendous resource to evaluate the mechanism of malignancy. However, it is not always possible to extrapolate findings made in animal models to humans<sup>159</sup>.

One of the most appreciated properties of antibodies is their binding to their target antigen with high specific selectivity, which is a prerequisite for their use in targeted therapy<sup>160</sup>. By contrast, it is less common for antibodies to bind the corresponding antigen from a different species, although such binding is a desirable attribute that would facilitate preclinical evaluation of efficacy and toxicity. Success in generating such species-cross-reactive antibodies depends on the sequence-similarity of the antigen in different species, especially conservation of the binding epitope and the method of antibody generation. In theory, phage-display technology<sup>161</sup> is particularly well suited for the generation of species-cross-reactive antibodies, because it is a fast and cheap method that circumvents immunization of animals and allows screening and direct selection of species cross-reactive antibodies<sup>162</sup>. In preclinical tumor angiogenesis models, human tumors are xenografted onto immunodeficient mice; the newly formed blood vessels in the transplanted tumor originate from the host (mouse), and conventional anti-human mAbs typically do not react with cell surface receptors displayed by mouse endothelial cells. In fact, the lack of cross-reactivity of humanized mouse mAbs directed to human integrin  $\alpha\beta3$  and human VEGFR-2 with the mouse antigen represents a major obstacle in their preclinical development<sup>163</sup>.

The specificity of VEGFR-2 expression, its location on the surface of the tumor vessels, and its predominant role in tumor angiogenesis make it a highly desirable target for the development of both antiangiogenic and vascular targeting drugs<sup>130</sup>. Mouse tumor models represent a major testing system to evaluate such drugs. Models of murine tumor angiogenesis and receptor-specific antibodies are required to assess



the roles of VEGF receptors in mouse models of human cancer. Human VEGFR-2 and murine VEGFR-2 share 85% amino acid sequence identity in their extracellular domain. The process of selection and characterization of anti-mouse-VEGFR-3 antibodies for their use in *in vivo* studies is described below.

5.2.

## Materials and methods

5.2.1.

### Production of recombinant mouse VEGFR-2 ECD

Purified mouse VEGFR-2 ECD was kindly provided by my colleague Mayanka Asthana. In brief, mouse VEGFR-2 ECD was expressed in transiently transfected HEK293-EBNA cells. ECD was purified by Ni-affinity chromatography (IMAC) and subsequently by size-exclusion chromatography (SEC). Purified protein was frozen at -80°C until further use.

5.2.2.

### Selection of mouse specific scFvs against VEGFR-2

5.2.2.1.

#### Selection of mouse specific scFvs from ETH-2 Gold library

Anti-mouse VEGFR-2 scFvs were selected as previously described for human specific scFvs.

5.2.2.2.

#### Selection of species cross-reactive scFv antibodies against mouse and human VEGFR-2 ECD

Phage display selection was performed as previously described for mouse specific scFvs except that a glycerol stock of TG1 bacteria bearing scFvs, previously selected with hVEGFR-2, was used instead of the ETH-2 Gold library.

### 5.2.2.3.

## Selection of mouse specific scFvs from R3 EPFL library

The R3 EPFL library was kindly provided by Prof. Christian Heinis from EPFL, Switzerland. The protein of interest was biotinylated using a biotinylation kit (21441, Thermo Scientific) and purified by PD-10 desalting columns (GE). The selection was performed in two rounds. In the first round, streptavidin beads were used, in the second, neutravidin beads. 1 ml of the glycerol stock of bacteria bearing scFvs obtained from EPFL was grown in 2xYT media containing chloramphenicol. When the culture reached OD<sub>600</sub> 0.5, both IPTG (0.5 mM) and 300 µl VCS helper phage were added. After 30 min of incubation at 37°C, 20% glucose was added, followed by 1 h of shaking and the addition of kanamycin. ScFvs were grown overnight at 30°C when cultures were pelleted, and 20% PEG/2.5 M NaCl (200 ml) was added, after which the phage was allowed to precipitate at 0°C. Biotinylated target protein mVEGFR-2 was displayed on the surface of streptavidin beads (Thermo Scientific). Both phages and beads were blocked with blocking buffer (10 mM Tris-Cl pH 7.4, 150 mM NaCl, 10 mM MgCl<sub>2</sub>, 1 mM CaCl<sub>2</sub>, 0.1% Tween-20, 1% BSA). Blocked magnetic beads bearing biotinylated protein of interest were added to the blocked phages. The magnetic beads were washed extensively with buffer (10 mM Tris-Cl pH 7.4, 150 mM NaCl, 10 mM MgCl<sub>2</sub>, 1 mM CaCl<sub>2</sub>). The tubes were replaced every two washing steps to eliminate binders to plastic. In the last step, the selected scFvs were eluted with low pH of glycine buffer (50 mM glycine, pH 2.2) and pH was normalized with Tris Buffer (1 M Tris-Cl, pH 8). The phages were added to TG1 cells and incubated for 30 minutes at 37 °C. Cells were pelleted by centrifugation at 4000 rpm for 15 minutes, suspended in 2 ml 2YT and plated on a large agar 2YT/chloramphenicol plate. The plate was incubated overnight at 37°C. The next day the colonies were scraped off the plate with 5 ml 2YT + 20% glycerol, frozen in liquid N<sub>2</sub> and stored as glycerol stock. ScFvs from the obtained glycerol stock were then purified for further use, in a procedure in which streptavidin beads were replaced with neutravidin beads in order to discard streptavidin-specific scFvs.

### 5.2.3.

## Sequencing of selected mouse scFvs

Extracted DNA from the binders giving the strongest absorbance signal in ELISA assay was sent for sequencing to mycosynth (<http://www.micosynth.ch/>) using sequencing primers.

(LMB3 long: CAGGAAACAGCTATGACCATGATTAC and Fdseq long: GACGTTAGTAAAT-GAATTTTCTGTATGAGG) and (primer 1: GGCTTCACCTTCAGCAGCTACG and primer 2: GCAGCACCTACTACGCCGATTC) for ETH-2 Gold library and R3 EPFL library respectively.

ScFvs bearing unique DNA sequences were produced in large scale expression and tested further.

5.2.4.

## Testing protein expression to select optimal bacterial strain

For all isolated phagemid vectors, an initial test expression assay was performed in different *E. coli* strains (Mach1, BL21(DE3)). The culture was grown in 5 ml LB-AMP media inoculated with several colonies of transformed bacteria. The cultures were incubated at 37°C on a shaker until they reached an OD<sub>600</sub> of 0.6 – 0.9. Protein expression was then induced with 1 mM IPTG final concentration. After incubation of the cultures overnight at 30°C on a shaker, they were centrifuged for 5 min (4000 g; 4°C) and 20 µl of the supernatants were taken for analysis. The pellets were re-suspended in 50 µl 3 M urea, incubated for 10 min at RT and centrifuged for 20 min (4000 g; 4°C). 20 µl aliquots of supernatants from the lysed cells were once again collected and analyzed by SDS-PAGE and western blot.

5.2.5.

## Expression and purification of scFvs against mouse VEGFR-2

5.2.5.1.

### Expression and purification of soluble scFvs from ETH-2 Gold library

ScFv antibodies were expressed as previously described for human VEGFR-2 specific scFvs.

5.2.5.2.

### Expression and purification of scFvs from R3 EPFL library

ScFv antibodies were expressed in *E. coli* Mach1. The bacteria were grown in 2xYT medium containing 100 µg/ml chloramphenicol and 0.1% glucose at 37°C until they reached an OD<sub>600</sub> of 0.8. IPTG was added to a final concentration of 1 mM to induce expression of scFv antibodies. Following 10 hours of incubation at 30°C, the bacteria were pelleted by centrifugation at 4000 g for 20 min. Cell pellets were resuspended in lysis buffer with the addition of 1 mg/ml lysozyme, 20 µg/ml DNase and 2 complete protease inhibitor tablets. The cells were homogenized with Turrax disperser (IKA) and lysed by high-pressure Emulsi-Flex C-3 (Avestin®) at 15000 psi. Unlysed cells, cell debris, and aggregates were removed by centrifugation at 17000 rpm for

45 minutes. ScFvs were purified from the filtered supernatant by Protein A chromatography. Typically, the obtained yield of scFvs from ETH-2 library was in the range of 1 – 4 mg from 1 l of bacterial culture and for scFvs obtained from R3 EPFL was ~1 mg from 200 ml of bacterial culture.

5.2.6.

## ELISA for binder specificity

Binder specificity was determined by enzyme-linked immunosorbent assay (ELISA) using immobilized recombinant mouse VEGFR-2 ECD protein D1-7, D1-3, D1-6. The assay was performed as previously described for human scFvs.

5.2.7.

## Cell culture

Primary mouse hemangioma cells (mEnd) were kindly provided by Prof. Dr. Kiefer from University of Muenster. MEnd cells were grown in Dulbecco's modified Eagle's medium (DMEM; BioConcept, Basel, Switzerland) supplemented with 10% fetal bovine serum (FBS) and 1% Penicillin–Streptomycin. Cells were propagated in a humidified atmosphere at 37°C and 5% CO<sub>2</sub>.

5.2.8.

## Receptor kinase activity assay

In this kinase activity assay, mEnd cells were used to test mouse-specific scFvs. The assay was performed as previously described for scFvs against human VEGFR-2.

5.2.9.

## HUVEC tube formation assay

The property of mEnd cells to form tube-like structures was used in tube formation assay, which was performed as previously described for HUVECs.

5.3.

# Results

5.3.1.

## Selection, production, and purification of scFvs antibodies

5.3.1.1.

### ETH-2 Gold library

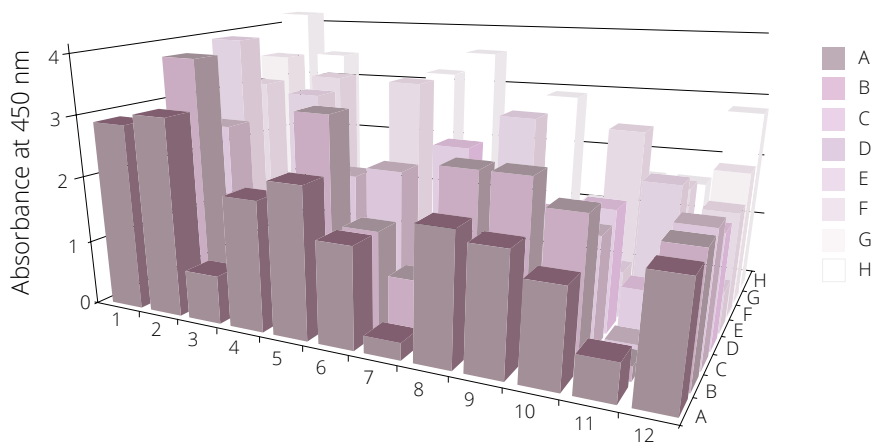
Selection, production, and purification of scFv antibodies was performed as previously described in chapter 2. To determine VEGFR-2 binders, scFvs were tested in ELISA (Figure 5.1, A). The best binders were sent for sequencing and scFvs with unique sequences (Figure 5.1, B) were expressed in high yield, and tested further. Antibodies were purified from lysed cell pellets using Protein A chromatography (Figure 5.3, A). The eluted peak fractions were loaded on 12% polyacrylamide gel and analyzed with a Coomassie blue staining (Figure 5.3, B). The ScFvs from ETH-2 Gold library presented here were selected by Nagjie Alijaj, with the exception of scFv MG6.

5.3.1.2.

### R3 EPFL library

ScFvs were selected against biotinylated mouse VEGFR-2 in two rounds from R3 EPFL library. Positive clones were chosen at random and tested for mVEGFR-2 specificity in ELISA (Figure 5.2, A). The binders with the best ELISA signal were sent for sequencing and scFvs with the unique DNA sequence (Figure 5.2, B) were expressed in large-scale expression. ScFv antibodies were expressed in *E. coli* Mach1 grown in 2xYT medium containing 100 µg/ml chloramphenicol and 0.1% glucose at 37°C until they reached an OD<sub>600</sub> of 0.8. IPTG was added to a final concentration of 1 mM to induce expression of scFv antibodies. Antibodies were purified from lysed cell pellets with Protein A chromatography.

### A) ETH-2 Gold library

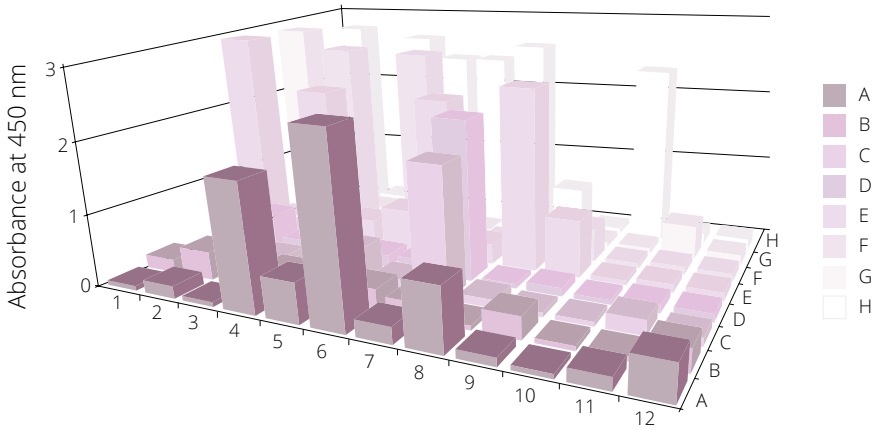


### B)

scFv	V <sub>H</sub>	V <sub>L</sub>	library	Tag	Domain specificity
P1B9	PGANRT	SGAFPA	DP47 DPK22	myc	D7
P1H1	PYVDRS	AGSIPV	DP47 DPK22	myc	D7
P2A11	PSHGRS	AGEFPP	DP47 DPK22	myc	D7
P2C1	PGPNRS	SGNLPP	DP47 DPK22	myc	D7
P1G6	PHWQRA	AGHSPV	DP47 DPK22	myc	D7
P1E8	PGPYRV	SGMLPV	DP47 DPK22	myc	D7

Figure 5.1. ELISA screening of scFvs from ETH-2 Gold library. A) ELISA screening with mouse VEGFR-2 ECD D1 – D7 coated MaxiSorp® plates. Each 96-well plate was incubated with the supernatants of TG1 colonies selected through three rounds of phage display with the ETH-2 Gold library. B) Overview of mouse specific scFv CDR3 sequences with library variants and domain specificity.

A) R3 EPFL library



B)

scFv	V <sub>H</sub>	V <sub>L</sub>	Tag	Domain specificity
A4	G G G P R E	S P S P A	myc	D4-7
A6	L T G S H R	R E N Y P Y	myc	D4-7
C7	P R S V S M	Q F D P P A	myc	D4-7
E1	P Y S M R L	S T I P S	myc	D4-7
E8	A R S L T F	S Y R P A	myc	D4-7
F3	A Y S M K Y	T H P R P T	myc	D4-7
F5	P Y S L T H	D S V G P T	myc	D4-7
G1	P Y R V S M	A Y T M E P L	myc	D4-7
H5	L Y S F R Y	E R Y K P A	myc	D4-7
F3	A Y S M K Y	T H P R P T	myc	D4-7

Figure 5.2. ELISA screening of scFvs from R3 EPFL library. A) ELISA screening with mouse VEGFR-2 ECD D1-D7 coated MaxiSorp® plates. Each 96-well plate was incubated with the supernatants of TG1 colonies selected through two rounds of phage display with the R3 EPFL library. B) Overview of mouse specific scFv CDR3 sequences with domain specificity.

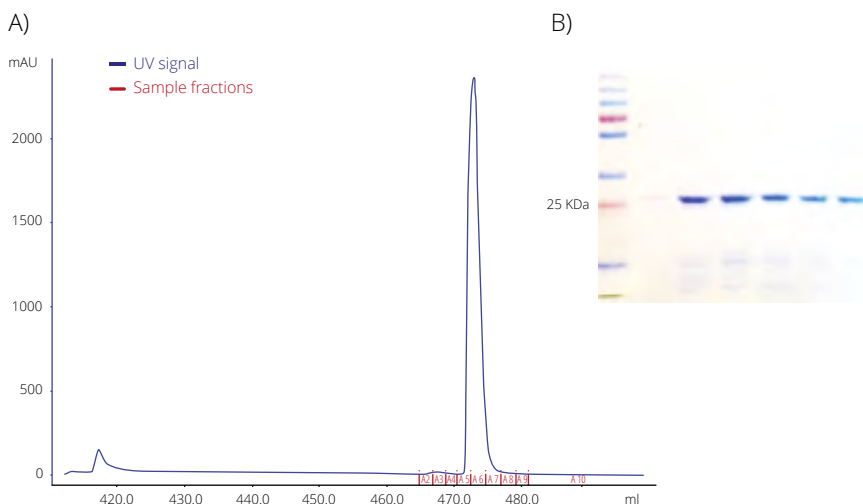


Figure 5.3. Mouse specific scFv purification. A) Elution profile of scFv MG6 after purification by protein A chromatography. B) The eluted peak fractions loaded on 12% polyacrylamide gel and analyzed with a Coomassie blue staining.

### 5.3.2.

## Functional inhibition of VEGFR-2 phosphorylation with mouse specific scFvs

ScFvs (1  $\mu$ M) selected against mouse VEGFR-2 were tested in a kinase activity assay as previously described, using mEnd cells. Activity assay results failed to show that mouse-specific scFvs selected from ETH-2 Gold library inhibited kinase phosphorylation at Y1173 and downstream signaling (Figure 5.4). However, scFv ME8 selected from R3 EPFL inhibited Y1173 phosphorylation of VEGFR-2 (Figure 5.5). The expression and phosphorylation of PLC $\gamma$ , AKT, and ERK were also examined, however, significant inhibition of downstream signaling for any of tested scFvs could not be confirmed. (Figure 5.5, A). All kinase assays were performed in triplicates and quantified with ImageJ software. Quantified data was analyzed with GraphPad (Figure 5.5, B).



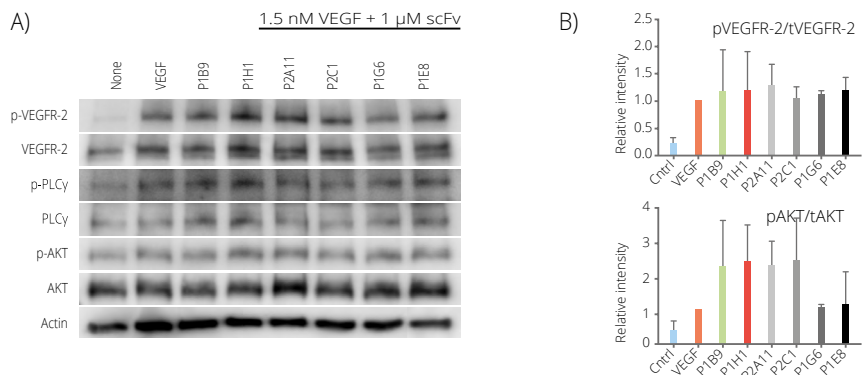
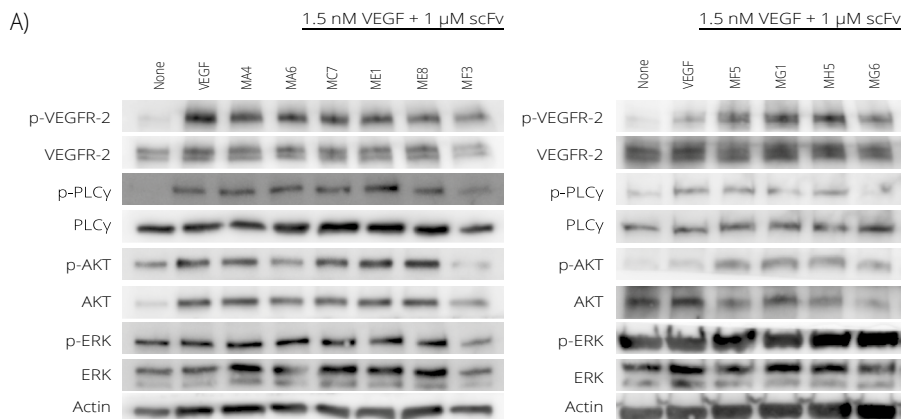


Figure 5.4. Testing of mouse specific scFvs obtained from ETH-2 Gold library. Effect of antibody treatment on VEGF-induced signaling in mEnd cells. A) The ability of scFvs (1  $\mu$ M) to inhibit phosphorylation of VEGFR-2 and AKT was tested in mEnd cells. The western blot data was analyzed and quantified with Image J. B) Quantification of data shown as n-fold increase over VEGF-induced signaling in the absence of mouse-scFv antibodies. Data distribution and statistical analysis were performed using GraphPad, Prism 7. Data distribution and statistical analysis were performed using GraphPad, Prism 7. A representative experiment is shown, out of three independent experiments. Error bars represent  $\pm$  SD. The statistical significance based on a Student's t-test is indicated by \* representing  $P < 0.05$ .



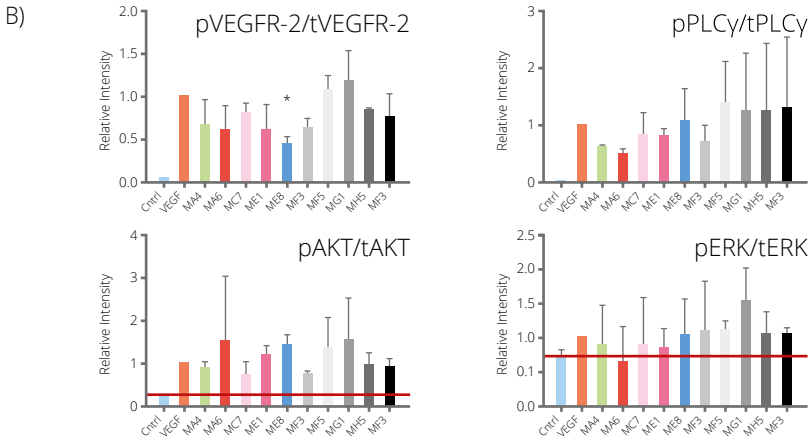


Figure 5.5. Testing of mouse specific scFvs obtained from R3 EPFL library. Effect of antibody treatment on VEGF-induced signaling in mEnd cells. A) The ability of scFvs (1  $\mu$ M) to inhibit phosphorylation of VEGFR-2, PLCy, AKT and ERK was tested in mEnd cells. The western blot data was analyzed and quantified with Image J. B) Quantification of data shown as n-fold increase over VEGF-induced signaling in the absence of mouse-scFv antibodies. Data distribution and statistical analysis were performed using GraphPad, Prism 7. Data distribution and statistical analysis were performed using GraphPad, Prism 7. A representative experiment is shown out of three independent experiments. Error bars represent  $\pm$  SD. The statistical significance based on a Student's t-test is indicated by \* representing  $P < 0.05$ .

5.3.3.

## Effect of antibodies on endothelial cell tube formation

We examined the effect of scFvs on the formation of capillary-like tubes by endothelial cells in Matrigel. mEnd cells were embedded in Matrigel and were treated for 8 h with VEGF in the presence or absence of 1  $\mu$ M of scFvs. Thereafter, the formation of tubes was examined in a phase contrast microscope. Results show that VEGF triggers the formation of a dense network of tubules when added to control mEnd in Matrigel. ScFv MA4 significantly repressed this effect when added (Figure 5.6).

A)

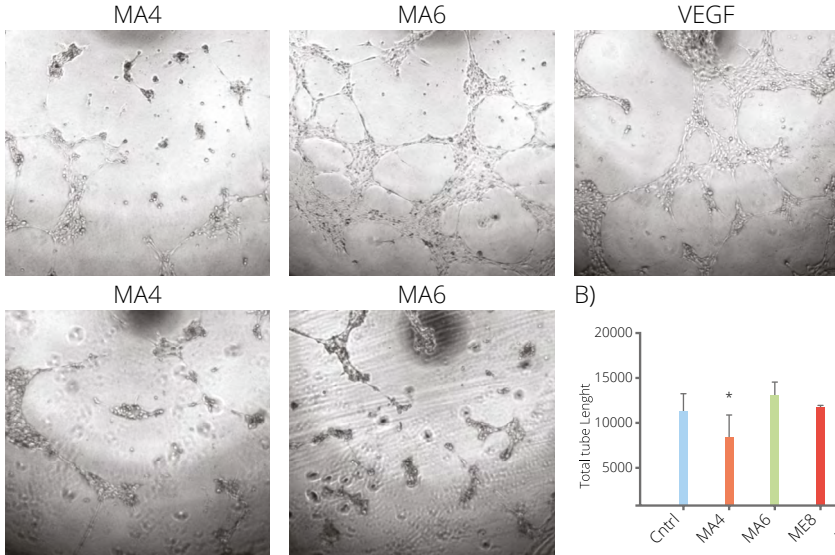


Figure 5.6. Effect of antibody treatment on VEGF-induced capillary-like tube formation in mEnd cells. A) Light microscopy of capillary-like tubes formed in presence and absence of 1  $\mu$ M of mouse-specific scFv antibodies. The total tube length was quantified with Wimasis online software (<http://ibidi.wimasis.com/>) B) Quantification of data shown as n-fold increase over VEGF-induced tube formation in the absence of antibodies. Data distribution and statistical analysis were performed using GraphPad, Prism 7.

5.4.

## Discussion

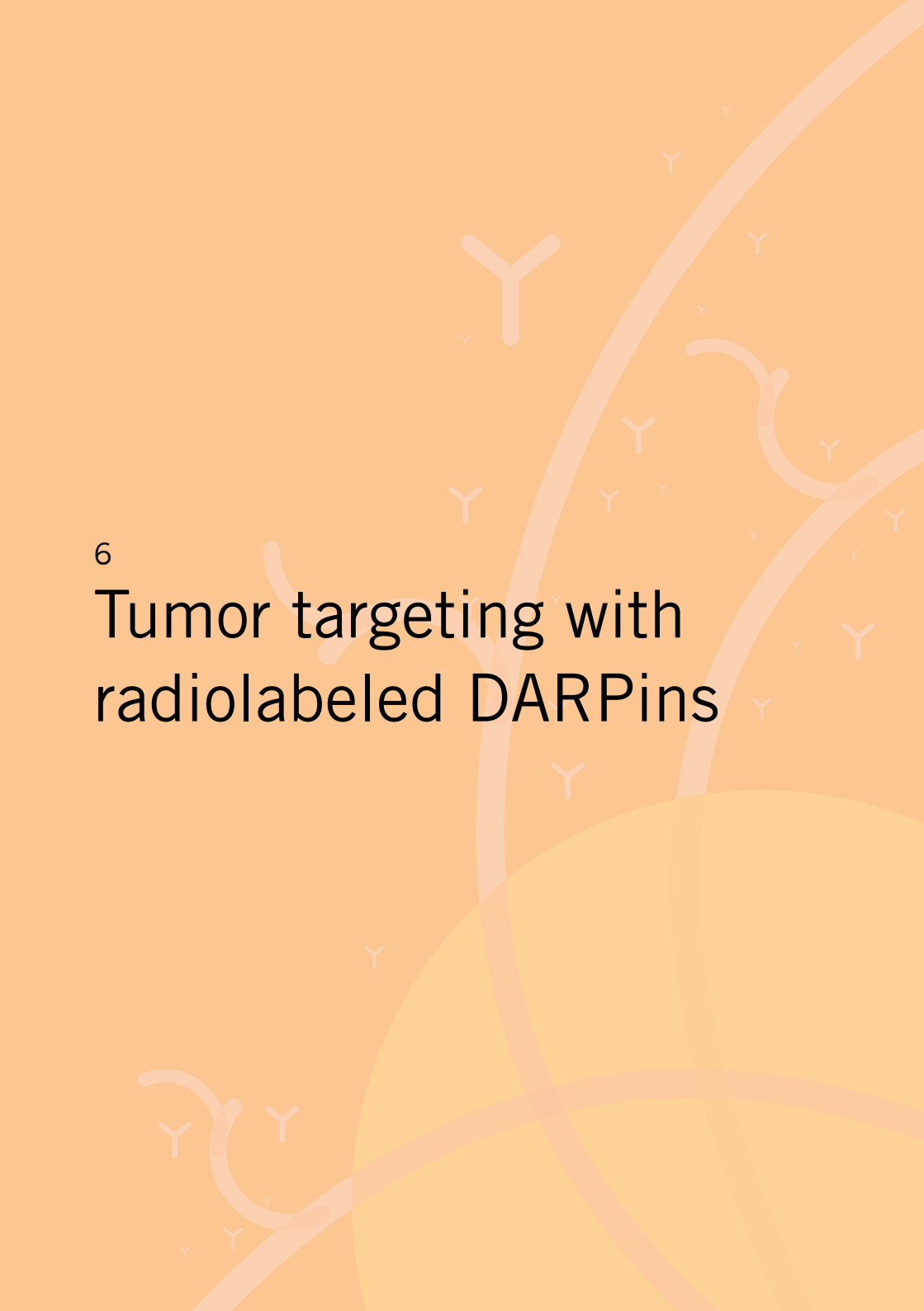
Two phage display libraries were used to select mouse-specific scFvs against mVEGFR-2. From both libraries, we identified 16 scFvs that were shown to bind mVEGFR-2 ECD in ELISA. ME8 showed significant inhibition of VEGFR-2 Y1173 phosphorylation. We also observed an inhibitory effect on endothelial cell tube formation with MA4. Further experiments to test these antibodies from both libraries should be performed in future projects.

Possible applications of mouse-specific scFvs are numerous. Firstly, such antibodies can be explored in preclinical tumor therapy<sup>164</sup>. By inhibiting VEGFR-2 activation, rapidly growing tumors would be deprived of nutrients and oxygen which would ultimately lead to tumor starvation and regression<sup>98,100</sup>. Secondly, these scFvs could be used as delivering platforms for toxins<sup>67</sup> and RNAs<sup>72</sup>. Thirdly, these antibodies can be useful reagents for monitoring the expression of the VEGFR-2 protein in mouse tumor models or in models of other diseases where VEGFR-2 plays a role and could potentially be utilized for vascular targeting and imaging<sup>58,89</sup> during tissue development.



6

# Tumor targeting with radiolabeled DARPins



6.1.

# Introduction

Lately, various antibody-based systems have been developed for noninvasive tumor imaging and tumor-targeted drug delivery<sup>16,55</sup>. VEGFR-2 is a major driver of angiogenesis<sup>165</sup> but it is also reported to be expressed in some cancer cell lines where it potentially plays a role in tumorigenesis<sup>166</sup>. Whether small antibody-like molecules against VEGFR-2 can be used to target the tumor for imaging or drug delivery remains an open question. In this study, radiolabeled Designed Ankyrin Repeat Proteins (DARPs) and xenograft human tumors were used to address this issue. DARPs are recombinant binding proteins composed of ankyrin repeats, which stack together to make a contiguous binding surface<sup>167,168</sup>. Each ankyrin repeat consists of 33 amino acids, which form a  $\beta$ -turn followed by two anti-parallel  $\alpha$ -helices and a loop binding to the  $\beta$ -turn of the next ankyrin repeat. Synthetic DARP libraries have been designed, from which specific binders can be selected and further evolved by methods such as ribosome display<sup>169,170</sup>. Due to their high affinity, receptor specificity and favorable molecular properties, DARPs offer application opportunities in diagnostic imaging and therapy using various conjugates<sup>171,172</sup>. The aim of this study was to evaluate the potential of <sup>99m</sup>Tc-labeled DARPs<sup>154,173,174</sup> designed to target specific domains of the extracellular domain (ECD) of VEGFR-2 for *in vivo* molecular imaging of tumors<sup>104,175</sup>.

6.2.

# Materials and methods

6.2.1.

## Cell lines used in the study

A549 lung cancer cells and SW-480 colon carcinoma cells were maintained in Ham's medium (Bioconcept). PAE KDR, Bovine aortic endothelial (BAE) cells, HeLa cervical carcinoma, OVCAR-3 ovarian cancer, SKOV-3 ovarian cancer, MCF-7 breast cancer and U87 glioblastoma cancer cell lines were cultured in Dulbecco's modified Eagle's medium (DMEM; BioConcept). Both media were supplemented with 10% fetal bovine serum (FBS) and 1% Penicillin–Streptomycin.

6.2.2.

## DARPs

All DARPs were obtained from Molecular Partners (Schlieren, Switzerland) and were previously tested by our group<sup>104</sup>.

6.2.3.

## Fluorescence activated cell sorting (FACS)

Cells propagated in standard culture conditions (described above) were detached from the plate surface by incubation with trypsin (GIBCO). The cell suspension containing 500 000 cells was washed with PBS and blocked with 5% BSA for 1 h at room temperature. Cells were incubated with primary antibody against VEGFR-2 (ab11939; Abcam) for 1 h at room temperature. After 3 washing steps with PBS, cells were incubated with fluorescently labeled secondary (1:10000) Dylight 488 antibody (Abcam) in PBS containing 5% BSA. Cells were sorted with FACS Aria™III (BD Biosciences, Denmark) using the green fluorescent channel.

6.2.4.

## Immunohistochemistry

Excised tumor tissue was collected and frozen, embedded in TissueTek (O.C.T. Compound; Sakura Finetek Europe B.V.), and stored at  $-80^{\circ}\text{C}$ . Frozen tumors were cut into sections of  $10\ \mu\text{m}$  using a microtome (Cryo-Star HM 560 M), fixed in 4% paraformaldehyde for 20 min at RT and blocked for 20 min at RT with 5% BSA. The sections were then incubated with primary VEGFR-2 (ab11939; Abcam) or CD31 antibody (Abcam) overnight at  $4^{\circ}\text{C}$ , followed by exposure to DAB/ $\text{H}_2\text{O}_2$  solution for visualization. Images were obtained on an Olympus IX81 phase-contrast microscope.

6.2.5.

## Labeling of DARPins with $^{99\text{m}}\text{Tc}(\text{CO})_3$

Commercially available molybdenum-99 (Mo-99) generator was used to obtain the decay product of Mo-99, Technetium-99  $^{99\text{m}}\text{Tc}(\text{CO})_3$ . 1 ml of freshly eluted  $^{99\text{m}}\text{TcO}_4$  was mixed with lyophilized sodium tartrate (8.5 mg),  $\text{Na}_2\text{B}_4\text{O}_7 \cdot 10\text{H}_2\text{O}$  (2.85 mg), 7.15 mg of sodium carbonate (7.15 mg) and sodium boranocarbonate (4.5 mg). The mixture was then heated for 40 s at  $150^{\circ}\text{C}$ , and 350  $\mu\text{l}$  neutralizing buffer solution (0.6 M phosphate buffer, pH 7.0 / 1 N HCL, 3:2) was added. DARPins were mixed with  $^{99\text{m}}\text{Tc}(\text{CO})_3$  in 0.125 M MES solution (pH 6.5), and the reaction was incubated at  $37^{\circ}\text{C}$  for 45 minutes. The final product was 100  $\mu\text{l}$  at 30 MBq/ $\mu\text{g}$  DARPIn. The quality control was performed by high-performance liquid chromatography (HPLC).

6.2.6.

## *In vivo* imaging

6.2.6.1.

### Animals

6 to 8 weeks old female athymic nude mice (CD-1 fox nu/nu) were purchased from Charles River Laboratories. (Sulzfeld, Germany). The animals were kept in standard housing conditions under a 12-hour light-dark cycle and provided with food and water *ad libitum*. All animal procedures were approved by the Veterinary Department of the Canton Aargau, Switzerland and performed under the license No. 75528/2010 issued to Dr. Eliane Fischer.

6.2.6.2.

### Cancer cell injections

Mice were injected subcutaneously (s.c.) with human SKOV-3.ip tumor cells subcutaneously injected at the lateral flanks with  $6 \times 10^6$  SKOV-3 cells in 100  $\mu$ l of PBS. When the tumors had reached a size of 0.5–1.5 cm<sup>3</sup>, approximately 21 days post inoculation, the animals were randomly divided into groups ( $n = 4$ /group), and each group was subjected to a different radiolabeled DARPIn derivative.

6.2.6.3.

### Tumor targeting with radiolabeled DARPins

To specifically target tumors, two different approaches and two different protocols were used. First, two DARPins: HSA-06G9 and HSA-NI2C were used (See Table 1). Four animals were used per group. In the second protocol, 3 DARPins were used: HSA-06G9, HSA-06C8, and HSA-07H4 where one-half of the animals were pre-injected with a 20-fold higher concentration of cold (not radioactively labeled) 06G9, 06G9 and 07H4 DARPins. The idea of the second approach was to block the specific signal with an excess of cold (unlabeled DARPins).

6.2.6.4.

### SPECT/CT imaging

Each mouse received a single dose of 10  $\mu$ g of <sup>99m</sup>Tc(CO)<sub>3</sub>-labeled DARPIn variant (300 MBq/mouse) intravenously, via the lateral tail vein in 100  $\mu$ l PBS. Blocking studies were performed with a 20-fold excess of non-labeled DARPIn in PBS and administered instantaneously before the radiotracer. Animals were anaesthetized under 4% isoflurane at time intervals of 2 h, 4 h, or 24 h after injection and immediately imaged. Combined single photon emission computed tomography (SPECT) data were



acquired for 30 min and reconstructed images were generated using the LumaGEM software (version 5.407; Gamma-Medica Inc.). SPECT / computed tomography (CT) imaging experiments were performed with an X-SPECT system (Gamma-Medica Inc.) with a single-head SPECT camera and CT detector. SPECT data were acquired for 30 min and reconstructed images were generated using the LumaGEM software (version 5.407; Gamma-Medica Inc.).

6.2.7.

## Biodistribution

The animals were euthanized, and selected tissues and organs were collected, weighed, and checked for radioactivity in a  $\gamma$ -scintillation counter (Cobra II Packard). The results are presented as the percentage of the injected dose per gram of tissue weight (%ID/g), using reference counts from a definite sample of the original injectate that was counted at the same time.

6.3.

## Results

In this study, we used DARPin-derivatives (Table 6.1) which were additionally modified to carry a human serum albumin-binding entity (HSA) via unique cysteine coupling at the COOH-terminal module. For the blocking study, we used DARPins previously characterized in our group.

DARPins	specificity	MW (Da)	Conc (g/l)
aHSA-06G9	D23	32727.70	11.7
aHSA-06C8	D4	32858.63	12.2
aHSA-07H4	D7	28949.32	9.5
aHSA-NI2C	non-binding	29270.68	11.8

Table 6.1. Overview of biophysical properties of VEGFR-2 ECD targeting DARPins.

To select the most promising tumor model, we performed a FACS analysis to quantify VEGFR-2 expression on the plasma membrane of a panel of tumor cell lines. The VEGFR-2 overexpressing PAE and BAE cell lines were chosen as the positive controls. The glioblastoma cell line U87 was chosen due to its reportedly high expression level of VEGFR-2 *in vivo*<sup>176</sup>. We detected membrane-bound VEGFR-2 in a sub-population of HeLa, MCF-7, SKOV-3 and OVCAR-3 cancer cell lines (Figure 6.1).

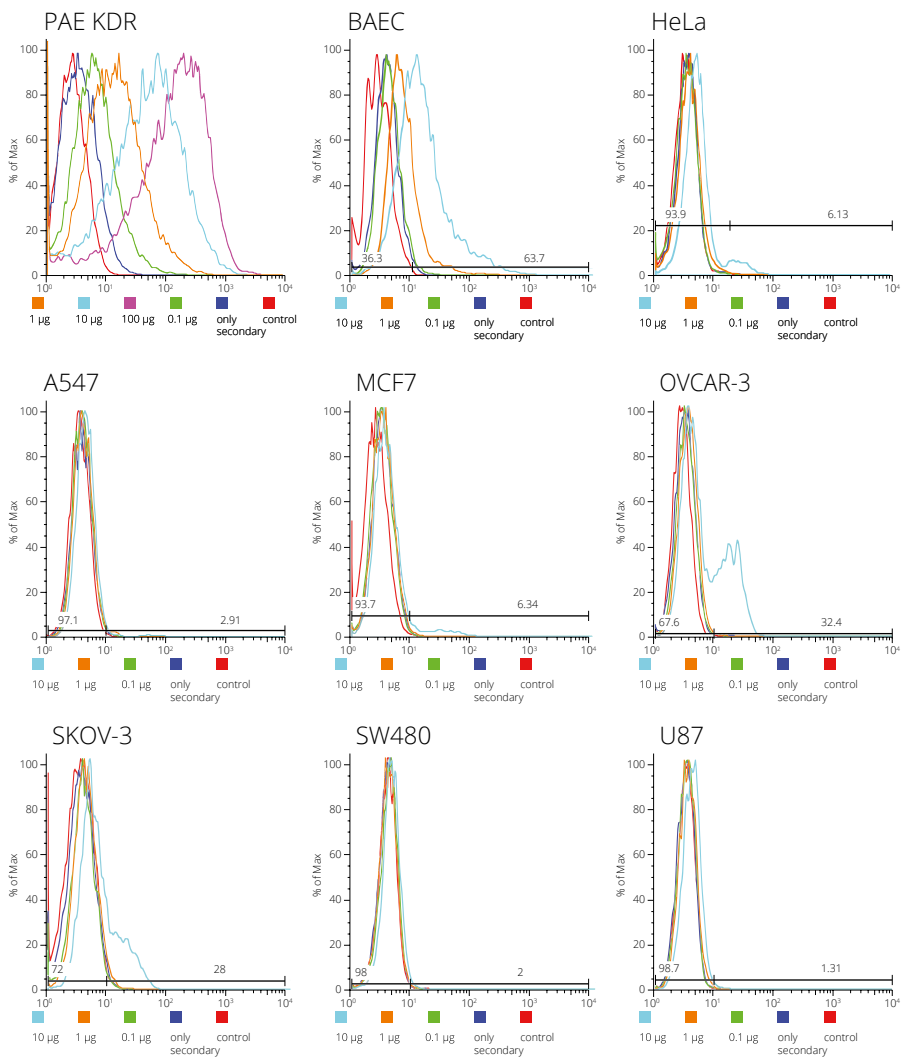


Figure 6.1. FACS analysis of membrane-bound VEGFR-2 on a panel of cancer cell lines.

Considering how the tumor microenvironment additionally influences protein expression in individual cells, an *in vitro* study does not necessarily correlate with *in vivo* expression profiles. For this purpose, tumors of palpable size were further analyzed by immunohistochemistry. HeLa tumor sections were analyzed for VEGFR-2 expression and the presence of blood vasculature by exposure to anti-VEGFR-2 and

anti-CD31 antibodies (Figure 6.2). High level of CD31 expression is an indication of tumor angiogenesis. Tumor tissue sections showed the presence of VEGFR-2 (brown) throughout the tumor mass, and tumor sections were CD31 positive.

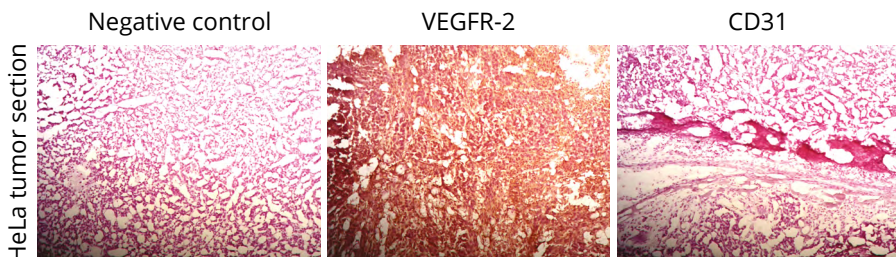


Figure 6.2. VEGFR-2 and CD31 expression levels in mouse tumor models.

To improve serum half-life, HSA-derivatives of each DARPIn variant were selected. DARPins were labeled with  $^{99m}\text{Tc}(\text{CO})_3$  via the  $\text{NH}_2$ -terminal his-tag at pH 6.5. Radiochemical purity was confirmed by the presence of a single radiochemical peak (HPLC), revealing complete incorporation of  $^{99m}\text{Tc}(\text{CO})_3$  with no free reduction products; radiochemical yield was  $\geq 95\%$  for all radioconjugates (Figure 6.3).

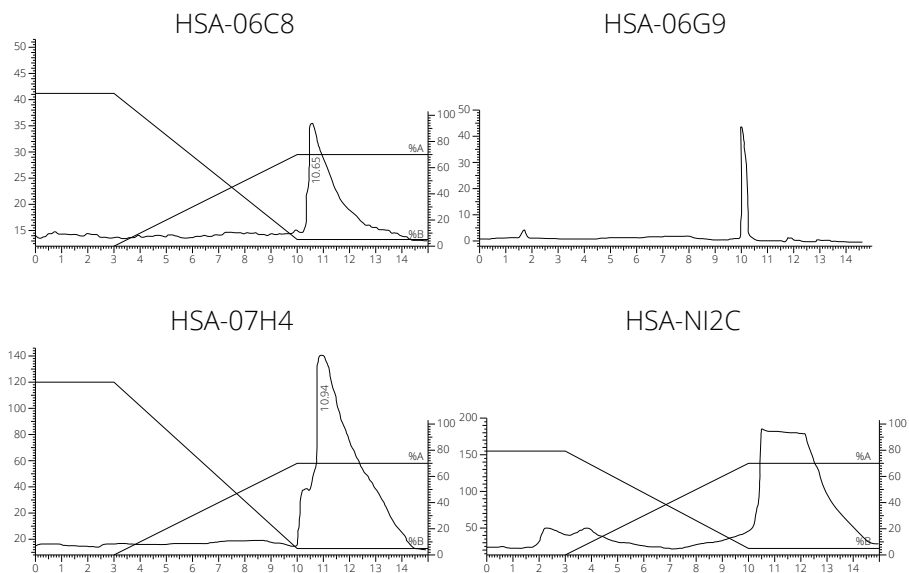


Figure 6.3. Radiochemical purity was determined by HPLC and revealed a single radiochemical peak corresponding to  $^{99m}\text{Tc}$ -labeled DARPins.

Next, SPECT/CT imaging was performed on SKOV-3 tumor-bearing mice injected with radioactively labeled DARPins. A whole-body SPECT/CT of mice bearing tumors was performed 2, 4 and 24 hours after i.v. injection. The scans of mice injected with  $^{99m}\text{Tc}(\text{CO})_3$ -labeled VEGFR-2 targeting DARPins were compared with the scans of the mice injected with  $^{99m}\text{Tc}(\text{CO})_3$ -labeled NI2C DARPIn (Figure 6.4) or mice pre-injected with cold DARPIn. (Figure 6.5). In all mice, high accumulation of radioactivity was detected in kidneys. Traceable radioactivity was detected in tumors, also in studies with non-binding DARPins (NI2C) and in the control group injected with an excess of cold DARPins.

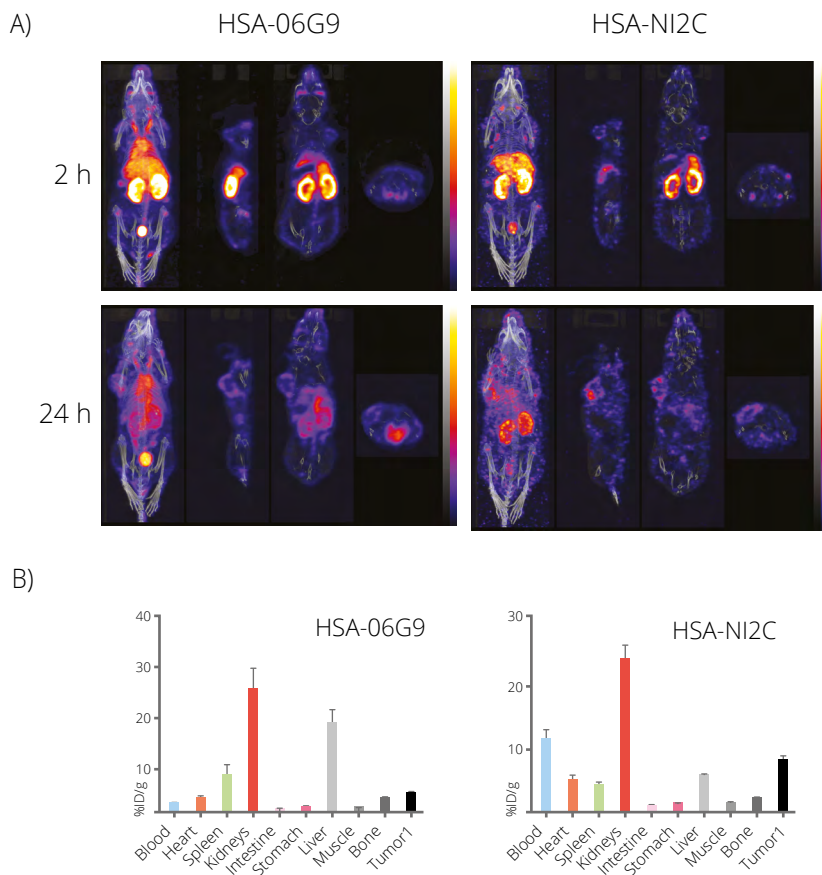
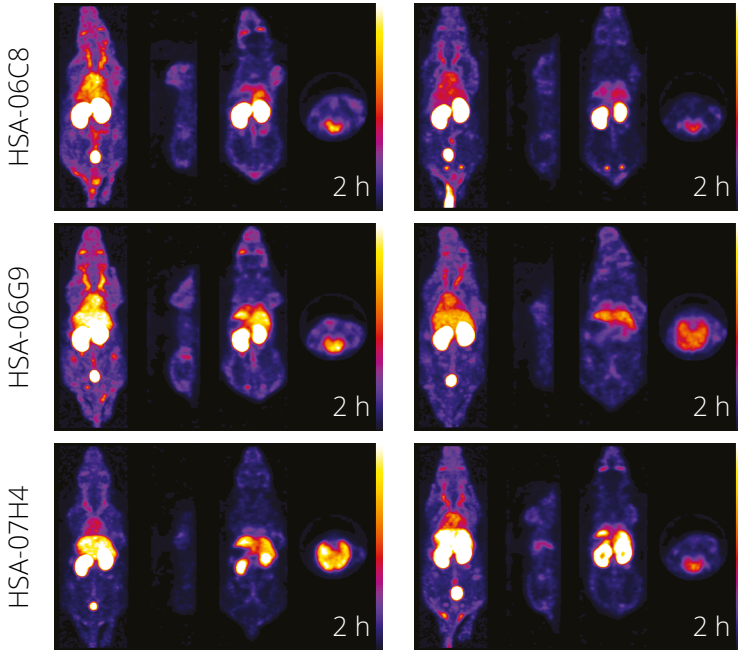


Figure 6.4. SPECT/CT images and biodistribution of anti-VEGFR-2  $^{99m}\text{Tc}$ -DARPins on SKOV-3 tumor-bearing mice. (A) SPECT/CT images of  $^{99m}\text{Tc}$ -labeled HSA-06G9 and NI2C. (B) Post-mortem biodistribution analysis.

A)

Blocked with cold DARPin



B)

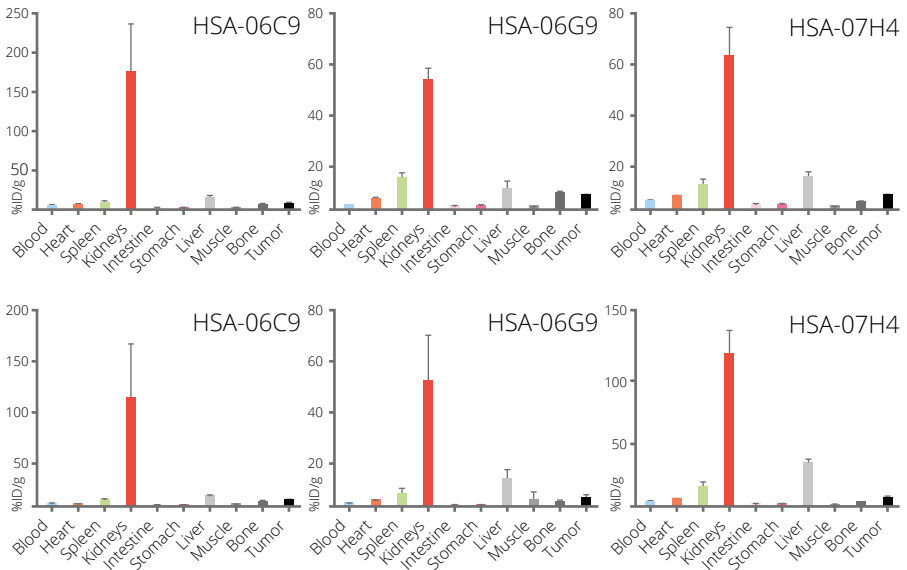


Figure 6.5. SPECT/CT images and biodistribution of anti-VEGFR-2  $^{99m}\text{Tc}(\text{CO})_3$ -DARPin on SKOV-3 tumor-bearing mice. (A) SPECT/CT images of  $^{99m}\text{Tc}(\text{CO})_3\text{HSA-06G9}$ ,  $\text{HSA-06C8}$ , and  $\text{HSA-07H4}$ . (B) Post-mortem biodistribution analysis.

6.4.

## Discussion

The goals of this study were to quantitatively test the ability of DARPins to target xenografted tumors in mice, examine if the optimal tumor-targeting format of DARPin is the HSA-derivative and evaluate if VEGFR-2 can be used as a tumor marker for *in vivo* imaging<sup>174</sup>. Due to its high affinity and small size, it was proposed that DARPins would be efficient tools for *in vivo* imaging<sup>172</sup> of xenograft tumors. In a pilot study (data not shown) fast blood clearance of DARPins was observed. Therefore, DARPin derivatives which contained an additional serum albumin binding entity attached to their C-terminus were employed. Although HSA-derivatives significantly prolonged blood circulation with notable levels of radioactivity still present at 24 h post injection, the increase in size due to the serum albumin-binding entity also led to non-specific accumulation in the tumor. To address this issue a second study was performed with the goal to block specific tumor intake<sup>177</sup>. However, no specific blocking of the radioactive signal in tumors was demonstrated.

A possible explanation is that the performance of DARPins *in vivo* was not as described *in vitro* and that DARPins simply don't reach VEGFR-2 in tumors in the mouse model used. High radioactivity in liver and kidney gives information about the elimination pathway of the DARPins. As expected, the small DARPins are predominantly eliminated via the kidney. High kidney values are observed for all monovalent DARPins, similar to scFv fragments<sup>173,178,179</sup> and camel  $V_{\text{H}}\text{H}$  domains<sup>180</sup>. Second possible explanation could be that the level of VEGF-2 expressed in SKOV-3 xenograft tumors was not high enough. To conclude, we failed to show that highly specific *in vitro* validated VEGFR-2 DARPins represent a potential tool for tumor imaging.

7

# Conclusions and Outlook



# Conclusions and Outlook

The concept that tumors are dependent on surrounding blood vessels and the idea that inhibiting the formation of new blood vasculature in cancer might inhibit the tumor appeared almost 40 years ago. Since then, a variety of anti-angiogenic drugs have been developed, and many of them have entered clinical trials. A promising target for anti-angiogenic therapies remains VEGFR-2, as the primary mediator of angiogenic signaling. Inhibiting VEGFR-2 is the main goal of this thesis. Although the evident purpose of this work was aimed at tumor angiogenesis inhibition, the inhibitors characterized herein, could be used for other angiogenesis-dependent conditions such as macular degeneration, diabetic retinopathy, atherosclerosis, rheumatoid arthritis, and other diseases. The study comprised generation and characterization of novel binders to the ECD of VEGFR-2 in different antibody formats such as scFvs, Fabs and IgGs that bind to D23, D6 or D7 and inhibit VEGFR-2 in an allosteric fashion not interfering with ligand-binding. The inhibitors in scFv, Fab, and IgG formats could have potential in clinical applications such as in tumor vasculature imaging, or as drug delivery platforms to inhibit angiogenesis. Imaging in live mice could be carried out with different technologies such as positron emission tomography (PET) or single-photon emission computed tomography (SPECT) using tagged variants of the scFvs and Fabs. Bioconjugation of the scFv to drugs for site-specific delivery of these drugs represents another possible use. Furthermore, the potential of using the full-length IgGs as angiogenesis inhibitors *in vivo* can be tested in HUVEC plug assays<sup>181</sup> in mouse models. In the end, the ability of DARPins to target xenografted tumors in mice was quantitatively tested and it was examined if the optimal tumor targeting format of DARPins is the HSA-derivative; it was also evaluated whether VEGFR-2 can be used as a tumor marker for *in vivo* imaging<sup>174</sup>. In two *in vivo* studies, it was not demonstrated that the highly VEGFR-2 specific DARPins would be promising tools for tumor imaging. The inhibitors described herein should be tested for application in VEGFR-2-induced ophthalmic pathologies and might represent alternatives to existing VEGF-inhibitory drugs<sup>182-184</sup>.



8

# Acknowledgements



# Acknowledgements

First and foremost, I would like to express my sincere gratitude to my advisor Prof. Dr. Kurt Ballmer-Hofer for giving me the opportunity to pro-actively and independently design and conduct my research on a highly stimulating subject matter, at the interface of basic research and translational medicine. I am also thankful to Prof. Dr. Gerhard M. Cristofori, official supervisor of my PhD thesis at the Basel University and PD Dr. med. Andrea Banfi, co-referee for their insightful comments and encouragement.

Extended thanks and acknowledgement of contributions go out to the following individuals from LBR and Radio Pharmacy group, who all played a pivotal role in making these past four years at PSI a better experience: in alphabetical order, Dr. Roger Benoit, Alain Blanc, Susan Cohrs, Daniel Frey, Antonietta Gasperina, Dr. Jürgen Grünberg, Dr. Anil Kumar, Dr. Lindenblatt Dennis, Daniel Mayer, Marcel Stangier, Prof Gebhard Schertler, Ulla Suter and Živa Vučkovič.

I thank my fellow lab mates for the endless practical help, stimulating discussions, and for all the fun we have had in the last four years in alphabetical order, Mayanka Asthana, Milica Bugarski, Dr. Philipp Berger, Dr. Caroline Hyde, Dr. Petra Hillmann-Wüllner, Julia Kostin, Dr. Sandro Manni, Dr. Sandra Marković-Müller, Dr. Maysam Mansouri, Dr. Maria Mitsi, Dr. Aurélien Rizk, Thomas Schleier, Katherine Thieltges, Cornelia Walther and Ye Xie. Special thanks to Nagjie Alijaj, Monigatti Massimo, Jonas Mechttersheimer and Sophie Huber who have been directly involved in the research and contributed with their hard work to the completion of my thesis.

Finally, I would like to express my sincere appreciation to my family. To my mother, father, and brother who have always been a great support and motivation. And, most importantly, to my partner Vukašin Nešović who has shown nothing but support and necessary encouragement in difficult moments.

9

# References



# References

1. Bittar, E. *Immunobiology*. (Elsevier, 1996).
2. Vidarsson, G., Dekkers, G. & Rispens, T. IgG subclasses and allotypes: from structure to effector functions. *Front Immunol* **5**, 520 (2014).
3. Copstead-Kirkhorn, L.-E. C. & Banasik, J. L. *Pathophysiology*. (Elsevier Health Sciences, 2014).
4. Harris, L. J., Skaletsky, E. & McPherson, A. Crystallographic structure of an intact IgG1 monoclonal antibody. *J. Mol. Biol.* **275**, 861–872 (1998).
5. Rogozin, I. B., Solovyov, V. V. & Kolchanov, N. A. Somatic hypermutagenesis in immunoglobulin genes. I. Correlation between somatic mutations and repeats. Somatic mutation properties and clonal selection. *Biochim. Biophys. Acta* **1089**, 175–182 (1991).
6. Morgan, G. & Levinsky, R. J. Monoclonal antibodies in diagnosis and treatment. *Arch. Dis. Child.* **60**, 96–98 (1985).
7. Köhler, G. & Milstein, C. *Continuous cultures of fused cells secreting antibody of predefined specificity*. 1975. *Journal of immunology (Baltimore, Md. : 1950)* **174**, 2453–2455 (2005).
8. Kontermann, R. E. & Dübel, S. *Antibody Engineering*. (Springer Science & Business Media, 2010). doi:10.1007/978-3-642-01144-3
9. Boss, M. A., Kenten, J. H., Wood, C. R. & Emtage, J. S. Assembly of functional antibodies from immunoglobulin heavy and light chains synthesised in *E. coli*. *Nucleic Acids Res.* **12**, 3791–3806 (1984).
10. Cabilly, S. *et al.* Generation of antibody activity from immunoglobulin polypeptide chains produced in *Escherichia coli*. *Proc. Natl. Acad. Sci. U.S.A.* **81**, 3273–3277 (1984).
11. Kinoshita, K. & Honjo, T. Linking class-switch recombination with somatic hypermutation. *Nature Reviews Molecular Cell Biology* **2**, 493–503 (2001).
12. Michnick, S. W. & Sidhu, S. S. Submitting antibodies to binding arbitration. *Nature Chemical Biology* **4**, 326–329 (2008).
13. Huston, J. S. *et al.* Protein engineering of antibody binding sites: recovery of specific activity in an anti-digoxin single-chain Fv analogue produced in *Escherichia coli*. *Proc. Natl. Acad. Sci. U.S.A.* **85**, 5879–5883 (1988).
14. Griffiths, A. D. *et al.* Isolation of high affinity human antibodies directly from large synthetic repertoires. *EMBO J.* **13**, 3245–3260 (1994).
15. Galeffi, P. *et al.* Functional expression of a single-chain antibody to ErbB-2 in plants and cell-free systems. *J Transl Med* **4**, 39 (2006).
16. Chaudhary, V. K. *et al.* A recombinant immunotoxin consisting of two antibody variable domains fused to *Pseudomonas* exotoxin. *Nature* **339**, 394–397 (1989).
17. Deng, X. K., Nesbit, L. A. & Morrow, K. J. Recombinant single-chain variable fragment antibodies directed against *Clostridium difficile* toxin B produced by use of an optimized phage display system. *Clin. Diagn. Lab. Immunol.* **10**, 587–595 (2003).

18. Clackson, T., Hoogenboom, H. R., Griffiths, A. D. & Winter, G. Making antibody fragments using phage display libraries. *Nature* **352**, 624–628 (1991).
19. Chaudhary, V. A rapid method of cloning functional variable-region antibody genes in *Escherichia coli* as single-chain immunotoxins. *Proc. Natl. Acad. Sci. U.S.A.* **87**, 1066–1070 (1990).
20. Finlay, W. J. J., Shaw, I., Reilly, J. P. & Kane, M. Generation of high-affinity chicken single-chain Fv antibody fragments for measurement of the *Pseudonitzschia pungens* toxin domoic acid. *Appl. Environ. Microbiol.* **72**, 3343–3349 (2006).
21. Zhang, J.-L. *et al.* Screening and evaluation of human single-chain fragment variable antibody against hepatitis B virus surface antigen. *HBPD INT* **5**, 237–241 (2006).
22. Marks, J. D. in *Antibody Engineering* **248**, 327–344 (Humana Press, 2003).
23. Shadidi, M. & Sioud, M. An anti-leukemic single chain Fv antibody selected from a synthetic human phage antibody library. *Biochem. Biophys. Res. Commun.* **280**, 548–552 (2001).
24. Ho, M., Nagata, S. & Pastan, I. Isolation of anti-CD22 Fv with high affinity by Fv display on human cells. *Proc. Natl. Acad. Sci. U.S.A.* **103**, 9637–9642 (2006).
25. Gram, H., Schmitz, R. & Ridder, R. in *Pichia Protocols* **103**, 179–192 (Humana Press, 1998).
26. Choo, A. B. H., Dunn, R. D., Broady, K. W. & Raison, R. L. Soluble expression of a functional recombinant cytolytic immunotoxin in insect cells. *Protein Expr. Purif.* **24**, 338–347 (2002).
27. Knaust, R. K. & Nordlund, P. Screening for soluble expression of recombinant proteins in a 96-well format. *Anal. Biochem.* **297**, 79–85 (2001).
28. Lesley, S. A. High-throughput proteomics: protein expression and purification in the postgenomic world. *Protein Expr. Purif.* **22**, 159–164 (2001).
29. Buchner, J. & Rudolph, R. Routes to active proteins from transformed microorganisms. *Current Opinion in Biotechnology* **2**, 532–538 (1991).
30. Bird, R. E. *et al.* Single-chain antigen-binding proteins. *Science* **242**, 423–426 (1988).
31. Skerra, A. & Plückthun, A. Assembly of a functional immunoglobulin Fv fragment in *Escherichia coli*. *Science* **240**, 1038–1041 (1988).
32. Better, M., Chang, C. P., Robinson, R. R. & Horwitz, A. H. *Escherichia coli* secretion of an active chimeric antibody fragment. *Science* **240**, 1041–1043 (1988).
33. Baneyx, F. Recombinant protein expression in *Escherichia coli*. *Current Opinion in Biotechnology* **10**, 411–421 (1999).
34. Jain, M., Kamal, N. & Batra, S. K. Engineering antibodies for clinical applications. *Trends Biotechnol.* **25**, 307–316 (2007).
35. Giménez-Llort, L., Rivera-Hernández, G., Marin-Argany, M., Sánchez-Quesada, J. L. & Villegas, S. Early intervention in the 3xTg-AD mice with an amyloid  $\beta$ -antibody fragment ameliorates first hallmarks of Alzheimer disease. *MAbs* **5**, 665–677 (2013).
36. Singh, A., Poshtiban, S. & Evoy, S. Recent advances in bacteriophage based

- biosensors for food-borne pathogen detection. *Sensors (Basel)* **13**, 1763–1786 (2013).
37. Smith, G. P. Filamentous fusion phage: novel expression vectors that display cloned antigens on the virion surface. *Science* **228**, 1315–1317 (1985).
  38. McCafferty, J., Griffiths, A. D., Winter, G. & Chiswell, D. J. Phage antibodies: filamentous phage displaying antibody variable domains. *Nature* **348**, 552–554 (1990).
  39. Wu, C.-C. *et al.* Identification of a new peptide for fibrosarcoma tumor targeting and imaging in vivo. *J. Biomed. Biotechnol.* **2010**, 167045–10 (2010).
  40. Wieland, W. H., Orzáez, D., Lammers, A., Parmentier, H. K. & Schots, A. Display and selection of chicken IgA Fab fragments. *Vet. Immunol. Immunopathol.* **110**, 129–140 (2006).
  41. Sheikholvaezin, A. *et al.* Optimizing the generation of recombinant single-chain antibodies against placental alkaline phosphatase. *Hybridoma (Larchmt)* **25**, 181–192 (2006).
  42. Takemura, S. *et al.* Construction of a diabody (small recombinant bispecific antibody) using a refolding system. *Protein Eng.* **13**, 583–588 (2000).
  43. Vaughan, T. J. *et al.* Human antibodies with sub-nanomolar affinities isolated from a large non-immunized phage display library. *Nat. Biotechnol.* **14**, 309–314 (1996).
  44. Sheets, M. D. *et al.* Efficient construction of a large nonimmune phage antibody library: the production of high-affinity human single-chain antibodies to protein antigens. *Proc. Natl. Acad. Sci. U.S.A.* **95**, 6157–6162 (1998).
  45. Winter, G., Griffiths, A. D., Hawkins, R. E. & Hoogenboom, H. R. Making antibodies by phage display technology. *Annu. Rev. Immunol.* **12**, 433–455 (1994).
  46. Knappik, A. *et al.* Fully synthetic human combinatorial antibody libraries (HuCAL) based on modular consensus frameworks and CDRs randomized with trinucleotides. *J. Mol. Biol.* **296**, 57–86 (2000).
  47. Hanes, J. & Plückthun, A. In vitro selection and evolution of functional proteins by using ribosome display. *Proc. Natl. Acad. Sci. U.S.A.* **94**, 4937–4942 (1997).
  48. Hanes, J., Schaffitzel, C., Knappik, A. & Plückthun, A. Picomolar affinity antibodies from a fully synthetic naive library selected and evolved by ribosome display. *Nat. Biotechnol.* **18**, 1287–1292 (2000).
  49. Hoogenboom, H. R. & Chames, P. Natural and designer binding sites made by phage display technology. *Immunol. Today* **21**, 371–378 (2000).
  50. Kumada, Y., Sasaki, E. & Kishimoto, M. Preparation of scFv-immobilized quartz crystal microbalance sensor by PS-tag-mediated solid-phase refolding. *J. Biosci. Bioeng.* **111**, 459–464 (2011).
  51. Lindner, P. *et al.* Specific detection of his-tagged proteins with recombinant anti-His tag scFv-phosphatase or scFv-phage fusions. *BioTechniques* **22**, 140–149 (1997).
  52. Klimka, A. *et al.* An anti-CD30 single-chain Fv selected by phage display and fused to Pseudomonas exotoxin A (Ki-4(scFv)-ETA) is a potent immunotoxin against a Hodgkin-derived cell line. *Br. J. Cancer* **80**, 1214–1222 (1999).

53. Kobayashi, N. *et al.* Generation of a single-chain Fv fragment for the monitoring of deoxycholic acid residues anchored on endogenous proteins. *Steroids* **70**, 285–294 (2005).
54. Marks, J. D. *et al.* By-passing immunization. Human antibodies from V-gene libraries displayed on phage. *J. Mol. Biol.* **222**, 581–597 (1991).
55. Mendler, C. T. *et al.* High contrast tumor imaging with radio-labeled antibody Fab fragments tailored for optimized pharmacokinetics via PASylation. *MAbs* **7**, 96–109 (2015).
56. Rosenblum, L. T., Choyke, P. L. & Kobayashi, H. Quantitative and specific molecular imaging of cancer with labeled engineered monoclonal antibody fragments. *Ther Deliv* **2**, 345–358 (2011).
57. Yokota, T., Milenic, D. E., Whitlow, M. & Schlom, J. Rapid tumor penetration of a single-chain Fv and comparison with other immunoglobulin forms. *Cancer Res.* **52**, 3402–3408 (1992).
58. Stipsanelli, E. & Valsamaki, P. Monoclonal antibodies: old and new trends in breast cancer imaging and therapeutic approach. *Hell J Nucl Med* **8**, 103–108 (2005).
59. Oriuchi, N., Higuchi, T., Hanaoka, H., Iida, Y. & Endo, K. Current status of cancer therapy with radiolabeled monoclonal antibody. *Ann Nucl Med* **19**, 355–365 (2005).
60. Marasco, W. & Dana Jones S. Antibodies for targeted gene therapy: extra-cellular gene targeting and intracellular expression. *Adv. Drug Deliv. Rev.* **31**, 153–170 (1998).
61. Krebs, B. *et al.* High-throughput generation and engineering of recombinant human antibodies. *J. Immunol. Methods* **254**, 67–84 (2001).
62. Deckert, P. M. Current constructs and targets in clinical development for antibody-based cancer therapy. *Curr Drug Targets* **10**, 158–175 (2009).
63. Ferris, R. L., Jaffee, E. M. & Ferrone, S. Tumor antigen-targeted, monoclonal antibody-based immunotherapy: clinical response, cellular immunity, and immunoescape. *J. Clin. Oncol.* **28**, 4390–4399 (2010).
64. Han, T. *et al.* Human anti-CCR4 minibody gene transfer for the treatment of cutaneous T-cell lymphoma. *PLoS ONE* **7**, e44455 (2012).
65. Olkhanud, P. B. *et al.* Breast cancer lung metastasis requires expression of chemokine receptor CCR4 and regulatory T cells. *Cancer Res.* **69**, 5996–6004 (2009).
66. Curiel, T. J. *et al.* Specific recruitment of regulatory T cells in ovarian carcinoma fosters immune privilege and predicts reduced survival. *Nature Medicine* **10**, 942–949 (2004).
67. Liu, W. *et al.* Recombinant immunotoxin engineered for low immunogenicity and antigenicity by identifying and silencing human B-cell epitopes. *Proc. Natl. Acad. Sci. U.S.A.* **109**, 11782–11787 (2012).
68. Kreitman, R. J. *et al.* Phase I trial of anti-CD22 recombinant immunotoxin moxetumomab pasudotoc (CAT-8015 or HA22) in patients with hairy cell leukemia. *J. Clin. Oncol.* **30**, 1822–1828 (2012).
69. Hassan, R. *et al.* Phase I Study of SS1P, a Recombinant Anti-Mesothelin Immunotoxin Given as a Bolus I.V. Infusion to Patients with Mesothelin-Ex-

- pressing Mesothelioma, Ovarian, and Pancreatic Cancers. *Clinical Cancer Research* **13**, 5144–5149 (2007).
70. Kuroki, M. *et al.* Specific targeting strategies of cancer gene therapy using a single-chain variable fragment (scFv) with a high affinity for CEA. *Anticancer Res.* **20**, 4067–4071 (2000).
  71. Li, X., Stuckert, P., Bosch, I., Marks, J. D. & Marasco, W. A. Single-chain antibody-mediated gene delivery into ErbB2-positive human breast cancer cells. *Cancer Gene Ther.* **8**, 555–565 (2001).
  72. Curigliano, G. *et al.* Vaccine immunotherapy in breast cancer treatment: promising, but still early. *Expert Review of Anticancer Therapy* **7**, 1225–1241 (2014).
  73. Soliman, H. Immunotherapy strategies in the treatment of breast cancer. *Cancer Control* **20**, 17–21 (2013).
  74. Alvarez, R. D. *et al.* A cancer gene therapy approach utilizing an anti-erbB-2 single-chain antibody-encoding adenovirus (AD21): a phase I trial. *Clinical Cancer Research* **6**, 3081–3087 (2000).
  75. Strube, R. W. & Chen, S.-Y. Characterization of anti-cyclin E single-chain Fv antibodies and intrabodies in breast cancer cells: enhanced intracellular stability of novel sFv-Fc intrabodies. *J. Immunol. Methods* **263**, 149–167 (2002).
  76. van der Meel, R., Vehmeijer, L. J. C., Kok, R. J., Storm, G. & van Gaal, E. V. B. Ligand-targeted particulate nanomedicines undergoing clinical evaluation: Current status. *Adv. Drug Deliv. Rev.* **65**, 1284–1298 (2013).
  77. Hardy, J. & Allsop, D. Amyloid deposition as the central event in the aetiology of Alzheimer's disease. *Trends in Pharmacological Sciences* **12**, 383–388 (1991).
  78. Alzheimer's disease: the amyloid cascade hypothesis. (1992).
  79. Robert, R. *et al.* Engineered antibody intervention strategies for Alzheimer's disease and related dementias by targeting amyloid and toxic oligomers. *Protein Eng. Des. Sel.* **22**, 199–208 (2009).
  80. Robert, R. & Wark, K. L. Engineered antibody approaches for Alzheimer's disease immunotherapy. *Arch. Biochem. Biophys.* **526**, 132–138 (2012).
  81. Ryan, D. A. *et al.* A $\beta$ -directed Single-chain Antibody Delivery Via a Serotype-1 AAV Vector Improves Learning Behavior and Pathology in Alzheimer's Disease Mice. *Molecular Therapy* **18**, 1471–1481 (2010).
  82. Wang, Y.-J. *et al.* Intramuscular delivery of a single chain antibody gene reduces brain Abeta burden in a mouse model of Alzheimer's disease. *Neurobiol. Aging* **30**, 364–376 (2009).
  83. Wang, Y.-J. *et al.* Intramuscular delivery of a single chain antibody gene prevents brain A $\beta$  deposition and cognitive impairment in a mouse model of Alzheimer's disease. *Brain, Behavior, and Immunity* **24**, 1281–1293 (2010).
  84. Frenkel, D. & Solomon, B. Filamentous phage as vector-mediated antibody delivery to the brain. *Proceedings of the National Academy of Sciences* **99**, 5675–5679 (2002).
  85. Cattepoel, S., Hanenberg, M., Kulic, L. & Nitsch, R. M. Chronic Intranasal Treatment with an Anti-A $\beta$ 30-42 scFv Antibody Ameliorates Amyloid Pa-



- thology in a Transgenic Mouse Model of Alzheimer's Disease. *PLoS ONE* **6**, e18296 (2011).
86. Xu, L., Jin, B.-Q. & Fan, D.-M. Selection and identification of mimic epitopes for gastric cancer-associated antigen MG7 Ag. *Mol. Cancer Ther.* **2**, 301–306 (2003).
  87. Rahbarizadeh, F., Rasaee, M. J., Forouzandeh Moghadam, M., Allameh, A. A. & Sadroddiny, E. Production of novel recombinant single-domain antibodies against tandem repeat region of MUC1 mucin. *Hybrid. Hybridomics* **23**, 151–159 (2004).
  88. Choi, S., Lee, J., Kumar, P., Lee, K. Y. & Lee, S.-K. Single chain variable fragment CD7 antibody conjugated PLGA/HDAC inhibitor immuno-nanoparticles: developing human T cell-specific nano-technology for delivery of therapeutic drugs targeting latent HIV. *J Control Release* **152 Suppl 1**, e9–10 (2011).
  89. Kobayashi, N. *et al.* Toward in Vivo Imaging of Heart Disease Using a Radio-labeled Single-Chain Fv Fragment Targeting Tenascin-C. *Analytical Chemistry* **83**, 9123–9130 (2011).
  90. Xu, W., Liu, L., Brown, N. J., Christian, S. & Hornby, D. Quantum Dot- Conjugated Anti-GRP78 scFv Inhibits Cancer Growth in Mice. *Molecules* **17**, 796–808 (2012).
  91. Sato, Y. *et al.* Genetically encoded system to track histone modification in vivo. *Scientific Reports* **3**, 2436 (2013).
  92. Tanenbaum, M. E., Gilbert, L. A., Qi, L. S., Weissman, J. S. & Vale, R. D. A Protein-Tagging System for Signal Amplification in Gene Expression and Fluorescence Imaging. *Cell* **159**, 635–646 (2014).
  93. Vigor, K. L. *et al.* Nanoparticles functionalised with recombinant single chain Fv antibody fragments (scFv) for the magnetic resonance imaging of cancer cells. *Biomaterials* **31**, 1307–1315 (2010).
  94. Kontermann, R. E., Wing, M. G. & Winter, G. Complement recruitment using bispecific diabodies. *Nat. Biotechnol.* **15**, 629–631 (1997).
  95. Emanuel, P. A. *et al.* Recombinant antibodies: a new reagent for biological agent detection. *Biosens Bioelectron* **14**, 751–759 (2000).
  96. Griep, R. A., van Twisk, C., van der Wolf, J. M. & Schots, A. Fluobodies: green fluorescent single-chain Fv fusion proteins. *J. Immunol. Methods* **230**, 121–130 (1999).
  97. Oelschlaeger, P., Srikant-Iyer, S., Lange, S., Schmitt, J. & Schmid, R. D. Fluorophor-linked immunosorbent assay: a time- and cost-saving method for the characterization of antibody fragments using a fusion protein of a single-chain antibody fragment and enhanced green fluorescent protein. *Anal. Biochem.* **309**, 27–34 (2002).
  98. Folkman, J. Tumor angiogenesis: therapeutic implications. *N. Engl. J. Med.* **285**, 1182–1186 (1971).
  99. Yang, Y., Xie, P., Opatowsky, Y. & Schlessinger, J. Direct contacts between extracellular membrane-proximal domains are required for VEGF receptor activation and cell signaling. *Proceedings of the National Academy of Sciences* **107**, 1906–1911 (2010).

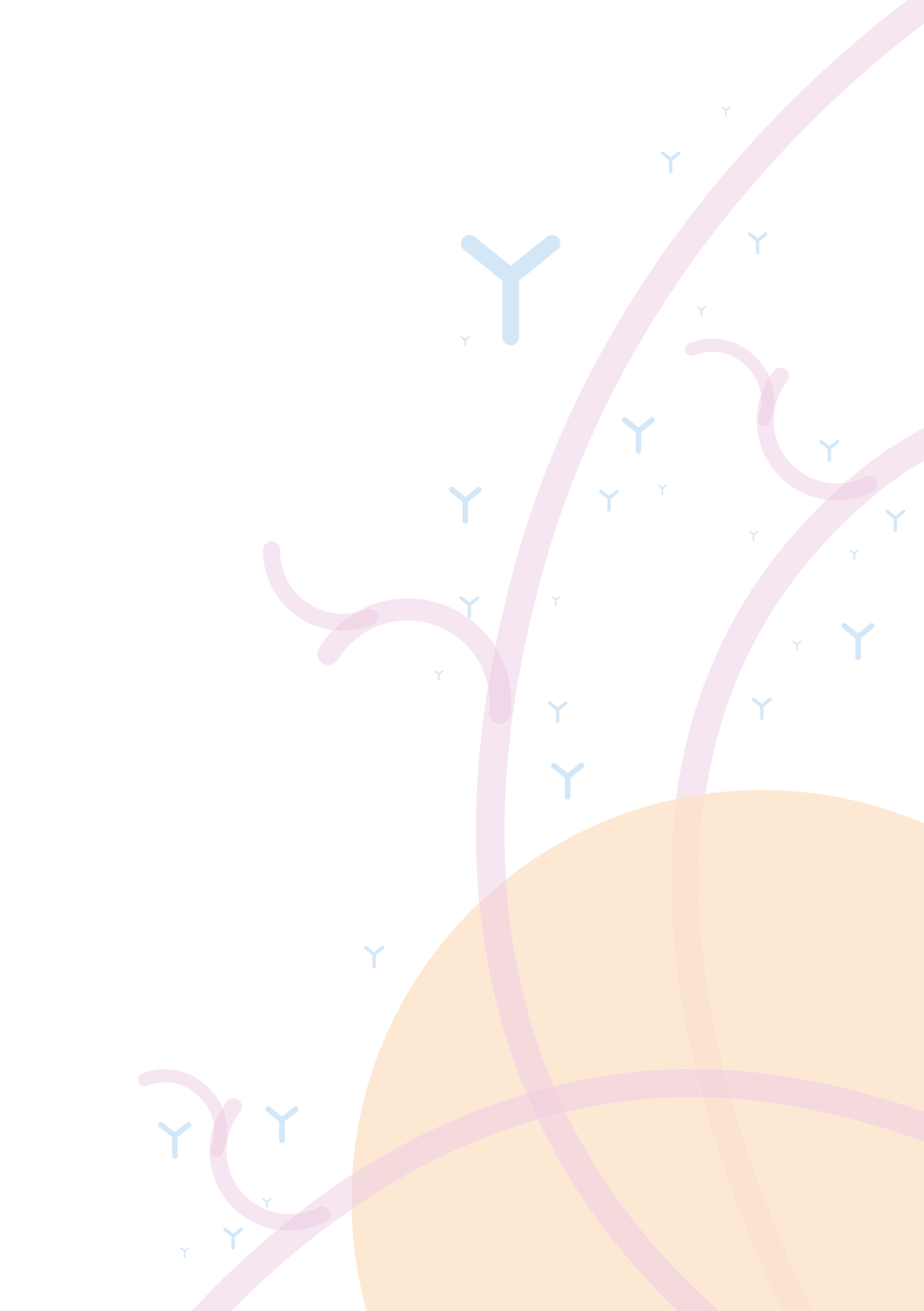
100. Hurwitz, H. *et al.* Bevacizumab plus Irinotecan, Fluorouracil, and Leucovorin for Metastatic Colorectal Cancer. *N. Engl. J. Med.* **350**, 2335–2342 (2004).
101. Brozzo, M. S., Leppanen, V. M., Winkler, F. K. & Ballmer-Hofer, K. VEGFR-2/VEGF-A COMPLEX STRUCTURE. (2012). doi:10.2210/pdb3v2a/pdb
102. Kisko, K. *et al.* Structural analysis of vascular endothelial growth factor receptor-2/ligand complexes by small-angle X-ray solution scattering. *FASEB J.* **25**, 2980–2986 (2011).
103. Ruch, C., Skiniotis, G., Steinmetz, M. O., Walz, T. & Ballmer-Hofer, K. Structure of a VEGF–VEGF receptor complex determined by electron microscopy. *Nature Structural & Molecular Biology* **14**, 249–250 (2007).
104. Hyde, C. A. C. *et al.* Targeting Extracellular Domains D4 and D7 of Vascular Endothelial Growth Factor Receptor 2 Reveals Allosteric Receptor Regulatory Sites. *Molecular and Cellular Biology* **32**, 3802–3813 (2012).
105. Silacci, M. *et al.* Design, construction, and characterization of a large synthetic human antibody phage display library. *PROTEOMICS* **5**, 2340–2350 (2005).
106. Böldicke, T. *et al.* Anti-VEGFR-2 scFvs for Cell Isolation. Single-Chain Antibodies Recognizing the Human Vascular Endothelial Growth Factor Receptor-2 (VEGFR-2/flk-1) on the Surface of Primary Endothelial Cells and Preselected CD34+ Cells from Cord Blood. *STEM CELLS* **19**, 24–36 (2001).
107. Adair, T. H. *Angiogenesis*. (Morgan & Claypool Publishers, 2010).
108. Risau, W. Mechanisms of angiogenesis. *Nature* **386**, 671–674 (1997).
109. Breier, G. & Risau, W. The role of vascular endothelial growth factor in blood vessel formation. *Trends in Cell Biology* **6**, 454–456 (1996).
110. Kim, K. J. *et al.* Inhibition of vascular endothelial growth factor-induced angiogenesis suppresses tumour growth in vivo. *Nature* **362**, 841–844 (1993).
111. Ide, A., Baker, N., Warren, S. & Clark, E. A Starting Point. *Am J Roentgenol* (1939).
112. H, A. G., W, C. H., Y, L. F. & D, P. H. *Vasculae Reactions of Normal and Malignant Tissues in Vivo. I. Vascular Reactions of Mice to Wounds and to Normal and Neoplastic Transplants*. (Oxford University Press, 1945). doi:10.1093/jnci/6.1.73
113. Algire, G. H. & Chalkley, H. W. *THE VASCULAR REACTION OF THE MOUSE TO NORMAL AND NEOPLASTIC TRANSPLANTS AND WOUNDS*. (CANCER ..., 1945).
114. Greenblatt, M. & Shubi, P. Tumor angiogenesis: transfilter diffusion studies in the hamster by the transparent chamber technique. *J. Natl. Cancer Inst.* **41**, 111–124 (1968).
115. Warren, B. A. The ultrastructure of capillary sprouts induced by melanoma transplants in the golden hamster. *Journal of Microscopy* **86**, 177–187 (1966).
116. Folkman, J. Angiogenesis in cancer, vascular, rheumatoid and other disease. *Nature Medicine* **1**, 27–31 (1995).
117. Folkman, J. Anti-angiogenesis: new concept for therapy of solid tumors. *Annals of Surgery* **175**, 409–416 (1972).
118. Shinkai, A. *et al.* Mapping of the Sites Involved in Ligand Association and Dissociation at the Extracellular Domain of the Kinase Insert Domain-containing Receptor for Vascular Endothelial Growth Factor. *J. Biol. Chem.* **273**,

- 31283–31288 (1998).
119. Fuh, G., Li, B., Crowley, C., Cunningham, B. & Wells, J. A. Requirements for binding and signaling of the kinase domain receptor for vascular endothelial growth factor. *J. Biol. Chem.* **273**, 11197–11204 (1998).
  120. Weber, M. *et al.* A Highly Functional Synthetic Phage Display Library Containing over 40 Billion Human Antibody Clones. *PLoS ONE* **9**, e100000 (2014).
  121. Hoogenboom, H. R., Raus, J. C. M. & Volckaert, G. Targeting of tumor necrosis factor to tumor cells: secretion by myeloma cells of a genetically engineered antibody-tumor necrosis factor hybrid molecule. *Biochimica et Biophysica Acta (BBA) - Molecular Basis of Disease* **1096**, 345–354 (1991).
  122. Rizk, A. *et al.* Segmentation and quantification of subcellular structures in fluorescence microscopy images using Squassh. *Nature Protocols* **9**, 586–596 (2014).
  123. Rizk, A., Mansouri, M., Ballmer-Hofer, K. & Berger, P. Subcellular object quantification with Squassh3C and SquasshAnalyst. *BioTechniques* **59**, (2015).
  124. Hoet, R. M. *et al.* Generation of high-affinity human antibodies by combining donor-derived and synthetic complementarity-determining-region diversity. *Nat. Biotechnol.* **23**, 344–348 (2005).
  125. Drebin, J. A., Link, V. C., Stern, D. F., Weinberg, R. A. & Greene, M. I. Down-modulation of an oncogene protein product and reversion of the transformed phenotype by monoclonal antibodies. *Cell* **41**, 695–706 (1985).
  126. Hudziak, R. M. *et al.* p185HER2 monoclonal antibody has antiproliferative effects in vitro and sensitizes human breast tumor cells to tumor necrosis factor. *Molecular and Cellular Biology* **9**, 1165–1172 (1989).
  127. Fan, Z. & Mendelsohn, J. Therapeutic application of anti-growth factor receptor antibodies. *Current Opinion in Oncology* **10**, 67–73 (1998).
  128. Zhu, W., Okollie, B. & Artemov, D. Controlled internalization of Her-2/ neu receptors by cross-linking for targeted delivery. *Cancer Biol. Ther.* **6**, 1960–1966 (2007).
  129. Bertelsen, V. & Stang, E. The Mysterious Ways of ErbB2/HER2 Trafficking. *Membranes (Basel)* **4**, 424–446 (2014).
  130. Olsson, A.-K., Dimberg, A., Kreuger, J. & Claesson-Welsh, L. VEGF receptor signalling — in control of vascular function. *Nature Reviews Molecular Cell Biology* **7**, 359–371 (2006).
  131. Carmeliet, P. *et al.* Synergism between vascular endothelial growth factor and placental growth factor contributes to angiogenesis and plasma extravasation in pathological conditions. *Nature Medicine* **7**, 575–583 (2001).
  132. Autiero, M. *et al.* Role of PlGF in the intra- and intermolecular cross talk between the VEGF receptors Flt1 and Flk1. *Nature Medicine* **9**, 936–943 (2003).
  133. Alam, A. *et al.* Heterodimerization with vascular endothelial growth factor receptor-2 (VEGFR-2) is necessary for VEGFR-3 activity. *Biochem. Biophys. Res. Commun.* **324**, 909–915 (2004).
  134. Andersen, D. C. & Reilly, D. E. Production technologies for monoclonal antibodies and their fragments. *Current Opinion in Biotechnology* **15**, 456–462 (2004).

135. Inoue, K., Itoh, K., Nakao, H., Takeda, T. & Suzuki, T. Characterization of a Shiga toxin 1-neutralizing recombinant Fab fragment isolated by phage display system. *Tohoku J. Exp. Med.* **203**, 295–303 (2004).
136. Maeda, F. *et al.* Production and characterization of recombinant human anti-HBs Fab antibodies. *J. Virol. Methods* **127**, 141–147 (2005).
137. Sharon, J., Liebman, M. A. & Williams, B. R. Recombinant polyclonal antibodies for cancer therapy. *Journal of Cellular Biochemistry* **96**, 305–313 (2005).
138. Weitkamp, J. H. *et al.* Generation of recombinant human monoclonal antibodies to rotavirus from single antigen-specific B cells selected with fluorescent virus-like particles. *J. Immunol. Methods* **275**, 223–237 (2003).
139. Wu, H. *et al.* Ultra-potent antibodies against respiratory syncytial virus: effects of binding kinetics and binding valence on viral neutralization. *J. Mol. Biol.* **350**, 126–144 (2005).
140. Yuan, F. *et al.* Vascular permeability in a human tumor xenograft: molecular size dependence and cutoff size. *Cancer Res.* **55**, 3752–3756 (1995).
141. Cabral, H. *et al.* Accumulation of sub-100 nm polymeric micelles in poorly permeable tumours depends on size. *Nat Nanotechnol* **6**, 815–823 (2011).
142. Longmire, M., Choyke, P. L. & Kobayashi, H. Clearance properties of nano-sized particles and molecules as imaging agents: considerations and caveats. *Nanomedicine (Lond)* **3**, 703–717 (2008).
143. Röthlisberger, D., Honegger, A. & Plückthun, A. Domain interactions in the Fab fragment: a comparative evaluation of the single-chain Fv and Fab format engineered with variable domains of different stability. *J. Mol. Biol.* **347**, 773–789 (2005).
144. Quintero-Hernández, V. *et al.* The change of the scFv into the Fab format improves the stability and in vivo toxin neutralization capacity of recombinant antibodies. *Mol. Immunol.* **44**, 1307–1315 (2007).
145. Reilly, R. M. *Monoclonal Antibody and Peptide-Targeted Radiotherapy of Cancer.* (John Wiley & Sons, 2010).
146. Batista, F. D. & Neuberger, M. S. Affinity dependence of the B cell response to antigen: a threshold, a ceiling, and the importance of off-rate. *Immunity* **8**, 751–759 (1998).
147. Steinwand, M. *et al.* The influence of antibody fragment format on phage display based affinity maturation of IgG. *MAbs* **6**, 204–218 (2014).
148. Menzel, C., Schirrmann, T., Konthur, Z., Jostock, T. & Dübel, S. Human antibody RNase fusion protein targeting CD30+ lymphomas. *Blood* **111**, 3830–3837 (2008).
149. Thie, H. in *Antibody Engineering* 397–409 (Springer Berlin Heidelberg, 2010). doi:10.1007/978-3-642-01144-3\_26
150. Zuberbuhler, K. *et al.* A general method for the selection of high-level scFv and IgG antibody expression by stably transfected mammalian cells. *Protein Engineering Design and Selection* **22**, 169–174 (2008).
151. Grünberg, J., Knogler, K., Waibel, R. & Novak-Hofer, I. High-yield production of recombinant antibody fragments in HEK-293 cells using sodium butyrate. *BioTechniques* **34**, 968–972 (2003).
152. Mansouri, M. *et al.* Highly efficient baculovirus-mediated multigene delivery

- in primary cells. *Nature Communications* **7**, 11529 (2016).
153. Al-Rubeai, M. *Antibody Expression and Production*. (Springer Science & Business Media, 2011).
  154. Nahta, R. The HER-2-Targeting Antibodies Trastuzumab and Pertuzumab Synergistically Inhibit the Survival of Breast Cancer Cells. *Cancer Res.* **64**, 2343–2346 (2004).
  155. Conn, P. M. *Animal Models for the Study of Human Disease*. (Academic Press, 2013).
  156. Houdebine, L.-M. in *The Laboratory Mouse* 97–110 (Elsevier, 2004). doi:10.1016/B978-012336425-8/50059-5
  157. Hutchinson, E. Mouse model: Reconstruction clues. *Nature Reviews Cancer* **4**, 332–332 (2004).
  158. Holland, E. C. *Mouse Models of Human Cancer*. (Wiley-Liss, 2004). doi:10.1002/0471675067
  159. Martic-Kehl, M. I., Schubiger, P. A., Mannhold, R., Kubinyi, H. & Folkers, G. *Animal Models for Human Cancer*. (John Wiley & Sons, 2016).
  160. Matzku. *Antibodies in Diagnosis and Therapy*. (CRC Press, 1999).
  161. Griffiths, A. D. & Duncan, A. R. Strategies for selection of antibodies by phage display. *Current Opinion in Biotechnology* **9**, 102–108 (1998).
  162. Popkov, M. *et al.* Human/mouse cross-reactive anti-VEGF receptor 2 recombinant antibodies selected from an immune b9 allotype rabbit antibody library. *J. Immunol. Methods* **288**, 149–164 (2004).
  163. Klohs, W. D. & Hamby, J. M. Antiangiogenic agents. *Current Opinion in Biotechnology* **10**, 544–549 (1999).
  164. Foulkes, R. Preclinical safety evaluation of monoclonal antibodies. *Toxicology* **174**, 21–26 (2002).
  165. Claesson-Welsh, L. Blood vessels as targets in tumor therapy. *Ups. J. Med. Sci.* **117**, 178–186 (2012).
  166. Waldner, M. J. *et al.* VEGF receptor signaling links inflammation and tumorigenesis in colitis-associated cancer. *The Journal of Experimental Medicine* **207**, 2855–2868 (2010).
  167. Stupp, M. T., Binz, H. K. & Amstutz, P. DARPinS: A new generation of protein therapeutics. *Drug Discovery Today* **13**, 695–701 (2008).
  168. Boersma, Y. L. & Plückthun, A. DARPins and other repeat protein scaffolds: advances in engineering and applications. *Current Opinion in Biotechnology* **22**, 849–857 (2011).
  169. Thom, G. & Groves, M. in *Therapeutic Antibodies* **901**, 101–116 (Humana Press, 2012).
  170. *Ribosome Display and Related Technologies.* **805**, (Springer New York, 2012).
  171. Goldstein, R. *et al.* Development of the designed ankyrin repeat protein (DARPin) G3 for HER2 molecular imaging. *European Journal of Nuclear Medicine and Molecular Imaging* **42**, 288–301 (2014).
  172. Zahnd, C. *et al.* Efficient tumor targeting with high-affinity designed ankyrin repeat proteins: effects of affinity and molecular size. *Cancer Res.* **70**, 1595–1605 (2010).
  173. Waibel, R. *et al.* Stable one-step technetium-99m labeling of His-tagged

- recombinant proteins with a novel Tc(I)-carbonyl complex. *Nat. Biotechnol.* **17**, 897–901 (1999).
174. Tang, Y. *et al.* Imaging of HER2/neu expression in BT-474 human breast cancer xenografts in athymic mice using [(99m)Tc]-HYNIC-trastuzumab (Herceptin) Fab fragments. *Nucl Med Commun* **26**, 427–432 (2005).
  175. Boersma, Y. L., Chao, G., Steiner, D., Wittrup, K. D. & Plückthun, A. Bispecific designed ankyrin repeat proteins (DARPin)s targeting epidermal growth factor receptor inhibit A431 cell proliferation and receptor recycling. *J. Biol. Chem.* **286**, 41273–41285 (2011).
  176. Yao, X. *et al.* Vascular endothelial growth factor receptor 2 (VEGFR-2) plays a key role in vasculogenic mimicry formation, neovascularization and tumor initiation by Glioma stem-like cells. *PLoS ONE* **8**, e57188 (2013).
  177. Müller, C., Schibli, R., Krenning, E. P. & de Jong, M. Pemetrexed improves tumor selectivity of 111In-DTPA-folate in mice with folate receptor-positive ovarian cancer. *Journal of Nuclear Medicine* **49**, 623–629 (2008).
  178. Schott, M. E. *et al.* Differential metabolic patterns of iodinated versus radiometal chelated anticarcinoma single-chain Fv molecules. *Cancer Res.* **52**, 6413–6417 (1992).
  179. Berndorff, D. *et al.* Radioimmunotherapy of solid tumors by targeting extra domain B fibronectin: identification of the best-suited radioimmunoconjugate. *Clinical Cancer Research* **11**, 7053s–7063s (2005).
  180. Gaijnkam, L. O. T. *et al.* Comparison of the biodistribution and tumor targeting of two 99mTc-labeled anti-EGFR nanobodies in mice, using pinhole SPECT/micro-CT. *Journal of Nuclear Medicine* **49**, 788–795 (2008).
  181. Alajati, A. *et al.* Spheroid-based engineering of a human vasculature in mice. *Nat. Methods* **5**, 439–445 (2008).
  182. Rosenfeld, P. J. *et al.* Ranibizumab for Neovascular Age-Related Macular Degeneration. <http://dx.doi.org/10.1056/NEJMoa054481> **355**, 1419–1431 (2009).
  183. Gragoudas, E. S., Adamis, A. P., Cunningham, E. T. J., Feinsod, M. & Guyer, D. R. Pegaptanib for Neovascular Age-Related Macular Degeneration. <http://dx.doi.org/10.1056/NEJMoa042760> **351**, 2805–2816 (2009).
  184. Vander, J. F. Ranibizumab and Bevacizumab for Neovascular Age-Related Macular Degeneration. *Yearbook of Ophthalmology* **2012**, 145–146 (2012).









Dragana Avramović  
Curriculum Vitae



### About me:

PhD, Angiogenesis, Cancer biology,  
Cell biology, Synthetic antibodies,  
Phage display

### Contact:

+41 78 6868546  
dragana\_avramovic@yahoo.com

### Personal details:

15.01.1984  
Belgrade, Serbia

## WORK EXPERIENCE

### 2012 - 2016

#### **PhD at Paul Scherrer Institute, Zurich area, Switzerland**

Project: Inhibiting angiogenesis with small antibody formats and antibody-like molecules

- Select antibodies from phage display libraries
- Expression and purification of antibodies
- Biophysical characterization of antibodies
- Testing antibodies on cells in kinase assays
- Testing antibodies in angiogenesis assays
- Testing antibodies in vivo

### 2011 - 2012

#### **Scientific associate at Novartis, Basel, Switzerland**

Project: Determination of hot spot mutation of TNK2 gene responsible for tumor development

- Mutagenesis
- Gain of function studies
- Transient and stable transfection
- BL2 viral transduction

**2010 - 2011**

**Internship contract at Novartis, Basel, Switzerland**

Projects:

I. Characterization of sensitivity to FGFR inhibitor in sarcoma cell lines  
II. Investigation of resistance after long term treatment in vivo with PIK3CA inhibitor in tumors

- Mutational analysis
- Gene-copy number analysis
- Gene expression analysis
- DNA methylation analysis

**2009 - 2010**

**Assistant of general director at University Children's Hospital, Belgrade, Serbia**

## EDUCATION

**2012 - 2016**

**PhD degree at Basel University, Switzerland**

Department: Cell biology

PhD Thesis: Inhibiting angiogenesis with different antibody formats and antibody-like molecules

**2003 - 2009**

**Bachelor and Master degree at University of Belgrade, Serbia**

Department: Molecular Biology and Physiology,

Study group: Experimental Biomedicine

Master thesis: Antigenic and genetic characteristics of swine-origin 2009 A (H1N1) influenza viruses circulating in humans

# SKILLS

## **In-vivo**

Tumor targeting with radioactively labeled antibodies  
LTK 1 course at University Zürich

## **In-vitro**

### **Cell biology technics**

Cell and tissue culture  
Kinase activation assay  
Transient and stable transfection  
BL2 viral transduction

### **Immunoassays**

Western Blot  
ELISA  
FACS  
Immunostaining  
Immunoprecipitation

### **Special technics**

Antibodies selection from phage library  
Antibodies characterization  
Antibodies formatting from ScFv to Fabs and full IgGs

### **Microscopy technics**

Wide field fluorescence microscopy  
Confocal fluorescence microscopy

### **Biochemistry technics**

Protein expression: Mammalian and bacterial vectors  
Protein purification:

- ÄKTA systems with Unicorn software
- IMAC affinity column
- Size-exclusion chromatography

## **Biophysical technics**

FSEC  
MALS  
ITC

## **Molecular biology technics**

Cloning, Restriction digestion, Mutagenesis, Mutational screening,  
PCR - based techniques

## **Bioinformatics tools**

Vector NTI, Ape, ImageJ, GraphPad

## **Computer skills**

MS Office, Illustrator, Photoshop

## LANGUAGES

English - Fluent  
German - C1  
French - Basic  
Spanish - Basic  
Serbian - Native speaker

